

I

Simulation of Air-to-Air Energy Recovery Systems for HVAC Energy Conservation in an Animal Housing Facility

by

Sebastian W. Freund

A Thesis submitted in partial fulfillment of the requirements for the degree

Masters of Science
Mechanical Engineering

Solar Energy Laboratory
University of Wisconsin - Madison
2003

Abstract

Implementation of energy conservation measures in buildings can extend our use of finite resources while simultaneously reducing our impact on the environment. This project summarizes efforts to identify economically-viable strategies to reduce HVAC related energy usage and improve the indoor air quality at a facility that houses primates and large cats. The primary focus of energy conservation strategies for the facility centered around air-to-air energy recovery concepts including enthalpy exchangers and runaround loops. Component and system models for transient computer simulations were developed for the existing facility and for several equipment alternatives including enthalpy exchangers and runaround loop heat exchangers. The model of the enthalpy exchanger is based on a new semi-empirical NTU Correction Factor Method. Given only two reference data points, the model is able to predict effectiveness for any balanced and unbalanced flow condition. The runaround loop is modeled as two counterflow liquid-to-air heat exchangers coupled by a heat transfer liquid. The model incorporates liquid flow rate and bypass control. Both models include various options of economizer control and frost control, as well as calculations of parasitic losses. Comparisons of frost control strategies for energy recovery systems were prepared and show that preheating of outdoor air is a favorable solution for enthalpy exchangers. The new simulation models are validated with experimental data. The building model is a detailed model including all internal gains, humidity and solar irradiation and is created in TRNSYS, a software package for transient simulations. The simulations were based on hourly weather data for one year. The simulations allow energy consumption and indoor air quality to be optimized. The findings of the simulations suggest that more than 80% of the heating energy and 45% of the cooling energy can be saved by implementation of air-to-air energy recovery and conservative control settings. The proposal for changes of the HVAC system includes specifications of energy recovery systems and an economic analysis. The environmental impact of the proposed systems regarding CO₂ production has been analyzed, showing that up to 73 tons can be saved per year.

Preface

Motivation

In connection with the looming threats of global warming and unavoidable increasing energy prices within the foreseeable future as a consequence of our amply usage of fossil fuel, the significance of high efficient HVAC systems should not be underestimated anymore.

Economic growth and upgraded requirements of comfort and indoor air quality lead to a steadily increasing energy demand in the commercial HVAC sector. Improved efficiency alone will not be sufficient to halt or reverse this trend in the future.

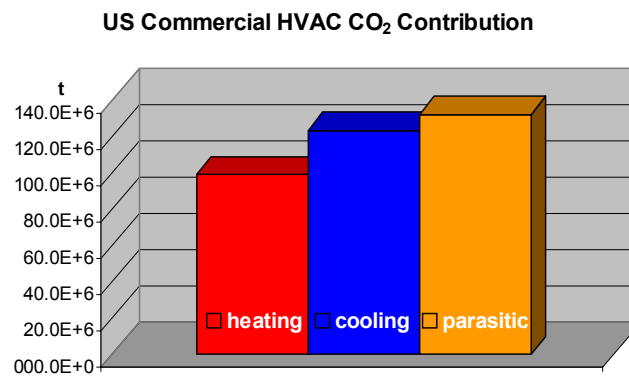


Figure 1: HVAC related CO₂ contribution by sector (estimated based on numbers from ADL Inc, 1995). Commercial HVAC accounts for 6% of US CO₂ production

Almost unnoticed by the public and widely ignored in the HVAC contractor business, energy recovery equipment can save substantial amounts of HVAC related energy and can lead to immediate payback.

Tools to investigate the options of more efficient energy usage are computer simulations of buildings and systems. May the models created here and the simulations help saving energy and are examples of measures to reduce building energy consumption.

Acknowledgements

I would like to express my gratitude to all people who gave me a very enjoyable time at the University of Wisconsin – Madison and created a comfortable working environment in the Solar Energy Lab. I would like to thank my friends, my fellow students and professors in the lab, namely Tim Shedd, and the TRNSYS engineer Michaël Kummert, who were always there to answer questions and helped me through many difficulties of this project.

A very special thanks goes to my great academic advisors: Professor Sanford A. Klein, an outstanding teacher of thermodynamics, and Douglas T. Reindl, from whose profound hands-on knowledge of the HVAC world I benefited a lot during this project.

Thanks also to Jim Hubing, the director of Vilas Zoo, and Bob Criscione from MG&E, for the good cooperation on the Primate House project.

Greatly acknowledged is John S. Nelson, whose generous Fellowship grant provided excellent funding for this project and my studies in Madison.

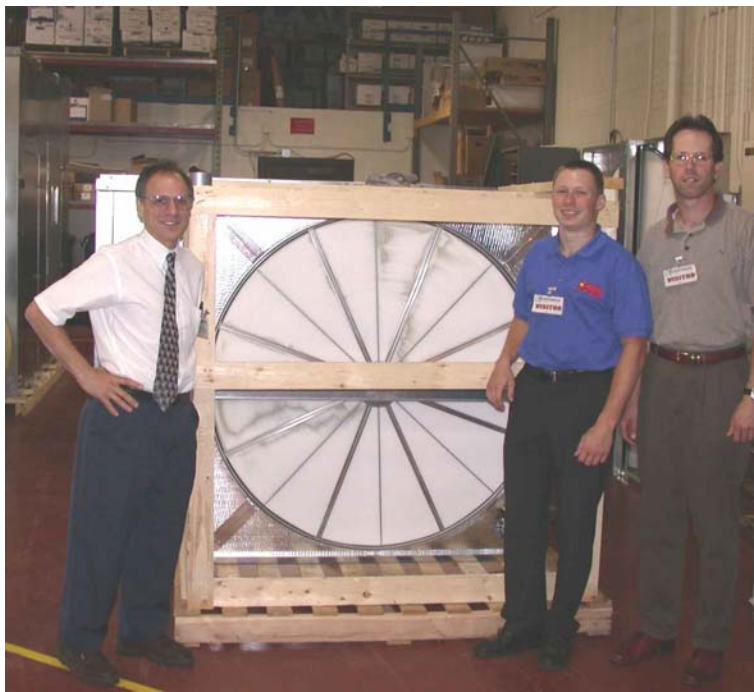


Figure 2: My advisors and me in front of an enthalpy exchanger at a factory

Table of Contents

Abstract.....	I
Preface.....	III
Motivation.....	III
Acknowledgements.....	IV
Table of Contents.....	V
Nomenclature.....	VIII
Chapter 1 Building Modeling.....	1
Internal Gains.....	4
Solar Gains.....	7
Basement Heat Losses.....	8
Chapter 2 Ventilation.....	11
Temperature Measurements to Calculate outside Air Flow Rates.....	13
Effect of Ventilation on the Building Energy Balance.....	15
Infiltration.....	16
Suggestions to Improve IAQ.....	17
Chapter 3 Indoor Humidity.....	19
Introduction.....	19
Characterizing Humidity in the Primate House – Existing Situation.....	20
Humidification Mode Limitation: Condensation.....	24
Humidification System: Existing Situation and Recommendations.....	26
Dehumidification System: Existing Situation and Recommendations.....	29
Calibration of the Data Loggers.....	32
Chapter 4 Enthalpy Exchangers.....	35
Introduction.....	35
Psychrometrics of Enthalpy Exchange.....	37
Transfer Mechanism and Governing Equations.....	41
Desiccants.....	45
Calculation of NTU.....	47
Discussion of the NTU Calculations.....	51

Introducing the NTU Correction Factor Method for Performance Prediction of Enthalpy Exchangers	52
Verification	55
Uncertainty Propagation for the NTU Correction Factor Method	58
Conclusion	60
Computer Modeling of Enthalpy Exchangers for TRNSYS	61
Outlet State Calculation	63
Frost Control	64
Pressure Drop and Fan Power	65
Enthalpy Exchanger Economizer Control	65
Output Plots	68
Chapter 5 Runaround Loop Heat Exchangers	70
Introduction	70
Transfer Fluid	71
Frost Control	74
Economizer Control	76
Heat Exchanger Equations	77
Verification	80
Computer Modeling	84
Outlet State Calculation	85
Wet Coil Analyses	86
Frost Control	90
Economizer Control	91
Fan and Pump Power	91
Output Plots	93
Chapter 6 Simulations of the Primate House	95
Validation of the Simulation Model	95
Simulation of the HVAC system including Enthalpy Exchangers	102
Simulation of the HVAC system including Runaround Loops	106
Energy Optimized Control Settings	109
Improved Indoor Air Quality	112

	VII
Improved IAQ settings without Energy Recovery.....	112
Improved IAQ settings applying Enthalpy Exchangers.....	113
Improved IAQ settings applying Runaround Loops.....	116
Extreme Weather Conditions and System Sizing.....	118
Conclusions of the Annual Building Energy Simulations.....	119
Chapter 7 Economic Analysis.....	121
Influence of Economic Parameters.....	123
Estimation of Energy Recovery Equipment Cost.....	126
Chapter 8 Environmental Impacts.....	128
Chapter 9 Conclusions and Recommendations.....	130
Appendix A: FORTRAN Source Code for TRNSYS Type 222 Enthalpy Exchanger.....	132
Appendix B: FORTRAN Source Code for TRNSYS Type 223 Runaround Loop.....	140
References.....	153

Nomenclature

A	absorption potential [kJ/kmol], area [m ²]
A _S	surface area [m ²]
cp _r	specific heat of air [kJ/kgK]
cp _m	specific heat of the matrix [kJ/kgK]
C _r *	ratio of matrix capacitance rate to the minimum fluid capacitance rate
CFX	Counterflow heat exchanger
D _h	Hydraulic diameter
EA	Exhaust air
EX	Enthalpy exchanger
ERV	Energy recovery ventilation
h	heat transfer coefficient between the matrix surface and air [W/m ² K]
h _w	mass transfer coefficient between the matrix surface and air [kg/m ² s]
h	specific enthalpy of the air [kJ/kg]
h _{sat}	specific enthalpy of moist air at saturation [kJ/kg]
i _f	specific enthalpy of fluid stream [kJ/kg]
i _m	specific enthalpy of matrix [kJ/kg]
i _w	specific enthalpy of water vapor [kJ/kmol]
k	Thermal conductivity [W/mK]
L	length of matrix in flow direction [m]
Le	Lewis number = NTU _w / NTU _T
m _{air}	mass flow rate of air [kg/s], both flow rates are the same in this study
M _f	fluid mass entrained in flow passages [kg]
M _m	mass of dry matrix [kg]
NTU	overall Number of Transfer Units
NTU _T	Number of Transfer Units for heat transfer
NTU _w	Number of Transfer Units for mass transfer
Nu	Nusselt number = D _h h/k
OA	Outside air
ps	saturation vapor pressure of water at a specified temperature [kPa]

p_v	actual vapor pressure of water [kPa]
R	universal gas constant, 8.314 kJ/kmol-K
Re	Reynolds number = vD_h/ν
RL	Runaround loop
REX	Rotary enthalpy exchanger
S	rotation speed [1/s]
t	time [s]
T	temperature [K]
T_{amb}	ambient temperature [K]
T_f	temperature of the air stream [K]
T_m	temperature of the matrix surface [K]
v	Velocity [m/s]
w_f	humidity ratio of the air stream
w_m	humidity ratio of air in equilibrium with the matrix
W_m	matrix humidity ratio, unit mass of absorbed water per unit mass of dry matrix [kg/kg]
x	position in matrix in flow direction [m]
z	dimensionless flow coordinate = x/L
ε	effectiveness
ε_{cf}	effectiveness for direct transfer counterflow heat exchangers
ε_t	heat exchanger temperature effectiveness
ε_w	mass exchanger effectiveness
ε_i	enthalpy exchanger effectiveness
Γ	mass flow rate ratio: $M_m S/m_{air}$
ν	Cinematic viscosity [m ² /s]
τ	dimensionless time $\tau = tS/\Gamma$

Chapter 1 Building Modeling

The building simulations are made in TRNSYS [10] for the Primate House, a facility that is part of the Vilas Zoo located in Madison, WI. The building is modeled as a TRNSYS Type 56 multi zone building. Type 56 is a TRNSYS component, which allows transient estimates of heating and cooling loads of buildings with more than one thermal zone. Due to its complexity, a user interface program called PreBid is used to generate the Type 56 model description code. All building data are entered in PreBid, e.g. dimensions, materials and orientation of all internal and external walls and windows, as well as internal heat gains, ventilation, heating and cooling data, with limited power with respect to the maximum power of installed equipment. The Primate House Type 56 model includes four zones, each served by an air-handling unit identical to the configuration in the actual building. All walls, windows and doors, outside, inside and between zones are modeled according to the blueprints of the building.

The building, a two story animal housing and visitor facility completely rebuilt in 1995, has a total floor area of 1516 m², and is divided into two zones on the ground level and two zones in the basement, **Table 1.1**.

Zone	Occupants	Floor space	Volume
1, Basement	Tigers and Lions	184 m ²	450 m ³
2, Basement	Primates and Staff	574 m ²	1440 m ³
3, 1 st Floor	Primates and Staff	516 m ²	2500 m ³
4, 1 st Floor	Visitors	242 m ²	1000 m ³

Table 1.1: The 4 Zones in the Primate House

The old building walls are made of concrete and face brick with an insulating air space (R-value 4.5), the new wall are either or two layer poured concrete with Styrofoam insulation (R-value 11), or concrete with 100mm Styrofoam (R-value 20). The basement also has concrete wall insulated with Styrofoam (R-value 8.5). The roofing is made of fiberglass insulated sheet metal (R-value 8.5), roofing area is 824 m², including skylights for the cages in the viewing area. Large east-facing windows in the visitor's zone and the viewing area

allow same daylight. The double-glazed insulated windows have an R-value of 2, the unbreakable windows of the cages in the viewing area are the least insulated with an R-value of 1.2 ft²F/BTUH.



Figure 1.1: East façade of the Primate House



Figure 1.2: west façade of the Primate House, with a condensing unit for Zone 3, exhaust air outlet (louwer upper right) and intake air inlet (louwer lower right).

The inputs for the Type 56 simulations are outside temperature and humidity, solar radiation and ground temperature. The outputs include each zone's temperature and humidity, the heating demand and the sensible and latent cooling demand. A detailed description of how Type 56 computes temperatures by means of thermal nodes for each zone and transfer functions for each wall can be found in the TRNSYS Manual [10]. Some aspects of building simulations are discussed in more detail in the following.

The building's HVAC system (without optional energy recovery equipment) is modeled in Type 56. Type 56 calculates sensible and latent energy demand for each zone based on all input conditions and the zone set points of temperature and relative humidity. For each zone the heating and cooling capacity is limited in accordance with the maximum capacity of the air-handling units, coils, boilers and condensing units:

- Zone 1: Heating 200000 kJ/h, Cooling 80184 kJ/h
- Zone 2: Heating 300000 kJ/h, Cooling 178304 kJ/h
- Zone 3: Heating 797306 kJ/h, Cooling 494821 kJ/h
- Zone 4: Heating 294255 kJ/h, Cooling 187800 kJ/h

The input weather data used for all yearly simulations is based on hourly measurements of temperature, humidity and solar radiation for Madison in 1999, obtained from NOAA and the Wisconsin State Climatologist. The usage of real historic weather data has the advantage that modeled data can be compared to data taken during the simulated time in the past.

The entire simulation model including additional components such as data readers and output printer is assembled in IISiBat, a graphical user interface program belonging to TRNSYS, where components are interlinked to each other with inputs and outputs lines. **Figure 1.3** shows an IISiBat window with the Primate House Project:

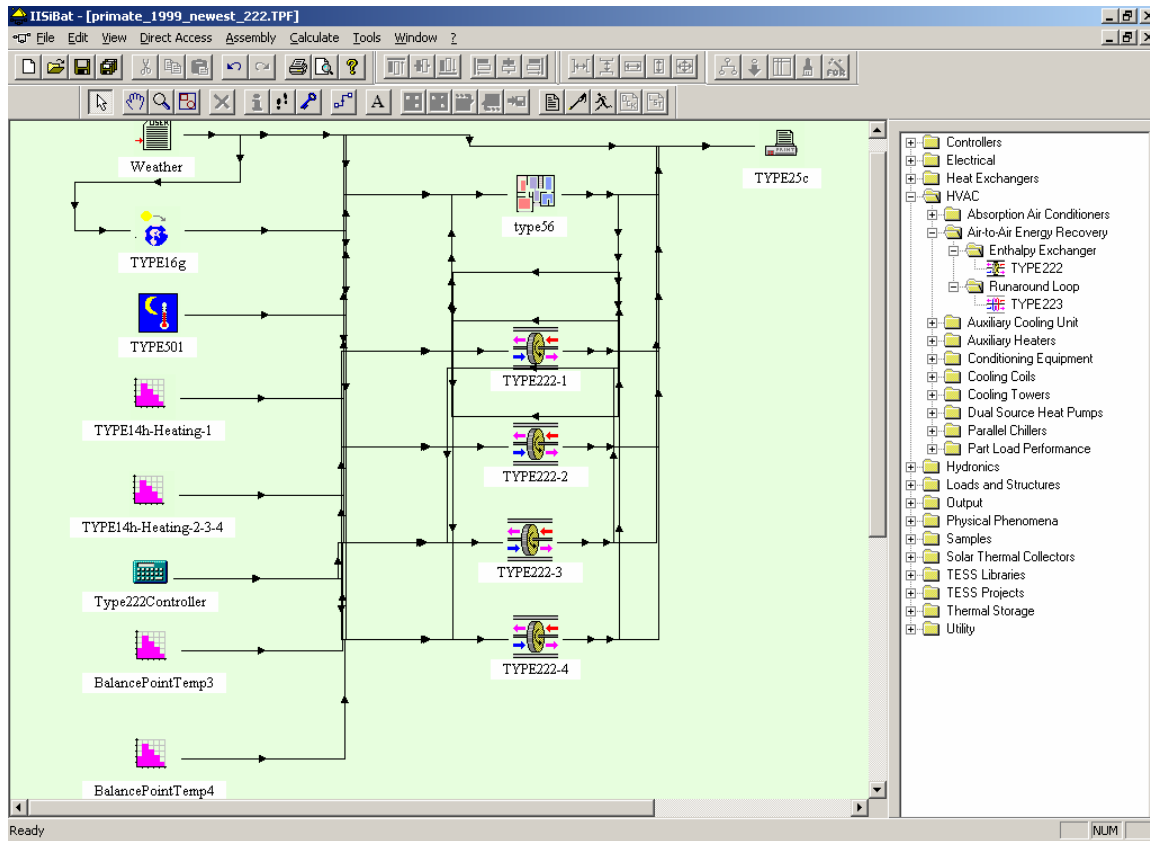


Figure 1.3: Screenshot IISiBat surface with Type 56 and Type 222 Enthalpy Exchangers.

Internal Gains

Internal gains in a building include heat and moisture generated by lights, equipment and occupants within the conditioned space. In the Primate House internal gains come from lights and electric equipment as well as from visitors, staff and animals and have to be considered in the building simulations.

Internal gains from electric sources include:

- Fans
- Lights
- Pumps

- Refrigerators and freezers

The heat gain of ventilation fans is assumed to be equal to the nominal horsepower divided by a motor efficiency of 0.8 and multiplied by a loadfactor of 0.75. The loadfactor takes into account that the fan motors are not always running under maximal load conditions, where the power output would be the nominal horsepower. All electric energy provided to the fan motors will finally be converted into heat. The same applies for the pumps for hot water; the heat gain is set equal to the nominal horsepower. Fans and pumps run continuously.

Gains from lighting represent the second largest heat gain with a total of 5 kW. The heat gain is equal to the total wattage. The number of lights and the wattage has been determined for each zone. The schedule for the lights is 8 AM – 5 PM for all zones but the visitors, where the light is on from 10 AM – 5 PM.

The heat gain of the refrigerators is based on the average yearly energy consumption of US household refrigerators of 1251 kWh/year respectively 142.8 W [DoE, 2001]. There are two refrigerators in Zone 1, one freezer in Zone 2 and the large cooler in Zone 3. The heat gain of the freezer is estimated to be equal to the standard refrigerator multiplied by a factor of three, the gain of the large cooler is assumed to be 3 times as high as a standard refrigerator. The walk-in freezer in Zone 2 has a condensing unit installed outdoors so that the heat gain inside Zone 2 is negative. Based on the estimated energy consumption of the unit, it is roughly assumed that the insulation losses are equal to those of 20 standard refrigerators. A summary of internal gains of equipment is presented in **Table 1.2**:

Zone No.	1, Tiger	2, Basement	3, 1 st Floor	4, Visitors
Lights	900 W	2220 W	1080 W	1110 W
Pumps		2860 W		
Fans	2097 W	5243 W	10486 W	5243 W
Refrigerators	143 W	-2285 W	571 W	
TV/PC		230 W		150 W

Table 1.2: Internal loads from electric equipment in the primate house

The heat and moisture gains from building occupants include:

- Visitors
- Keepers
- Animals

To estimate the sensible and latent heat gain of humans, tables according to ISO 7730 are used showing the heat gain depending of the level of activity. The visitors in Zone 4 are assumed to generate 75 W sensible and latent heat each at an activity level described as “Seated, light work”. The number of people is scheduled to be 10 persons every day between 10 AM and 5 PM. Two keepers are assumed to be in the building, one person in Zone 2 and one in Zone 3. Due to a higher activity, their sensible and latent heat gain is higher, 100 W / 130 W respectively.

The heat gain of the animals is calculated based on metabolic rate M and average weight W . The Average Total Heat Gain (AHTG) can be calculated with equation (2.1) according to Wood et al. 1972, Gordon et al. 1976, in [9]:

$$AHTG = 2.5M, \quad M = 3.5W^{0.75} \quad (2.1)$$

A summary of the AHTG of the animals is given in **Table 1.3**:

Individual	AHTG [W]	No. of Individuals	Zone No.
Orangutan	303	6	2, 3
Chimpanzee	218	5	2, 3
Tiger / Lion	273	7	1
Gibbon / Colobus / Lemur	29	14	2, 3

Table 1.3: AHTG of the animals in the primate house

Tigers and lions are scheduled to be inside the building only between 5 PM and 10 AM, while the monkeys are assumed to be inside all day, living in Zone 2 and 3.

In the TRNSYS Type 56 building model, the internal gains can be conveniently entered when using PreBid. **Figure 1.4** shows a PreBid input window for internal gains for Zone 3. Internal gains are specified in PreBid as gain types, e.g. Orangutan or Fans, and scaled and time-scheduled for each zone.

Gains [Zone: 31FVIEWING]

Persons

degree of activity

off ISO 7730 Table light bench work

on VDI 2078 Table

scale: S: 1*08_17

Computer

off on

Artificial Lighting

related floor area: 108 m²

off on

total heat gain: 10 W/m² control strategy: S: 1*08_17

convective part: 40 % Leuchtstoffröhre scale: 1

Other Gains

Type	Scale	Geo Position
ORANGUTAN	3	
FANS	13	
LEGIBOLD	12	
REFRIGERAT	4	

gain type: ORANGUTAN new ...

scale: 3

Figure 1.4: Input window for internal gains in PreBid

Solar Gains

Solar heat gains are caused by solar radiation entering the building through fenestration or by absorbed radiation warming the building envelope. The solar radiation incident on each building surface is calculated for each surface orientation based on input solar data and simulation time by a TRNSYS Type 16 radiation processor. The input data from the weather data file is hourly beam radiation and total horizontal radiation, together with the local latitude and time, the total radiation on any surface can be evaluated. Type 56 accounts for

solar radiation by calculating transmittance, absorbance and emittance of any exposed surface, based on viewfactors and surface orientation.

For the Primate House, solar gains are relatively small, since the building does not have large south- or west-facing or horizontal windows and the envelope is well insulated and has a light color, so that neither much solar radiation is transmitted through fenestration, nor will the absorption of the roof cause a large heat flux into the zones on the first floor. However, solar gains are included in the simulations and contribute to summer peak loads.

Basement Heat Losses

In contrast to the calculation of heat losses for a structure above the surface, where heat is conducted through the wall driven by the temperature difference from inside and outside air temperature, the calculation of basement heat losses requires different assumptions and methods since the basement walls and the slab are surrounded by layers of sand and soil with different temperatures from the outside air. In a certain depth below surface, ground temperature will be equal to the yearly average temperature and constant. Closer to the surface, ground temperature fluctuations will show an increase in amplitude, seasonal and near the surface even daily fluctuations. Ground temperature can be estimated by means of the Kusuda-Equation, (2.2), developed by Kusuda and Archenbach, 1965, [15],

$$T = T_{\text{mean}} - T_{\text{amp}} \cdot \exp\left[-Z \cdot \left(\frac{\pi}{365 \cdot \alpha}\right)^{0.5}\right] \cdot \cos\left[2 \cdot \frac{\pi}{365} \cdot \left(t_{\text{year}} - t_{\text{shift}} - \frac{Z}{2} \cdot \left[\frac{365}{\pi \cdot \alpha}\right]^{0.5}\right)\right] \quad (2.2)$$

where T_{mean} is the annual local mean temperature (9.22°C), T_{amp} is the local ground surface temperature amplitude (15K), Z the depth below surface, α is the thermal diffusivity of the ground (0.05573 m²/day), t_{year} is the day of the year and t_{shift} is the difference between the coldest surface temperature and the begin of the year (14); values in parenthesis valid for Madison in 1999.

The approach to simulate heat loss through basement walls in TRNSYS is to divide the wall in an upper and a lower half, and setting the boundary temperatures as ground temperatures in 0.5 m and 1.5 m depth provided by TRNSYS Type 501. The assumption made here is that the ground temperature is undisturbed i.e. not influenced by heat losses of the building. Since the soil around the wall heats up, actual temperature may be higher and losses may be slightly lower than calculated.

To estimate the heat losses from the basement floor [18], a 2D finite element model was created using the program FEHT [17]. The model includes the basement slab made of concrete with a thickness of 0.2 m, the foundation footer with an $R=7.5$ insulation layer, a 0.2 m layer of sand below the slab and that all surrounded by 5 m of soil. Ground temperature 5 m off the building can be considered as undisturbed, [15], and was set to the annual mean of 9.22 C. The temperature distribution found in this analysis is shown in **Figure 1.5**.

Losses have been found to be averagely 1.64 W/m^2 for a basement slab surface temperature of 22°C and a ground temperature of 9.22°C . That leads to a total heat loss of 1250 W. For modeling this loss as conduction through the slab with a constant boundary temperature, a temperature difference is calculated according to the equation $q = k \Delta T$. The corresponding temperature difference to a heat transfer coefficient of $k = 3.875 \text{ W/m}^2\text{K}$ equals 0.43 K. Boundary temperature is set to the zone temperature minus 0.43 K.

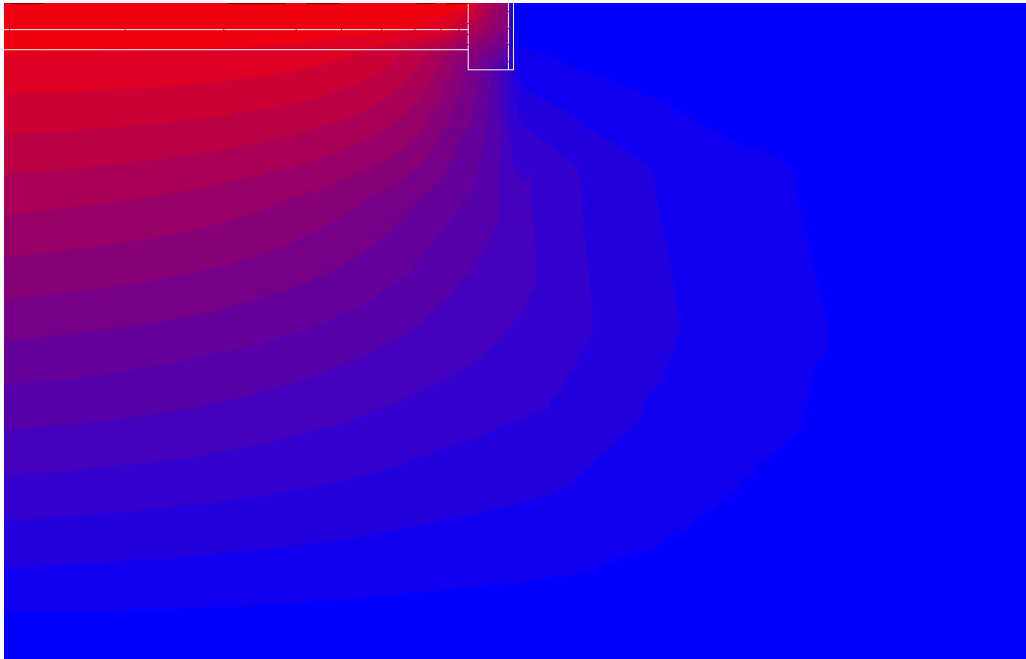


Figure 1.5: Finite element model by FEHT of basement slab and surrounding soil, colors indicating temperatures ranging from 22°C to 9.22°C

Effects of changed ground temperatures at the basement slab level on heat losses turned out to be negligible, since temperature below the slab will be close to indoor temperature and is hardly affected by seasonal changes of ground temperature as calculated by the Kusuda-Equation.

Chapter 2 Ventilation

Thermal comfort and appropriate indoor air quality (IAQ) are important factors for occupants in a building. The way to maintain acceptable IAQ is to bring fresh outside air into a building by mechanical ventilation. In order to satisfy indoor temperature and humidity requirements, outside air has to be conditioned in an air-handling unit (AHU), **Figure 2.1**.



Figure 2.1: Air-handling unit for Zone 3, air flow from left to right: mixed air duct, filter box, heating coil (piping with white insulation), cooling coil (piping black insulation), fan box, supply air duct in the back

Heating, ventilation and air-conditioning of commercial buildings are rather energy intense processes, 6% of the total US energy usage, or currently ca. 6,300,000,000 GJ are consumed by HVAC systems in the commercial sector [34]. The largest share of this consumption is due to the conditioning of outside air to meet ventilation requirements; henceforth the amount of fresh air brought into a building is of great importance in terms of energy usage and HVAC costs, **Figure 2.2**.

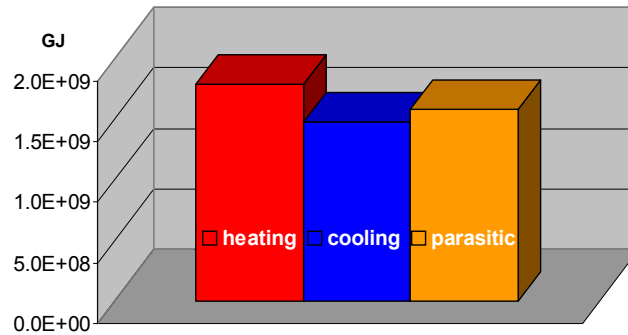


Figure 2.2: Primary HVAC energy consumption by application of commercial buildings in the US in 1995 [34]

There are different standards to ensure sufficient ventilation for buildings. ASHRAE Standard 62-2001 “Ventilation Requirements for Acceptable Indoor Air Quality” [6], recommends a minimum ventilation rate of 8 l/s (15 cfm) outside air per person for places of assembly and spectator areas, as what the visitor area Zone 4 of the Primate House may be considered. Required minimum ventilation rate in accordance to the Wisconsin Department of Commerce Chapter Comm 64.05 “Inside Design Temperatures and Ventilation Requirements” is two air changes per hour for public buildings. More applicable for the Primate House may be the recommendation from “Guide for the Care and Use of Laboratory Animals”[16], of 10 to 15 air changes per hour in non-human primate cages.

Higher ventilation rate means enhanced dilution of odors, gases, vapors and particles, hence better IAQ. The amount of energy required for heating or cooling the intake air increases proportionally with the ventilation rate. Due to the large affect of the ventilation rate on the building’s energy balance, it is essential to know the ventilation rate for building simulations. Measurements were undertaken to investigate the ventilation rates in different zones of the Primate House.

Temperature Measurements to Calculate outside Air Flow Rates

In an AHU outside air is mixed with return air to create a “mixed air” state prior to conditioning. To offset the sensible and latent space load in a zone, the mixed air is heated above or cooled below indoor temperature in the AHU and distributed through supply air ducts. The outside airflow rate can be determined by the fraction of outside air in the mixed air and either based on the scheduled return or supply airflow rate. Given the temperatures of outside, mixed and return air, the outside air fraction f_{OA} of the mixed air can be calculated:

$$f_{OA} = (T_{return} - T_{mix}) / (T_{return} - T_{outside}) \quad (2.1)$$

When including a mass balances, airflows can be calculated e.g.:

$$T_{outside} = 0$$

$$T_{return} = 21.55$$

$$T_{mix} = 8.7$$

$$m_{O,A} = 5496.3$$

$$m_{O,A} \cdot T_{outside} + m_{return} \cdot T_{return} = m_{total} \cdot T_{mix}$$

$$m_{total} = m_{return} + m_{O,A}$$

$$f_{O,A} = \frac{m_{O,A}}{m_{total}}$$

The measurements of temperatures were taken on a clear and windless day in January 2002. The measurements revealed a significant thermal boundary layer outdoors. Surface temperature was 0°C, while temperature at an altitude of 2 m was found to be -1.5°C and at 4.4 m -4.7°C.

Calibration and accuracy of the thermometers: both thermometers, the digital Tri Sense (readout-precision 0.05°F) and the analog (readout-precision 0.5°C) showed good agreement after a sufficient time to reach steady state: 21.44°C vs. 21.5°C. Results when measuring mixed air temperature in the filter compartments of the air-handling units were reasonable close but deviations between 0.1°C and 1.4°C occurred. However, when measuring return air temperature, analog thermometers showed always up to 1.3°C less than the digital one. When temperatures measured with the digital thermometers and one or two analog seemed to be

reasonable, the arithmetic mean value was used, rounded with respect to the digital temperature measurements.

An uncertainty-propagation for the outside airflow was carried out using an EES [11] program, assuming an uncertainty of 0.5 C for the temperatures.

Zone 2, Basement

T_{Mixed}^1	T_{Return}^1	$T_{Outdoor}^1$	$f_{outsideair}^2$	Out Air Flow ^{2/3}	Exh Flow ³	Supply Flow ^{3/2}	VR ⁴
15.6	22.1	-4.7	0.24	1682+/-201 2004.8	2004.8	8036.3 8266+/-812	1.17 1.4

Zone 3, 1st Floor Animals

T_{Mixed}^1	T_{Return}^1	$T_{Outdoor}^1$	$f_{outsideair}^2$	Out Air Flow ^{2/3}	Exh Flow ³	Supply Flow ^{3/2}	VR ⁴
8.7	21.55	0	0.596	13115+/-629 5496.3	5496.3	21985.2 9218+/-442	5.25 2.2

Zone 4, 1st Floor Visitors

T_{Mixed}^1	T_{Return}^1	$T_{Outdoor}^1$	$f_{outsideair}^2$	Out Air Flow ^{2/3}	Exh Flow ³	Supply Flow ^{3/2}	VR ⁴
16.9	21.8	-2	0.21	1585+/-209 1699	1699	7696.5 8087+/-1045	1.58 1.69

Table 2.1: Temperatures and airflow rates, Explanation:

¹) Measured value, average from analog and digital thermometers when both applicable

²) Calculated value, based on scheduled supply airflow or on scheduled exhaust airflow

³) Scheduled value, acc. to blueprints HVAC schedule

⁴) Resulting ventilation rate in air changes per hour, based on zone volume and outside airflow

All flow rates in m³/h, Temperatures in °C.

In Zones 2 and 4, measurements of ventilation rates agree fairly well with scheduled values from the building plans. Outside airflow is assumed to equal exhaust airflow, relief fans are off and dampers closed; ventilation rates are set to 1.4 ACH for Zone 2 and 1.7 ACH for Zone 4. In Zone 3 occurs a difference between scheduled and calculated supply airflow. Since relief fans are off, outside airflow is assumed to equal exhaust airflow plus 20%, corresponding to a ventilation rate of 2.68 air changes per hour. For Zone 1 no measurements were taken. Ventilation rate is assumed to be 2.4 based on scheduled exhaust flow rate and

additional 20% relief air. The ventilation rate averaged for the entire building and used in simulations is 2.13 air changes per hour.

Effect of Ventilation on the Building Energy Balance

To investigate the effect the ventilation rate has on heating and cooling energy demand for the building, simulations were carried out with ventilation rates ranging between zero and 5 air changes per hour. The results are shown in **Figure 2.3**.

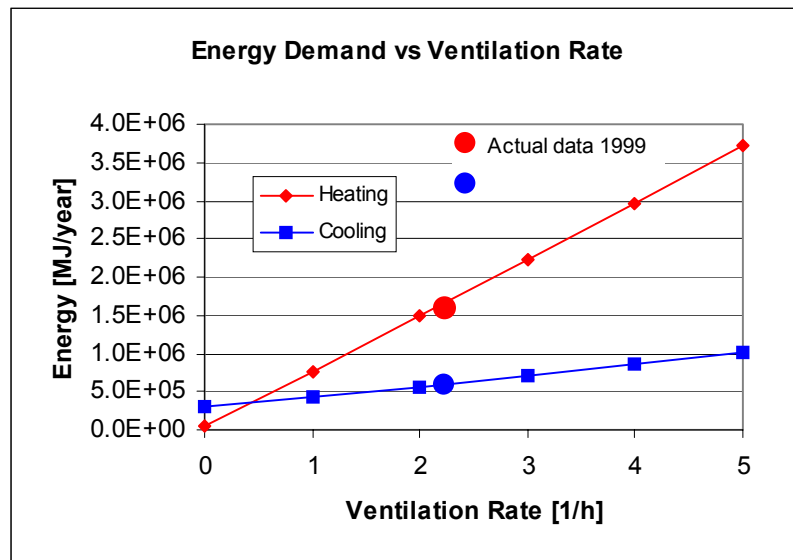


Figure 2.3: Yearly heating and cooling energy consumption for different ventilation rates for 1999 weather data.

Correlations of the simulation data yield the following equations (2.2) and (2.3) for the annually heating respectively cooling energy demand in MJ as functions of ventilation rate VR for the year 1999:

$$E_{heat} = 51329 + 710650 VR + 4533 VR^2 \quad (2.2)$$

$$E_{cool} = 314453 + 108257 VR + 6879 VR^2 \quad (2.3)$$

When solving Equations (2.2) and (2.3) using actual heating and cooling energy consumption, the resulting ventilation rates are 2.16, 2.13, respectively. These values agree well with the assumed average ventilation rate of 2.13.

Furthermore, the results for actual ventilation rate show that the major part of the heating energy consumption, 96%, is used to heat the ventilation air. The impact of the ventilation rate on the cooling energy demand is smaller. A part of the cooling energy is used to offset internal gains; this part is constant over the ventilation rate and accounts for about 54% of the energy. The other 46% are used to cool and dehumidify the ventilation air.

Infiltration

Uncontrolled ventilation caused by pressure differences between indoor and outdoors through open doors, windows and leakages in the building envelope is called infiltration. When the building is positively pressurized with respect to the ambient, exfiltration instead of infiltration takes place when conditioned air uncontrolled leaves the building. The effect of infiltration / exfiltration is an increase in space conditioning load due to higher amount of outside air coming in; similar to an increase in ventilation rate, but uncontrolled and often unwanted. Since the Primate House envelope has few windows and is tightly constructed, infiltration occurs mainly through doors. The infiltration settings for simulation are the following:

- Zone 1: 0.2 air changes per hour.
- Zone 2 and 3: 0.3 air changes per hour from 8 AM until 5 PM, when keepers are present, 0.1 during the night.
- Zone 4: 0.5 air changes per hour from 10 AM until 5 PM, when visitors are present, and 0.1 during the night.

In the TRNSYS Type 56 model, infiltration is modeled as a heat- and moisture gain depending on inside and outside temperatures and infiltration air mass flow.

Suggestions to Improve IAQ

IAQ in the Primate House is not acceptable in general; air change rates are too low in all zones.

Air change rates in the visitor area are not in accordance with ASHRAE Standard 62 [6], the minimum outdoor air requirement for the visitor area Zone 4 is 15 cfm per person or 8 l/s per person. Recommended minimum ventilation rate in accordance to the Wisconsin Department of Commerce Chapter Comm 64.05 “Inside Design Temperatures and Ventilation Requirements” is two air changes per hour. Actual air change rate in Zone 4 is only about 1.6 per hour or 1600 m³/h. That is sufficient for up to 55 persons according to ASHRAE Standard 62, but does not agree with Chapter Comm 64.05. Considering the unpleasant odor in the visitor area, an increase in the ventilation rate to three air changes per hour is suggested. Positive pressure in Zone 4 with respect to animal areas to avoid infiltration from Zone 3, would also lead to better IAQ. However, it would also have the effect that air from the visitor zone potentially containing harmful microorganisms could enter the animal cages.

Minimum ventilation in the basement Zone 2 is only 1.4 air changes per hour and this Zone too does not fulfill criteria of odorless fresh air. Recommendation from “Guide for the Care and Use of Laboratory Animals” [16] is 10 to 15 air changes per hour in non-human primate cages. Considering that the area of the cages is only about half of the total area of the zone, and that usually not all cages at a time are occupied, an increase to 3 air changes per hour is suggested. The same applies for Zone 3, the ventilation rate of 2.6 is too low and increasing to at least three air changes per hour would result in better IAQ in the zone.

The ventilation rate in Zone 1 is 2.4 air changes per hour. The low temperature in this zone coupled with the water used for cleaning and added by the animals results in high relative humidity. Increased ventilation rate would lead to dryer climate, and may also reduce

dehumidification demand. Since the tigers and lions spend most of the day in outside cages, an air change rate according to actual occupation schedule would be an option, unless the cleaning would require high ventilation to dry the floors. Also for this Zone, an increase in ventilation rate to three air changes per hour is suggested.

The enhanced ventilation rates in all zones could be technically made possible by opening and adjustment of intake air dampers and relief air dampers; no major changes at fans or ductwork would be necessary. The supply air fans are capable of handling larger volumes since the systems are designed to run with relief air and higher outside air fractions.

Chapter 3 Indoor Humidity

Introduction

Achieving humidity control in indoor environments is an important facet of indoor environmental quality. In the context of the Vilas Zoo Primate House, indoor air humidity affects both the comfort of humans (staff and visitors) and animals (primates and large cats). In situations where the indoor air is too dry, both humans and animals will experience symptoms of discomfort that span from dry skin to respiratory irritation. When the air is too humid, the probability of microbial growth substantially rises along with increased likelihood of building material deterioration.

ASHRAE has developed a thermal comfort standard (ASHRAE Standard 55-1992, [19]) that identifies temperature and humidity conditions that will satisfy 80% or more of building occupants. Standard 55-1992 recommends that relative humidity be maintained in a range between 30 – 60%. The risk of mold growth for relative humidity not higher than 60% is low and statistically 80% of all people feel comfortable at these humidity levels for normal room temperatures and normal grades of activity. Since the Primate House occupants also include animals, additional considerations must be included in establishing recommended ranges of humidity control for this facilities' mixed use. For primates, the National Institutes of Health recommends in their "Guide for the Care and Use of Laboratory Animals" [16] that the relative humidity be controlled in the range between 30 – 70%. Although many primates are exposed to higher humidity conditions in their natural habitat, such high humidity in a built environment is not attainable; consequently, we must rely on the animal's ability to adapt themselves to a wider range of lower humidity conditions. To minimize mold growth and meet human comfort requirements, a reasonable goal would be to maintain the space relative humidity in a range between 30 – 60%, as suggested by ASHRAE.

Without active humidification or dehumidification systems, the actual humidity level achieved in a ventilated building will depend on the outside air humidity, ventilation rate, and rate of moisture generation within the space. During wintertime operation, humidification is

required to counter the effects of low moisture contents of outdoor air, drying the indoor spaces. The humidity ratio of the air in ventilated buildings that do not utilize humidification systems in the winter tends to follow the humidity ratio of the outdoor air. However, in case of humidity gains or active humidification, care must be exercised to avoid too high levels of relative humidity during wintertime since the probability of condensation on cold surfaces (fenestration systems, exposed beams, etc.) increases dramatically.

During summertime operation, equipment must be in place and operated to dehumidify warm and moist outdoor air in order to maintain space humidity levels below 60%. The most common approach for humidity control during the summertime is by operation of refrigerant-based air-conditioning systems to accomplish temperature control directly and humidity control indirectly by condensing excess moisture from the supply air stream.

Characterizing Humidity in the Primate House – Existing Situation

Sources of moisture gains for the primate house are listed in **Table 3.1**. Note that visitors have the greatest potential for contributing moisture to the space but that moisture addition only occurs in during the day between 10 AM to 5 PM. In addition, the total moisture added depends on the actual number of visitors and their duration in the building. Moisture gains from the primates are assumed constant with time. The tigers and lions are adding humidity from 5 PM to 10 AM since they spend the day in their outside cages.

Moisture gains in the primate house are listed in **Table 3.1**, most moisture is added by the visitors, but only in the time of 10 AM to 5 PM and depending on the actual number, while the moisture gain of the monkeys is assumed to be the same 24 h a day. The tigers and lions are adding humidity only from 5 PM to 10 AM, they spend the day in their outside cages. Moisture gains of the animals are calculated under the assumption of a latent heat ratio of 0.33 of the average total heat gain (see also chapter internal gains).

Gain type / Individual	Added Moisture [kg/h]	No. of Individuals	Zone
Visitor	0.11 ¹	20	4
Keeper	0.19 ¹	2	2, 3
Orangutan	0.15	6	2, 3
Chimpanzee	0.125	5	2, 3
Tiger / Lion	0.15	7	1
Gibbon / Colobus / Lemur	0.02	14	2, 3

Table 3.1: Internal moisture gains in the primate house. ¹) according to ISO Standard 7730

Presented in **Figure 3.1** are measured and simulated humidity ratios in the basement Zone 2 for the time of February 1 – 8, 2002. The variable ω_{Error} denotes the difference between measurement and simulation. In this case, it can be seen that the simulated and measured humidity ratios are close to the outside humidity ratio. Two conclusions can be drawn from this information. First, the humidification system at the Primate House does not appear to be active, this conclusion was later validated by a site survey. Second, the effect of internal moisture gain is small as observed by the small difference between ω_{measured} and ω_{outside} . Finally, the phase shift between the measured and outside air humidity ratios is indicative of moisture buffering in the building. Virtually all building simulation/analysis programs neglect moisture capacitance in their models; however, moisture can be stored in absorptive plaster, concrete walls and building furnishings. The relative error $\omega_{\text{Error}} / \omega_{\text{measured}}$ is maximal 14 %, a value that validates the simulation results as not far off, considering the uncertainties of measurements, especially for the outside humidity which was measured miles away.

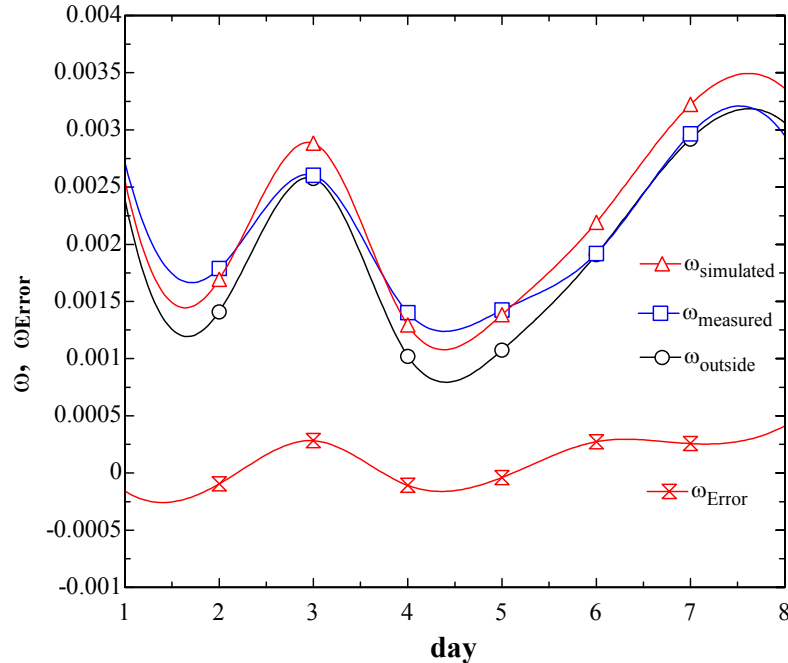


Figure 3.1: Measured and simulated humidity ratios and absolute error for the basement Zone 2 for February 1 – 8 2002 measured at 1AM

The rate of internal moisture gain in Zone 2 during the night without human activity is estimated to be 0.59 kg/h. This gain results in an internal zone average humidity ratio of 0.00023 kg water/kg dry air according to measured data during the time of February 1 - 8. Assumed in the simulation is a moisture gain of 0.74 kg/h or 0.00028 kg water/kg dry air due to the animals. During the day, humidity in the Primate House typically rises. The rise in humidity is caused by a higher outside humidity ratios as well as human activity, for example, the keeper adds moisture at a rate of ca. 0.191 kg/h, and the cages and floors in the basement are regularly cleaned with a water hose. Daily peaks can be seen on relative humidity plots of data collected on-site with automatic data loggers. Analyzing the humidity data shows that the cleaning in Zone 2 increases relative humidity by an average 13.9% for a time of one hour usually between 10 AM and 11 AM on a weekday basis. 13.9% relative humidity increase corresponds to an increase in humidity ratio of 0.0023. With a zone volume of 1440 m³ and assuming 1.5 air changes per hour, a total of 5.9 kg of water has to be evaporated to the zone air during one hour to yield the measured increase in zone humidity.

The effect of moisture gains in a conditioned space on the HVAC system is a decrease in humidification demand and an increase in latent cooling coil load when relative space humidity reaches the dehumidifying set point, i.e. on warm and humid days. Since the moisture gains as illustrated in **Figure 3.1** are small compared to outside air humidity, the affect of these gains on the coil load is small. The following example may demonstrate the effects of increased moisture gains during the time of cleaning.

The humidity ratio of the air due to moisture added during cleaning is about one order of magnitude lower than the outside humidity ratio on a hot and humid day (0.002 vs. 0.02). Assuming an outside air fraction $f_{OA} = 0.25$, an outside humidity ratio of 0.02 and an inside set point of 71°F (21.7°C) and 50% RH which corresponds to a humidity ratio of 0.008, the moisture difference to be extracted from the supply air equals 0.00471 kg water per kg dry air. Of the total value of 0.00471, 0.003 is due to humidity brought in with outside air, 0.00021 is due to internal gains and 0.0015 is attributable to cleaning. In this case internal moisture gains account for 39% of the latent load. Without moisture added by cleaning only 0.00321 kg water per kg dry air have to be removed, only 9% of this is caused by internal gains and the load on the cooling coil is 32% lower.

In view of the fact that the humidity rise due to cleaning activity only lasts for about an hour and then only affects the HVAC system in dehumidifying mode, its consequence on the overall building energy balance can be considered to be negligible. Nonetheless, it can have a significant impact on the peak cooling coil load during certain times and hence is included in the simulations.

With higher ventilation rates, the effect of internal moisture gains decreases, since more air is exhausted, while less moisture containing return air is mixed to supply air. The latent cooling coil load then is solely depending on the outside humidity.

In Zone 3 on the first floor moisture gains are higher than in the basement, but zone volume, outside air fraction f_{OA} and ventilation rate are higher too, effects of internal gains are very small. An analysis of the logged data shows no significant increase due to cleaning.

Humidity in Zone 1 mostly follows outside humidity similar to Zone 2. Small internal gains occur during evening and over night, when animals are present. During the day, relative humidity jumps up 50% for about one hour when the floor and the cages are cleaned around 11 AM. This is equivalent to a moisture gain of ca. 8.6 kg/h and is included in the simulations.

During wintertime, the average relative humidity in Zones 2, 3 and 4 is about 16 %. This is well below the recommended value of at least 30 %. Although humidification equipment is installed, it was not running in winter 2001 / 2002 when the measurements were taken. The colder Zone 1 has an average relative humidity of 40 %, a reasonable value, but shows large fluctuations between 20 % and up to 100 % during cleaning.

Humidification Mode Limitation: Condensation

Condensation is the most frequent factor limiting the maximum allowable indoor air relative humidity during wintertime operation. As the relative humidity of indoor air increases, condensation of moisture will occur on any indoor air surface with a temperature below the indoor air dew point temperature. Condensation has a number of undesirable effects including: providing a moisture source that contributes to mold and fungal growth and deterioration of building materials. Locations in buildings where condensation most often occurs are fenestration systems since their insulating values tend to be low, leading to cold interior surfaces. As the outdoor air temperature decreases, these indoor air surface temperatures decrease. With decreasing interior surface temperatures, the relative humidity of indoor air must also decrease to maintain the indoor air dew point temperature lower than the lowest interior surface temperature.

To estimate the maximum relative humidity that can be maintained in the wintertime without condensation, the least insulated inside surface temperatures as function of outdoor and indoor temperature are calculated and compared to the dew point of the indoor air. These

surfaces are in the Primate House the 1.5” laminated glass windows of the cages in Zone 3, with a U-value of $26 \text{ W/m}^2\text{K}$, and convection coefficients of $h_i = 7.2 \text{ W/m}^2\text{K}$ at the inside and $h_o = 29 \text{ W/m}^2\text{K}$ at the outside for winter conditions (values according to ASHRAE Fundamentals, [9]). **Figure 3.2** shows the maximum allowable relative humidity in Zone 3 as a function of outdoor temperature over a range of indoor temperatures:

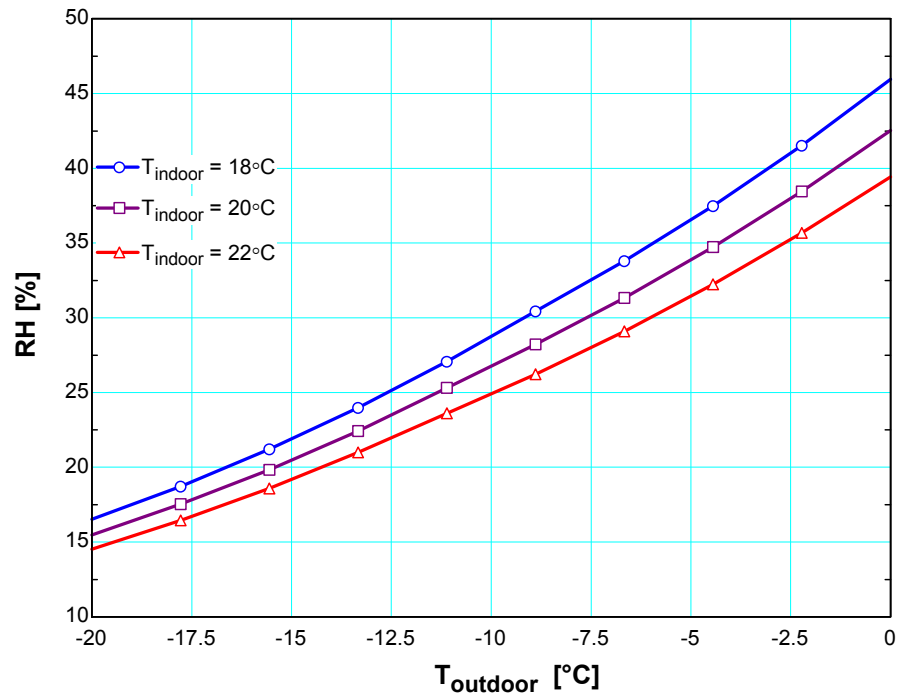


Figure 3.2: Maximal relative humidity in the Primate House to prevent condensation on windows in Zone 3

As one would expect, decreasing the indoor air set point temperature allows the maximum allowable relative humidity to increase.

Humidification System: Existing Situation and Recommendations

The humidification system in the Primate House includes humidifiers for the air-handling units for Zone 1, 2 and 3. These humidifiers are electric resistance heaters, generating steam under atmospheric pressure that will be diffused into the supply air duct. The respective humidification capacities of Zones 1, 2, and 3 are 12, 24 and 70 lbs of steam per hour, or 6.9, 10.3 and 27.5 kW electric power, respectively. In all cases, the humidification systems for each zone are sized to meet the highest moisture demand in winter to ensure at least 25% RH in Zone 3 under the current ventilation rate of 2.68 air changes per hour. A humidity sensor downstream in the duct measures the relative humidity and activates the humidification system controller. Humidity and temperature measured with automatic data loggers over two months during the winter are plotted in **Figure 3.3 - Figure 3.5**. It is obvious, that the average relative humidity is very low and it follows the outside temperature curve. It is evident that, while the indoor temperature is basically constant, the indoor air relative humidity is directly depending on the outdoor humidity, and it can be concluded that the humidification equipment was not operated during this time. However, daily peaks up to 100% RH in Zone 1 indicate the water evaporated during cleaning and providing some very limited humidification within the zone. Zone 1 has the lowest temperature, hence the highest relative humidity of averagely ca. 30%, Zone 2, 3 and 4 operate significantly dryer with average relative humidities of ca. 15%. These zones, in particular, require active humidification to meet the recommendations for the minimum relative humidity of 30%.

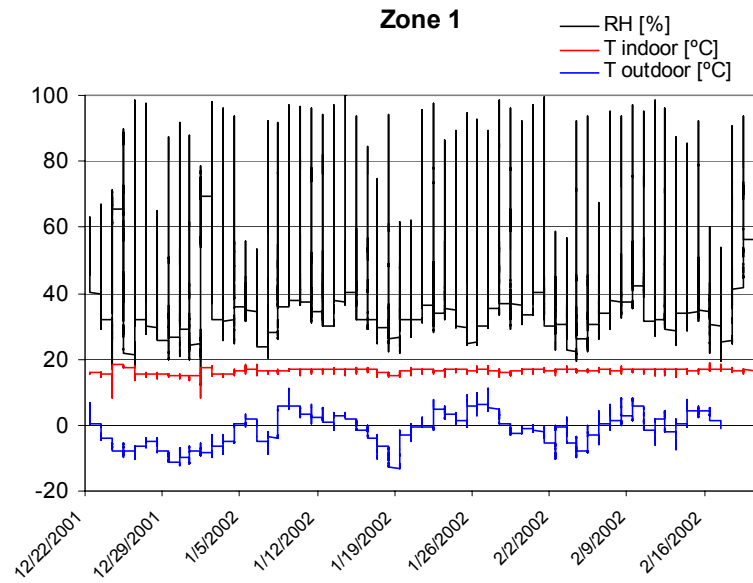


Figure 3.3: Temperature and humidity in Zone 1 measured from 12/22/01 to 2/20/02

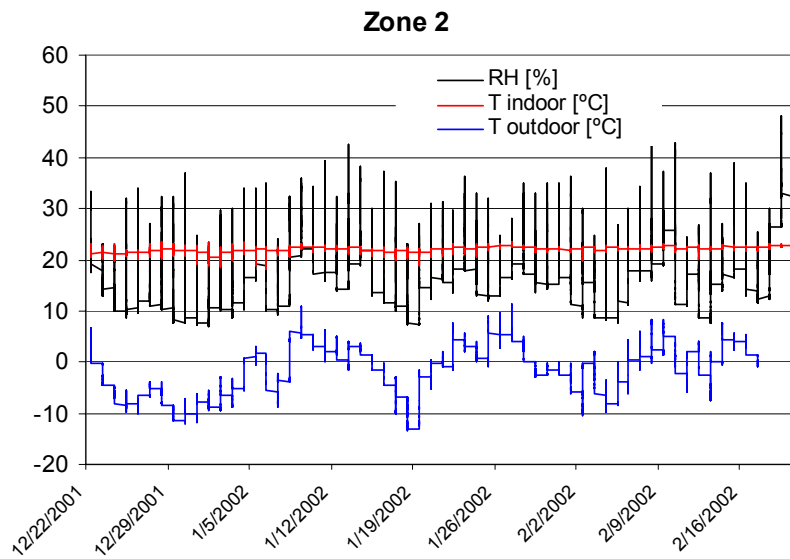


Figure 3.4: Temperature and humidity in Zone 2 measured from 12/22/01 to 2/20/02

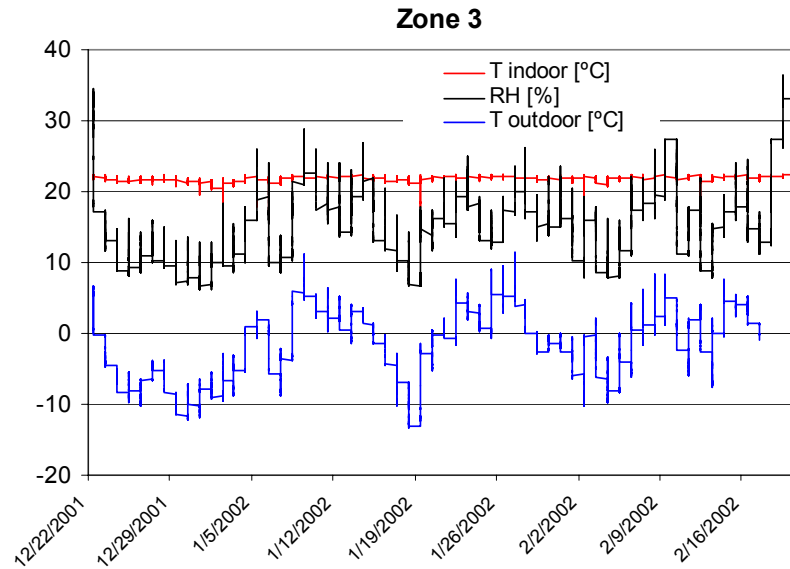


Figure 3.5: Temperature and humidity in Zone 3 measured from 12/22/01 to 2/20/02

The energy required to humidify the building with electric fueled steam humidifiers to reach a minimum of 30% relative humidity can be estimated based on hourly building simulation results. The calculation is accomplished by the following procedure: the difference Δw of simulated humidity ratio and the humidity ratio corresponding to 30% RH in the zone is multiplied with the ventilation air flow and the enthalpy of vaporization h_{fg} of the water in the humidifier (3.1):

$$\dot{E} = \dot{m}_{air} \Delta w h_{fg} \quad (3.1)$$

The integral over the energy of each time step over the year 1999 results in 65,300 kWh, assuming a price of electricity of \$0.0478/kWh [MG&E, 2002], this would sum up to \$3,121 for the Zones 2 and 3.

At this point, the recommendation to increase IAQ during the winter is to operate the humidifiers in the Zones 2 and 3 to ensure a minimum relative humidity of 30%, unless the outdoor air is extreme cold, then switch back to lower humidity levels of about 20% to

reduce condensation and energy consumption. For Zone 4, no humidification equipment is currently installed. Considering that visitors normally spend only a short time here, it may not be necessary to invest in equipment and spend about \$1,000 or 13,000kWh for humidification.

The application of enthalpy exchangers would mitigate the problem of low humidity and significantly reduce the amount of energy needed for humidification in the winter since humidity from the exhaust stream would be transferred into the intake stream.

Dehumidification System: Existing Situation and Recommendations

The dehumidification system in the Primate House consists of cooling and dehumidification coils in each air handling unit. These coils are finned tube direct expansion coils operating with refrigerant R22. The capacities of the air-cooled condensing units are:

1. 22kW / 7.5ton
2. 50kW / 15ton
3. 138kW / 40ton
4. 50kW / 15ton

The control schedule of the cooling equipment activates the condensing units when the return air temperature rises above the cooling set point (approximately 23°C for Zones 2, 3 and 4) or return air relative humidity exceeds a predetermined set point. **Figure 3.6** shows the relative humidity and temperature of the supply air stream in Zone 3 over a period of three days in 10-minute time steps. It can be seen, as the cooling coil is cycled on and off, the leaving supply air temperature fluctuates between 15-17°C when equipment is on and up to 23°C when the coil is off. The maximal relative humidity in the space at 23°C when supply air relative humidity approaches 100% at 16°C during dehumidification is 60%. However, on some very humid days, outdoor state 27°C, 76% RH, the data show that supply air becomes saturated at temperatures of about 20°C.

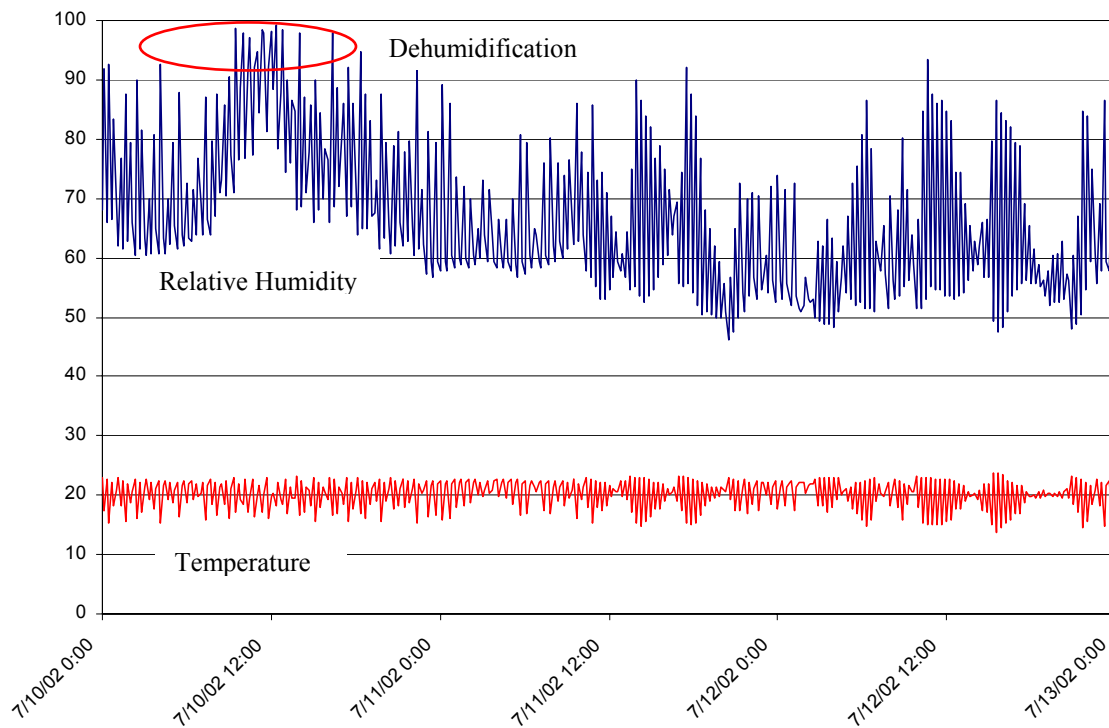


Figure 3.6: Typical summer conditions of supply air relative humidity and temperature measured in Zone 3

To maintain the space at temperature no lower than 23°C, the equipment will cycle on and off and supply air of averagely 21°C and nearly 100% RH. This operation will lead to space relative humidity of up to 90% for short time periods, it is concluded that the humidity control at least during the time of these measurements did not operate as intended. Supply air temperatures would have to be lower in order to reduce humidity, without supply air reheat the indoor set point of 23°C cannot be reached when maintaining relative humidity below 60% under these conditions. Another problem occurring during part load operation is re-evaporation of condensed moisture from the coils when the condenser remains in the off-cycle. Re-evaporation will increase the humidity in the supply air stream and cause unwanted high relative humidity in the space. The re-evaporation can be concluded from measured data, **Figure 3.7**, when relative humidity stays high and decays over a few time steps after

supply air temperature jumps up 4-5 K when the coils shut off, as shown in the psychrometric chart **Figure 3.8**.

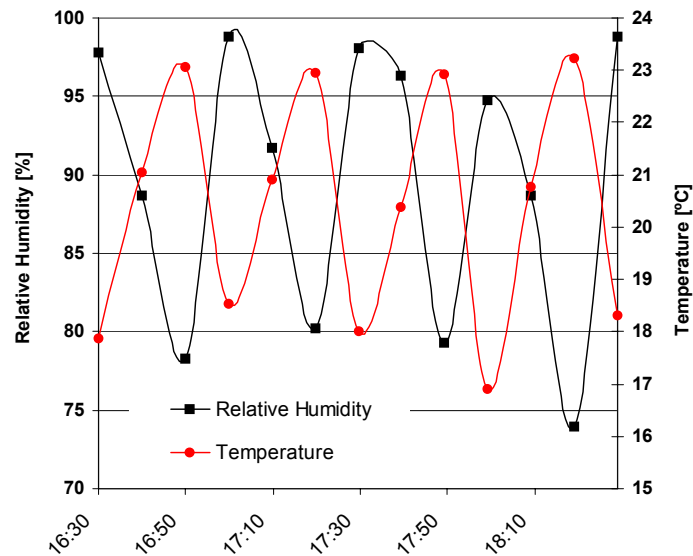


Figure 3.7: Supply air conditions of Zone 3 on June 19 2002

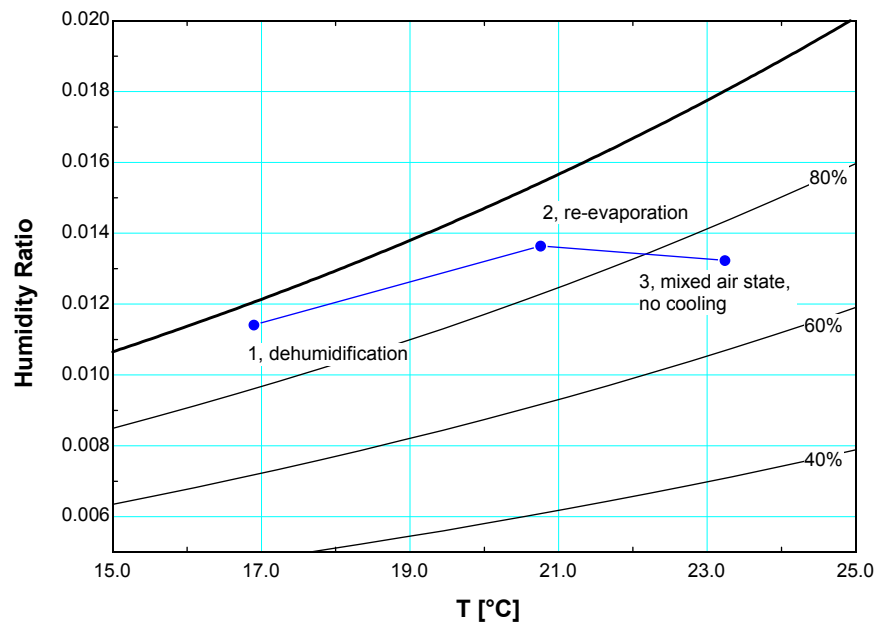


Figure 3.8: psychrometric chart representing three supply air states for Zone 3 on 6/19/02 18:00 – 18:20h. Outdoor state is 22.5°C, 78.3%, space state is 23°C, RH rising from 65 to 75% after cycling off the coil, re-evaporation of moisture takes place (2), until supply air reaches state 3, where humidity level equals combination of outdoor and indoor humidity for an outside air fraction of 0.6.

A method to maintain the space at the desired temperature without exceeding reasonable limits of relative humidity on humid days is to lower the supply air temperature when exceeding space humidity set point and either reheat with booster coils or lower the space temperature set point. A control strategy, which overrides the temperature control when return air humidity level becomes higher than 60%, is suggested. This should be applicable with installed equipment according to the HVAC schedule. In this case, the required supply air temperature to (neglecting internal moisture gains) would be not higher than 15°C for a space temperature of 23°C and 60% RH. Depending on outside temperatures, solar irradiance and internal heat gains, the inside temperature may drop below 23°C, leading then to higher relative space humidity and requiring even lower supply air temperature to maintain maximal relative humidity.

A better way to achieve humidity control without overcooling the building or the need of reheat would be to dehumidify only the outdoor air instead of the mixed air stream of return and outdoor air. The flow rate of outdoor air is lower than the mixed air flow rate, lower temperatures and hence higher dehumidification of the intake air stream could be achieved with the same amount of cooling energy but higher mixed air temperatures. However, this solution would require rearrangements of coils, ductwork, piping and controls.

Calibration of the Data Loggers

The data loggers used to measure temperature and humidity over periods up to 3 months in the Primate House in five-minute time steps were Hobo H8 Pro Series made by Onset Computer Corp. In order to compare the accuracy of the data loggers, they were put in a glass container with controlled humidity. Humidity control was achieved by giving a saturated aqueous salt solution into the closed container. Saturated solutions of hygroscopic salts have the capacity of maintaining a characteristic level of relative humidity due to absorption and desorption of moisture. **Table 3.2** lists the relative humidity achieved with different salts after reaching equilibrium state in an enclosed volume at 25°C:

Salt	RH
Lithium Chloride	11%
Magnesium Chloride	33%
Potassium Carbonate	43%
Sodium Bromide	58%
Sodium Chloride	75%

Table 3.2: Equilibrium relative humidity values at 25°C for salt solutions used in isotherm experiments from Greenspan (1977).

Figure 3.9 shows a plot of relative humidity and temperature measurements of six identical data loggers. The loggers were kept in a chamber with saturated magnesium chloride solution for five days. Equilibrium is reached after about one day, and then the relative humidity inversely follows the temperature fluctuations. The measured temperatures are in tolerance of 1K or less than 1% of the normal temperature range; the humidities measured with different loggers vary within 2%, suggesting that uncertainties of humidity measurements are higher than for temperatures. A similar experiment has been carried out with a sodium chloride solution, having similar results at a relative humidity of 75%. It is concluded, that the data obtained with different data loggers is sufficiently consistent and accurate to be used to study and simulate the indoor climate in the Primate House.

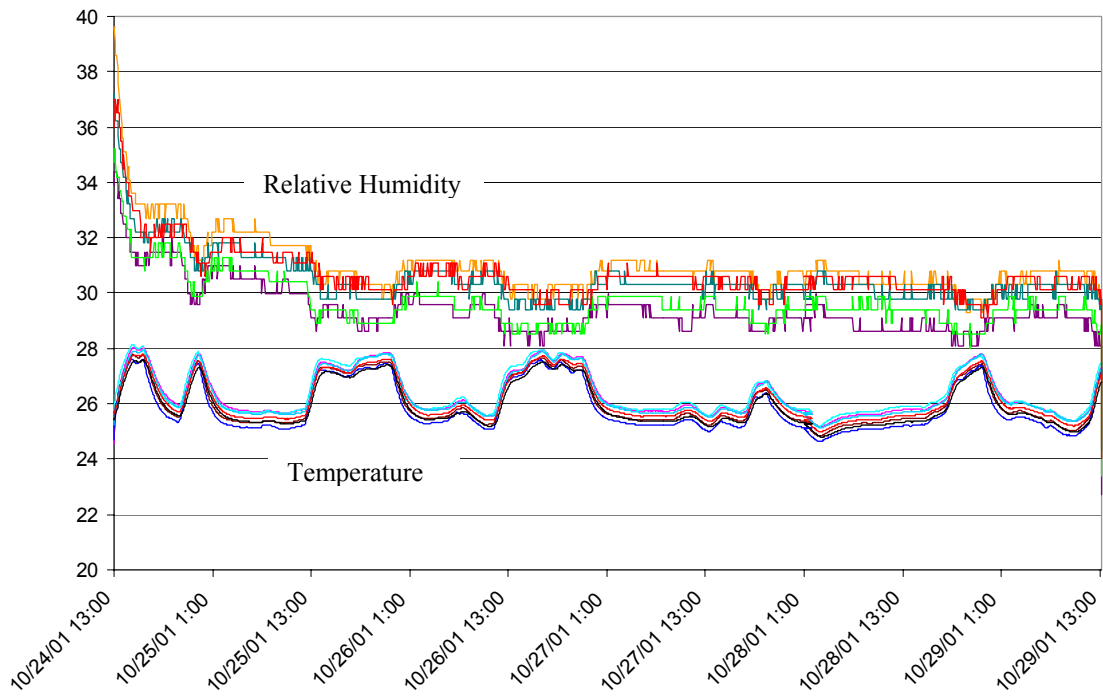


Figure 3.9: Relative humidity and Temperature measured with seven data loggers in MgCl controlled climate

Chapter 4 Enthalpy Exchangers

Introduction

Enthalpy exchangers used in HVAC applications are rotary regenerative heat and mass exchangers. These devices can reduce air-conditioning costs for sensible heating and cooling as well as for removing or adding humidity by recovering latent energy from the exhaust air and transferring it to the ventilation air stream entering the building. Using energy recovery systems in HVAC applications can significantly reduce energy consumption and costs by utilizing otherwise wasted energy from exhaust air. In addition, occupant comfort could benefit from increased ventilation rates and thus better indoor air quality (IAQ) without high operation cost premiums. Since heating and cooling loads due to preconditioned ventilation air decrease, downsizing of HVAC systems is possible, leading to additional savings by lower HVAC equipment capital cost. Considering the number of HVAC systems and the amount of energy currently needed for ventilation air heating and conditioning, the wide use of enthalpy exchangers can have a significant impact in reducing energy consumption.

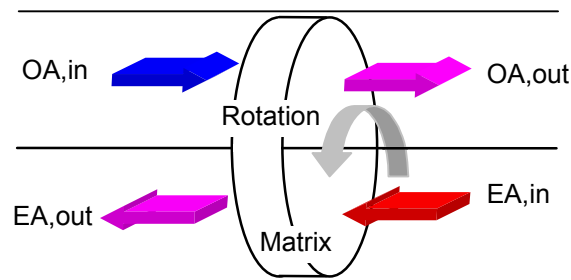


Figure 4.1: Schematic of a rotary enthalpy exchanger, OA = outside air, EA = exhaust air.

A rotary heat exchanger is a regenerative heat exchanger, which, in contrast to a recuperator, operates intermittently between a hot and a cold fluid. A wheel rotates between two separated fluid ducts such that each fluid passes axially through one half of the wheel. The fluids flow in opposite directions; a rotary heat exchanger can be considered a counterflow heat exchanger. The wheel is cylindrical and has numerous very small parallel passages for the

fluids with a preferably large surface area. The wheel matrix is made of either desiccant coated aluminum foil or a polymer membrane containing a desiccant substance such as silica gel, a molecular sieve or lithium chloride. In the hub of the wheel is an axis fixed in bearings. The wheel is driven via a belt with an electric motor.

To predict energy consumption of buildings for heating and cooling, calculations and computer simulations are carried out using models of buildings and HVAC equipment. To investigate the effect and saving potential of enthalpy exchangers in HVAC systems, a model has to be created that shows the same behavior as the actual equipment i.e. delivers the same outputs for the same inputs. For example, given the temperature and humidity of outside air and exhaust air, the enthalpy exchanger model should predict the temperature and humidity values of the two leaving air streams as outputs.

As a preface to developing the computer model, two different rotary enthalpy exchangers were studied in detail. One was made of corrugated aluminum coated with a layer of a hygroscopic polymer; the other one was constructed of polystyrene coated with a silica gel. The computer model of the enthalpy exchanger was created as a component to be used in the transient simulation program TRNSYS in order to simulate the HVAC system. Input and outputs of the model are the intake and exhaust airflow rates temperatures and humidities. The focus for calculating the performance is on determining the number of transfer units (NTU) for heat and mass transfer and exchanger effectiveness for sensible heat and for humidity. To model the thermodynamic behavior, convective heat transfer coefficients and adsorption potential of the surface were analyzed. Four coupled hyperbolic differential equations were obtained, and based on numerical solutions of these equations, simplified equations were developed to describe effectiveness as a function of input parameters including rotation speed. Comparisons of results yielded by the computer model based on those simplified equations and experimental data obtained from manufacturers showed excellent agreement for one of the analyzed geometries (Carnes). However, calculations for the other enthalpy exchanger design (Airxchange) demonstrated that this method of analysis could not be generalized. A new simulation model to predict the performance of enthalpy

exchangers and make predictions of energy savings feasible has been developed. The model is based on general equations and experimental reference data.

Psychrometrics of Enthalpy Exchange

Enthalpy exchange operation during the heating season means that cold and dry outside air enters the exchangers on one side, drying and cooling the exchange matrix while warming and increasing in humidity. On the other side, warm and humid indoor air from the exhaust stream enters the exchanger, warming the matrix and humidifying the desiccant material coated on the matrix. In the cooling season this situation is reversed: warm outside air is cooled and dehumidified, while cooler and drier inside air from the exhaust regenerates and cools the matrix.

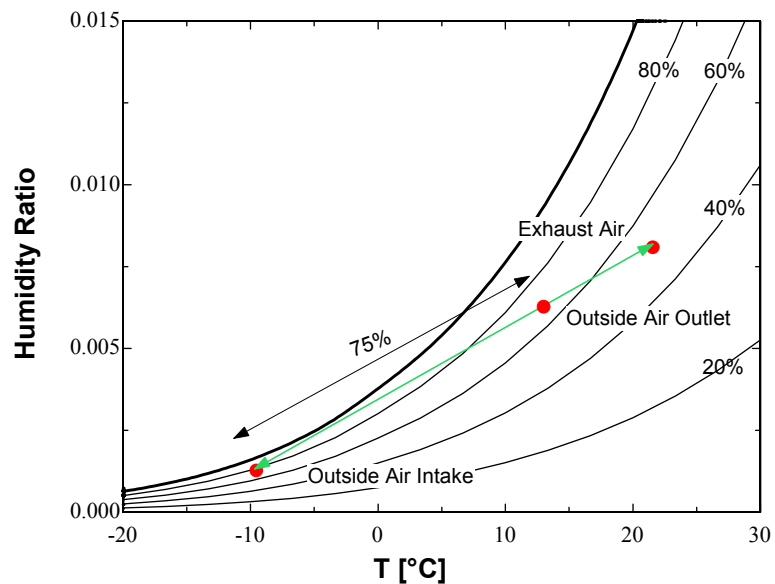


Figure 4.2: Psychrometric chart representing state points of outside air and exhaust air during heating mode operation. Outside air is -10°C , 80% RH, inside conditions are 21°C , 50% RH. Ventilation air outlet state is 13°C , 65% RH. Effectiveness of the enthalpy exchanger is 75%.

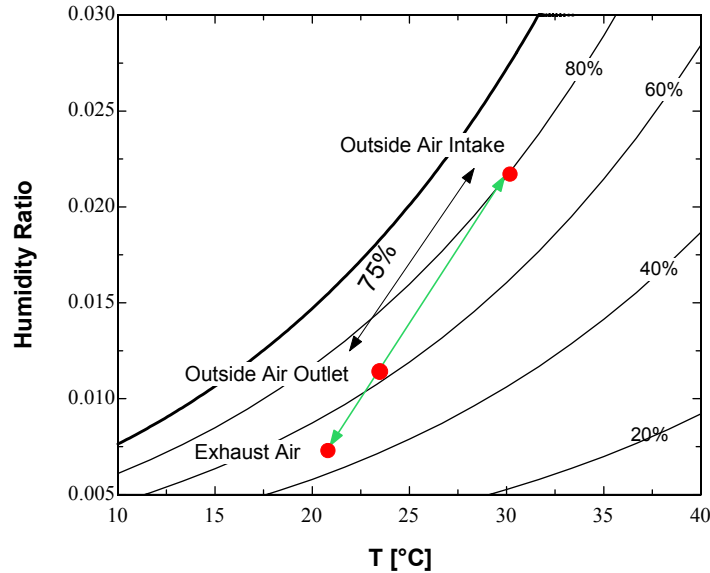


Figure 4.3: Psychrometric chart representing state points of outside air and exhaust air during cooling mode operation. Outside air is 30°C, 80% RH, inside conditions are 21°C, 50% RH. Ventilation air outlet state is 23°C, 62% RH. Effectiveness of the enthalpy exchanger is 75%.

As shown in **Figure 4.2** and **Figure 4.3**, leaving air state points on a psychrometric chart are on a straight line between outside and exhaust air states, assuming a Lewis number of unity and sufficient rotation speed [2, 4, 23]. The Lewis number is the ratio of mass and heat transfer NTU's. For an ideal enthalpy exchanger with balanced flow the thermodynamic state of the leaving fluid and the entering fluid would be the same, hence effectiveness would be unity.

If the line connecting the entering outside air and exhaust air states intersects the saturation curve, condensation can occur. If this happens at temperatures below freezing, ice crystals may accumulate in the channels of the enthalpy exchanger matrix, increase the pressure drop or block the air flow, interrupting ventilation. The temperature below which freezing can occur depends on the exhaust air relative humidity and is typically in the range of -25°C to -10°C .

There are two strategies for preventing an enthalpy exchanger wheel from freezing:

- Decrease rotation speed of the wheel

- Preheat of the outside air at the intake

Lowering the rotation speed causes a sharp drop in latent effectiveness due to the effects of intermittent flow: higher matrix temperatures on the exhaust side causes the relative humidity to be lower and lower temperatures on the intake side leading to higher relative humidity of the air in the matrix. Both results in a lower humidity gradient between matrix and air, thereby reduces the driving force of moisture transfer. Very low rotation speed also allows defrosting and evaporating of water of the surface in the warm exhaust air stream. This strategy reduces the sensible and latent effectiveness significantly. Since this would happen right when energy recovery is most needed to reduce heating power, heaters would have to be oversized to meet the full winter load without recovery. This solution is neither economical, nor does it conserve much energy during cold winter days when consumption is the highest. A more efficient way to inhibit frost is to heat the air in the intake section with an additional coil, fueled electrically or by hot water. The enthalpy wheel then operates under optimal effectiveness only reduced by a part of the amount of heat added by the preheater (Figure 4.4).

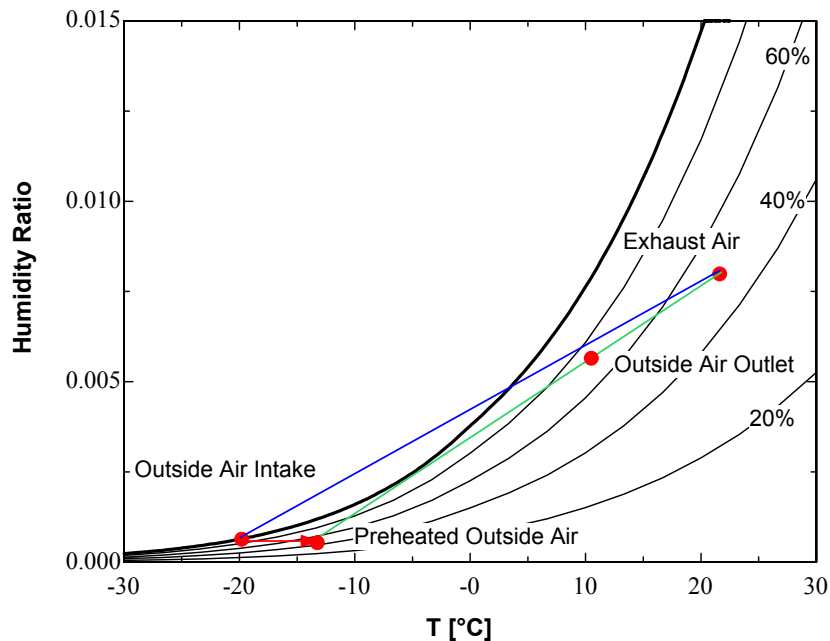


Figure 4.4: Intersected saturation curve, frost buildup likely. The arrow indicates the heat added by the preheater.

A comparison of the two frost control strategies is shown in **Figure 4.5**. The energy is the additional heating energy required to prevent the wheel from frosting for the preheat case, and the required additional energy to heat and humidify the air to the same outlet state as for the preheat case for the slowed down wheel. Exhaust air state is constant 21°C, 50% RH, outside air has a relative humidity of 80%, temperature varying from -25°C to -11°C, above where no frost control is required. The data used in this simulation are correlated from experimental manufacturer's data, sensible and latent effectiveness of this enthalpy exchanger at maximum speed is 0.714.

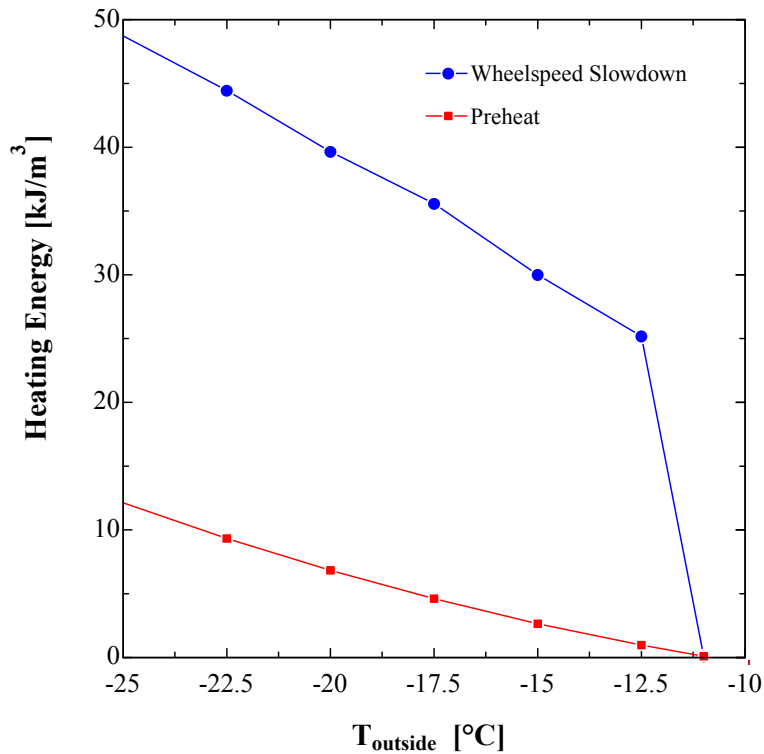


Figure 4.5: Comparison of wheel speed slow down versus preheat for frost control

Transfer Mechanism and Governing Equations

Regenerative exchangers transfer heat and mass periodically from one air stream to another. During the first period, heat and moisture is transported from one stream to a solid matrix and during the second period from the matrix to the other stream. The dominant heat transfer mechanism is convection; mass is transferred in combination with phase change at the matrix surface: condensation -evaporation or adsorption –desorption.

The two fluid streams considered primary are assumed to have equal heat capacity rates. A simplification justified by the fact that property variations between exhaust air (EA) and outside air (OA) are negligible, and mass flow rates are equal.

Rotary enthalpy exchangers have been found to have similar characteristics as direct transfer counterflow heat exchangers [3] under certain conditions. The following definitions of effectiveness for heat and mass transfer, respectively, will be used:

$$\mathcal{E}_T = \frac{T_{OA, in} - T_{OA, out}}{T_{OA, in} - T_{EA, in}} \quad (4.1)$$

$$\mathcal{E}_w = \frac{W_{OA, in} - W_{OA, out}}{W_{OA, in} - W_{EA, in}} \quad (4.2)$$

Effectiveness, in terms of Number of Transfer Units (NTU) for balanced direct counterflow heat exchanger is defined as:

$$\mathcal{E}_{CFX} = \frac{NTU}{NTU + 1} \quad (4.3)$$

For rotary sensible energy exchanger, the effectiveness is given by Kays and London (1984):

$$\mathcal{E}_T = \frac{NTU}{1 + NTU} \left(1 - \frac{1}{9 * C_r^{*1.93}} \right) \quad (4.4)$$

where C_r^* is the dimensionless wheel capacitance rate, given in [1] as:

$$C_r^* = \frac{MCp_m \omega}{mCp_a} \quad (4.5)$$

The Number of Transfer Units for heat and mass transfer are related by the Lewis Number:

$$Le = \frac{NTU_w}{NTU_T} \quad (4.6)$$

Assuming the Lewis number to be unity [1,2], the temperature and humidity exchange effectiveness become identical. The assumption of a Lewis number on the order of one is based on the comparison of simulation and manufacturers data, as well as the fact that $Le = 1$ leads to the best performance. However, for different enthalpy exchanger designs the Lewis Number varies, mass transfer is often slightly less effective than heat transfer, or $Le < 1$.

A functional analysis yields the common set of equations widely accepted in literature [5, 3, 1] governing the enthalpy exchange:

$$\text{Mass conservation} \quad \frac{\partial w_f}{\partial z} + \frac{M_f \partial w_f}{M_m \partial \tau} + \frac{\partial W_m}{\partial \tau} = 0 \quad (4.7)$$

$$\text{Absorbed water change} \quad \frac{\partial W_m}{\partial \tau} = NTU_w (w_f - w_m) \quad (4.8)$$

$$\text{Energy conservation} \quad \frac{\partial i_f}{\partial z} + \frac{M_f \partial i_f}{M_m \partial \tau} + \frac{\partial I_m}{\partial \tau} = 0 \quad (4.9)$$

$$\text{Matrix enthalpy change} \quad \frac{\partial I_m}{\partial \tau} = NTU_T \frac{\partial i_f}{\partial T_f} (T_f - T_m) + NTU_w i_w (w_f - w_m) \quad (4.10)$$

The following assumptions are made in the development of (4.7) - (4.10):

1. Steady state: after one revolution of the wheel, all air and matrix properties are the same as under initial conditions.
2. Uniform properties of the matrix and both air streams at each axial position over the regenerator.
3. Affect of pressure drop on properties is negligible.
4. Temperature and moisture differences across the matrix surface are negligible, uniform inlet and outlet streams.
5. Heat conduction and vapor diffusion in angular and axial direction are negligible.
6. Carryover of air entrained in the matrix is negligible, estimated about 3% according to [2]
7. The regenerator operation is adiabatic overall.

The coupled partial differential equations have no analytical solution, but have been solved numerically using the computer program MOSHMX [5, 2]. Solutions for various temperature and humidity conditions and different rotation speeds exist in the literature [2, 4]. Based on these solutions, curve fits have been prepared [4] in the form of:

$$\varepsilon_i = \frac{NTU}{NTU + 1} \left(1 - \exp \left[a\Gamma^3 + b\Gamma^2 + c\Gamma \right] \right) \quad (4.11)$$

where Γ is the mass flow rate ratio $M_m S / m_{air}$. a, b, c are curve fit coefficients.

Comparing the functional values of the curve fit to MOSHMX generated data points results in the graph shown in **Figure 4.6** [2].

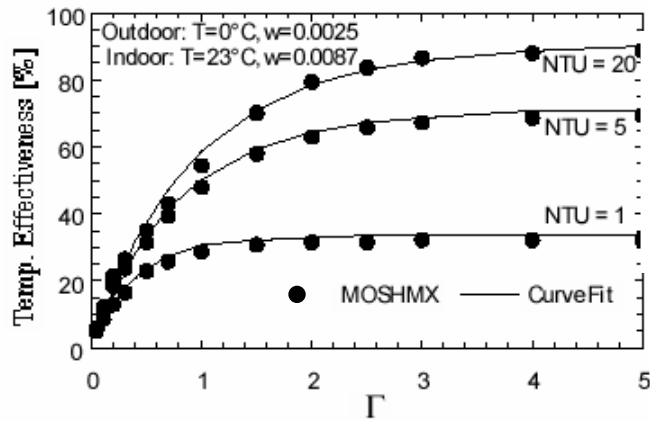


Figure 4.6: Effectiveness curves over mass flow rate ratio Γ for different NTU [2]

As Γ increases, i.e. higher rotational speed, the changes in the matrix states over time from one period to the other are getting smaller, while effectiveness reaches its maximum. As Kays' and London's equation (4.4) suggests, for increasing C_r^* the effectiveness becomes the same as for direct counterflow heat exchangers and is solely dependent on the NTU. **Figure 4.7** shows a comparison of different effectiveness curves. Above a Γ of 3.5, corresponding to a speed of 10.5 min^{-1} for the analyzed geometry and mass flows, effectiveness calculated by solving the governing equations by MOSHMX becomes nearly the same as the effectiveness calculated with equation (4.3) and the direct transfer counterflow heat exchanger effectiveness. These results are independent of temperature and humidity conditions and the desiccant characteristics. For this enthalpy exchanger matrix, the calculated efficiency values agree very well with experimental results. The manufacturer (Carnes) gives an experimental effectiveness of 0.73 for the analyzed conditions, with the calculated values approaching 0.72.

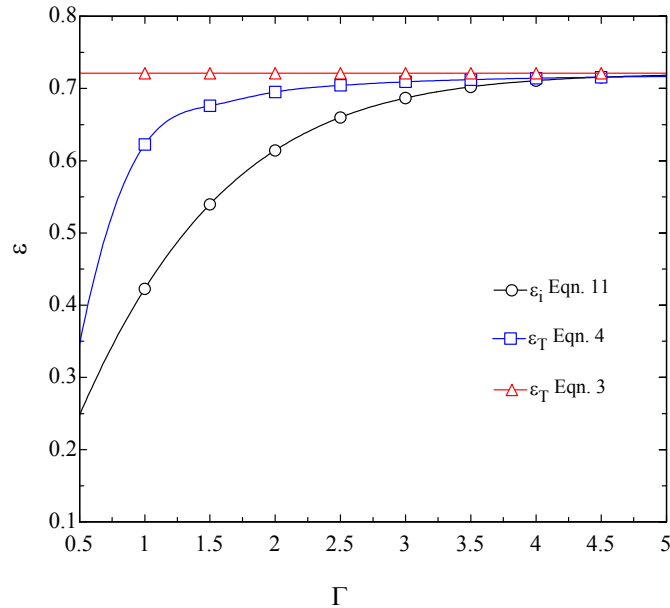


Figure 4.7: Effectiveness curves over mass flow rate ratio Γ obtained from different equations for $NTU = 2.6$

The amount of air entrained in the matrix has not been taken into account; it is proportional to the wheel speed and effectiveness will be lowered due to mixing when speed increases. Hence, effectiveness will have a maximum, at a certain optimum speed where the wheel should be operated. Since the effect of mixing is small at reasonable speed, the wheel speed S should be relative to a Γ of about four as **Figure 4.7** suggests. This correlates to an S of about 14 min^{-1} .

Desiccants

The capability of a desiccant to adsorb moisture is dependent on the relative humidity and temperature of the air. The driving force for the moisture transfer is the non-equilibrium state of the air and desiccant, and the energy liberated during the adsorption process (similar to heat of condensation). Experiments with desiccant material and moist air in equilibrium state show an exponential increase in the humidity ratio of the desiccant matrix with the relative humidity of the air. Adsorption is slightly higher for lower temperatures. **Figure 4.8** shows

the adsorption isotherms in equilibrium state for a polymer desiccant coated matrix (manufacturer: Carnes) [2].

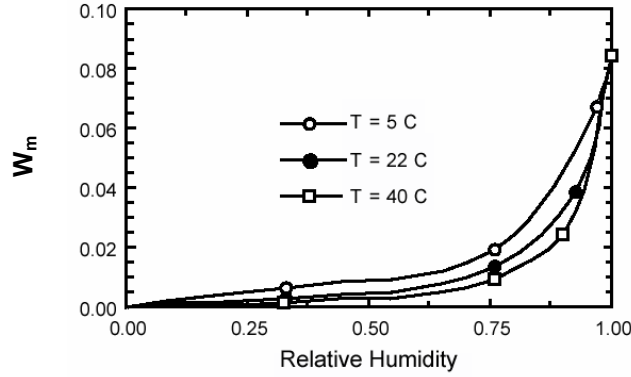


Figure 4.8: Adsorption isotherms, matrix humidity ratio W_m vs. relative humidity, [2]

The isotherms are represented by the Dubinin-Polstyanov equation (Dubinin, 1975),

$$W_m = 0.0385 \cdot \exp\left[-\left(\frac{A}{620}\right)^{0.5}\right] + 0.0460 \cdot \exp\left[-\left(\frac{A}{20}\right)^{1.5}\right] \quad (4.12)$$

where W_m is the mass of adsorbed water per unit mass of dry matrix and A is the adsorption potential defined as:

$$A = RT \ln(p_s/p_v) \quad (4.13)$$

The Dubinin-Polanyi Adsorption Potential Theory of a desiccant relates the amount of moisture adsorbed by the desiccant to the temperature and relative humidity of the air (Dubinin, 1975). **Figure 4.9** shows the adsorption potential versus matrix water content [2].

The matrix humidity ratio W_m as a function of saturation pressure goes into the governing differential equations (equations 4.7, 4.8) and characterizes the behavior of the desiccant.

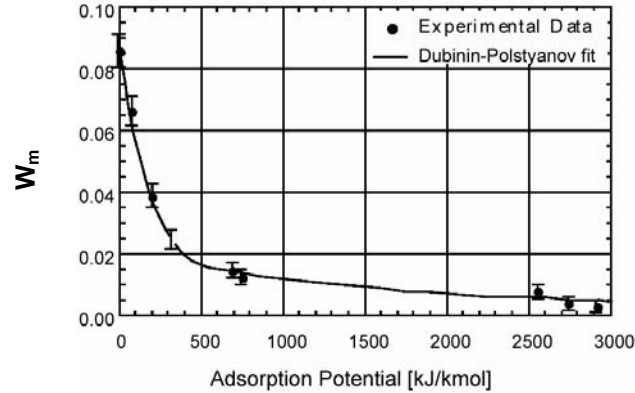


Figure 4.9: Matrix humidity ratio W_m vs. adsorption potential A of polymer desiccant, [2]

Calculation of NTU

Calculating the NTU is a crucial point in the enthalpy exchanger analysis. The NTU is factored directly into the governing equations. The NTU depends on the geometry of the matrix and the airflow. The effectiveness calculated based on the NTU, equation (4.3) indicates the upper limit for the rotary enthalpy exchanger effectiveness.

The first matrix examined here (manufacturer: Carnes) consists of isoscele-triangular passages of 2.54 mm *3.175 mm and is made of thin aluminum foil coated with a desiccant polymer. For a mass flow rate of 2.28 kg/s (data taken from literature [2]) the recommended wheel has a diameter of 0.828 m, cross-sectional area of 0.539 m² and is 0.203 m deep. Total surface area for heat and mass transfer is $A_S = 255 \text{ m}^2$. The hydraulic diameter ($D_h = 4A/P$) of a single passage is 1.72 mm.

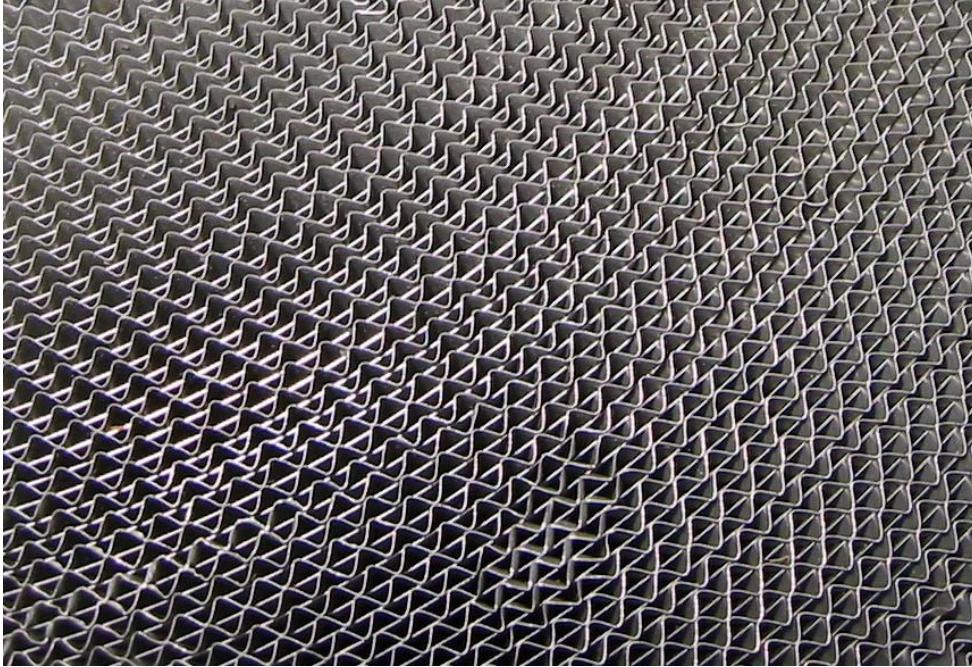


Figure 4.10: Enthalpy exchanger matrix from Carnes, made of corrugated aluminum coated with a molecular sieve

The Reynolds number for air flow through this matrix is:

$$\begin{aligned}
 Re &= vD_h/\nu & \nu &= 15.08 \cdot 10^{-6} \text{ m}^2/\text{s} & \text{for air at } 20^\circ\text{C} \\
 v &= 3.62 \text{ m/s} & & & \text{for given mass flow and cross-sectional} \\
 & & & & \text{area} \\
 Re &= 412.8 & & & < R_{crit} = 2300
 \end{aligned}$$

Thus, we have laminar flow through the passages. Constant heat flux and fully developed flow due to high length/diameter ratio are assumed. Nusselt Number for laminar flow in an isosceles triangular duct under these boundary conditions is given in [7] with the following equation:

$$Nu = 2.059(1 + 0.7139\alpha + 2.954\alpha^2 - 7.8785\alpha^3 + 5.645\alpha^4 - 0.2144\alpha^5 + 1.1387\alpha^6)$$

$$Nu = 3.113 \quad \text{for base-height ratio } \alpha = 2.54/3.175$$

Having determined the Nusselt Number, the convection coefficient h can readily be calculated:

$$h = Nu k / D_h \quad k = 0.02563 \text{ W/m-K for air at } 20^\circ\text{C}$$

$$h = 46.4 \text{ W/m}^2\text{K}$$

With known h , the NTU_T becomes:

$$NTU_T = h A_S / \dot{C} \quad \dot{C} = 2.28 \text{ kg/s} * 1004 \text{ J/kgK}, A_S = 255 \text{ m}^2$$

$$NTU_T = 5.17$$

The actual NTU is half of the calculated value, since heat transfer takes place not directly, but in two periods between one fluid and one half of the matrix area. This value for NTU assumes a Lewis Number of unity, the effectiveness is the same for heat and for mass transfer and it was used to solve the governing equations, as discussed before.

The other matrix analyzed here (manufacturer: Airxchange) is made of a coil of silica gel coated polystyrene straps 38.1 mm width and 0.2 mm thin. The concentric annular channels between the straps are 0.329 mm wide, small nubs on the straps maintain the gap. Aluminum spokes and rims support the straps. The surface area A_S can be obtained by multiplying the total length of all straps with two times the axial width. Total length equals the number of straps, $n = 708$, times the average perimeter. The outer radius, R , equals 457.2 mm and the inner radius, r , is 82.6 mm.



Figure 4.11: Enthalpy exchanger matrix from Airxchange, made of polystyrene straps coated with silica gel.

The Reynolds number becomes:

$$\begin{aligned}
 Re &= v D_h / \nu & \nu &= 15.08 \cdot 10^{-6} \text{ m}^2/\text{s} & \text{for air at } 20^\circ\text{C} \\
 v &= 1.195 \text{ m/s} & & & \text{for design conditions airflow of } 1000 \\
 & & & & \text{scfm (} 0.472 \text{ m}^3/\text{s)} \\
 D_h &= 4A/P = 0.658 \text{ mm} \\
 Re &= 52 & & & < R_{crit} = 2300
 \end{aligned}$$

For such a low Reynolds Number the flow will be laminar. Again, constant heat flux and fully developed flow due to high length/diameter ratio are assumed. The Nusselt Number for laminar flow in an annular duct with a radii ratio of one under these boundary conditions is given in [7] as:

$$Nu = 8.23$$

$$h = Nu k/D_h \quad k = 0.02563 \text{ W/mK} \quad \text{for air at } 20^\circ\text{C}$$

$$h = 320.4 \text{ W/m}^2\text{K}$$

NTU_T becomes:

$$NTU_T = h A_S / \dot{C} \quad \dot{C} = 0.472 \text{ m}^3/\text{s} * 1.2 \text{ kg/m}^3 * 1004 \text{ J/kgK}$$

$$A_S = 91.46 \text{ m}^2$$

$$NTU_T = 51.37$$

The actual NTU_T for the wheel equals 25.69, a rather high value for a heat exchanger of this kind and about ten times larger than the NTU_T for the other matrix (Carnes).

Discussion of the NTU Calculations

Agreement within 1.5% between catalog/experimental data and results from solving the governing equations has been achieved for the first analyzed matrix (Carnes). The curves shown in **Figure 4.7** even suggest that, when operating the enthalpy exchanger under optimum conditions, the effectiveness can be predicted solely with the counterflow heat exchanger effectiveness (equation 4.3).

While the analysis method works almost perfectly for the first analyzed matrix (Carnes), it fails to yield results within an acceptable range of tolerance for the second exchanger matrix (Airxchange): Calculating the counterflow heat exchanger effectiveness leads to $\varepsilon_T = 0.96$. The experimental value for the same conditions is $\varepsilon_T = 0.83$. NTU_T derived from $\varepsilon_T = 0.83$ with equation (4.3) gives a value of 5.06, in contrast to the calculated 25.69. Similar deviations between experimental and calculated values occur for $\varepsilon_w = 0.78$ and 0.96 under the assumption of $Le = 1$. Deriving the Lewis Number from experimental NTU_T and NTU_w gives $Le = 0.69$.

Why is the effectiveness in the second case over predicted? A first approach leads to the conclusion that lower conductivity of the polystyrene material of only 0.14 W/mK exacerbates heat transfer into the matrix material and non-ideal equal flow distribution through the matrix channels reduces the effective surface area. No further studies have been carried out yet to investigate these effects.

Introducing the NTU Correction Factor Method for Performance Prediction of Enthalpy Exchangers

The NTU method of heat exchanger analysis does not yield correct results for rotary enthalpy exchangers, as it has been shown before. Comparing experimental results and classic NTU based calculations shows that the effectiveness of enthalpy exchangers is usually over predicted when treating them as counterflow heat exchangers. However, introducing an effectiveness correction factor defined in equation (4.14), allows using the same equations for enthalpy exchangers as used to predict performance of counterflow heat exchangers (CFX). This factor takes into account that the enthalpy exchangers are, in general, less effective than a CFX with the same theoretical UA due to non-ideal flow through the matrix channels, fluid crossover leakage, axial conduction etc. The correction factor is a characteristic constant of each enthalpy exchanger operating at optimum capacity rate ratio of matrix and fluid. The values for the correction factor were found to be in the range of 0.87 to 1 for all analyzed enthalpy exchanger data (manufacturers: Airxchange, Novelaire, Venmar, Rotor Source, Rotary Desiccant Intern, Carnes).

The correction factor can be obtained from experimental data and it is heavily dependent on the reference data's accuracy and coherence. However, since also the NTU is obtained the same way, possible inaccuracies cancel out eventually when calculating the effectiveness, so that the effect on performance prediction i.e. temperature and humidity ratio differences will be relatively small, as shown later in the uncertainty calculation. Usually the manufacturer or

testing organizations provide effectiveness ratings for at least two different flow rates, based on experimental results.

The prerequisite for this analysis is a sufficient rotational speed of the enthalpy exchanger matrix, fast enough to eliminate the effects of periodic flow, which significantly reduce effectiveness. This speed is the normal operation speed of an enthalpy exchangers and it correlates to a matrix capacity-rate ratio on the order of 10.

$$\varepsilon_{REX} = \varepsilon_{CFX} c \quad (4.14)$$

Where the counterflow heat exchanger effectiveness,

$$\varepsilon_{CFX} = \frac{1 - e^{-NTU(R_C + 1)}}{1 - R_C e^{-NTU(1 - R_C)}} \quad (4.15)$$

is a function of the NTU ,

$$NTU = \frac{UA}{\dot{C}_{\min}} \quad (4.16)$$

and the ratio of the minimum of outside and exhaust air flow to the maximum airflow:

$$R_C = \frac{\dot{C}_{\min}}{\dot{C}_{\max}} \quad (4.17)$$

To calculate effectiveness of an enthalpy exchanger with equation (4.14) and (4.15) the NTU , equation (4.16), and the correction factor c are necessary. The reference effectiveness data ε_1 and ε_2 for two capacitance flow rates \dot{C}_1 and \dot{C}_2 are used to solve (4.20) to obtain UA and equation (4.19) to determine the correction factor $c_{balanced}$ for balanced flow. The

effectiveness ratings are for balanced flow i.e. $R_C = 1$, (4.17). In this case, equation (4.15) simplifies to (4.18) (rule of l'Hospital):

$$\varepsilon_{CFX} = \frac{NTU}{NTU + 1} \quad (4.18)$$

Equations (4.14), (4.16) and (4.18) can be combined to equation (4.19):

$$c_{balanced} = \varepsilon_{REX} \left(\frac{\dot{C}}{UA} + 1 \right) \quad (4.19)$$

Since UA and c are constant for all balanced flow rates, UA can be calculated putting ε_1 and \dot{C}_1 , ε_2 and \dot{C}_2 , respectively, into equation (4.19) and setting both equal in (4.20):

$$UA = \frac{\dot{C}_1 \varepsilon_1 - \dot{C}_2 \varepsilon_2}{\varepsilon_2 - \varepsilon_1} \quad (4.20)$$

For unbalanced flow, $R_C < 1$, the correction factor needs to be a function of R_C , as the following consideration may point out: For extreme unequal flow rates in a heat exchanger, R_C approaches zero and the effectiveness for the minimum flow approaches 1. The same behavior should apply for an enthalpy exchanger, so that effectiveness will approach CFX-effectiveness and be close to unity for a very small flow rate. Thus, the correction factor c for unbalanced flow will be higher than for balanced flow and it will be estimated as a linear function of R_C :

$$c = c_{balanced} \left(R_C + \frac{1}{c_{balanced}} - \frac{R_C}{c_{balanced}} \right) \quad (4.21)$$

With known UA and c , the effectiveness of an enthalpy exchanger finally can be computed using equations (4.14) and (4.15). Having the effectiveness, equation (4.22) can be solved to obtain the outlet temperatures for the outside air stream:

$$\varepsilon = \frac{\dot{C}_{OA}(T_{OA,out} - T_{OA,in})}{\dot{C}_{\min}(T_{OA,out} - T_{EA,in})} \quad (4.22)$$

The same procedure can be applied to calculate the mass transfer effectiveness. For mass transfer UA , c and ε have different values; mass transfer effectiveness is usually about 10% lower than the heat transfer effectiveness, the Lewis number smaller than one.

Verification

In order to verify the data computed with the method described above, the results have been compared to available manufacturers data (Airxchange Catalog, [12], Equipment selection software from Greenheck Fan Corp: CAPS 1.9, Rotor Source Inc: ESelect 2.0.3 and Carnes Co: Energy Recovery-C-Lect 2.0). The calculated effectiveness was usually within 1% for balanced as well as for unbalanced flow in the normal range of operation, from ca 50% to 200% of rated flow.

Table 4.1 presents NTU and UA calculated from a flow rate – effectiveness table for balanced flow taken from the Airxchange Catalog [12] for ERV-3615:

Flow Rate [m ³ /s]	Effectiveness [%]	NTU	UA [kW/K]
0.3776	85.2	10.23	4.730
0.4248	84.3	9.133	4.752
0.4719	83.5	8.325	4.813
0.5191	82.7	7.636	4.856
0.5663	81.8	6.974	4.838
0.6135	80.9	6.405	4.814
0.6607	80.1	5.964	4.827
0.7079	79.2	5.527	4.792
0.7551	78.4	5.182	4.793
0.8023	77.5	4.835	4.751

Table 4.1: NTU and UA

For $c = 0.9353$, the calculated UA has a value of about 4.8 kW/K, UA is constant over the flow rate since the flow regime is laminar. Finding the correction factor in this case is an iterative process; the factor also could be obtained using two reference flow rates and effectiveness's, as described earlier. Any other value for c would not yield the same UA for different flow rates. The small variations of the UA are presumably due to inaccurate and uncertain effectiveness values for given flow rates. Similar tables have been created for enthalpy exchanger performance data from other manufacturers (Novelaire, Venmar, Rotary Desiccant Intern) with comparable results.

Figure 4.12 compares the results of effectiveness calculated using the method described above with effectiveness data of a commercial available enthalpy exchanger obtained with the manufacturer's selection software (CAPS 1.9 from Greenheck Fan Corp.) for unbalanced flow. Reference data for two balanced flow rates was also obtained from the software.

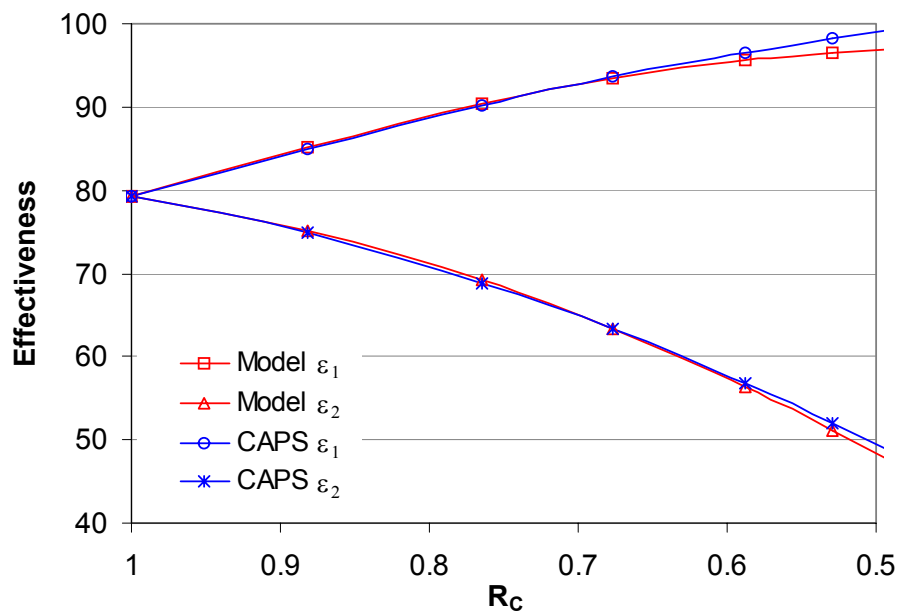


Figure 4.12: Comparison between manufacturer's data and model predicted data generated for imbalanced flow for Greenheck Fan Corp. enthalpy exchanger ERV-361S. Flow rate 2 is 0.8 m³/s while flow rate 1 varies from 0.8 to 0.4 m³/s

In **Table 4.2**, two sets of experimental test data from a commercial manufacturer are compared to performance data yielded by the model. The reference data for the model is taken from Airxchange Catalog [12] for ERV-3615 which the manufacturer uses; reference points at flow rates of $0.7551 \text{ m}^3/\text{s}$, $\varepsilon_T = 0.784$ and $0.4719 \text{ m}^3/\text{s}$, $\varepsilon_T = 0.835$.

Flow [m^3/s]	$T_{\text{OA,in}} [^\circ\text{C}]$	$T_{\text{EA,in}} [^\circ\text{C}]$	$T_{\text{OA,out,test}} [^\circ\text{C}]$	$T_{\text{OA,out,model}} [^\circ\text{C}]$	$\Delta T_{\text{OA,out}} [\text{K}]$	$\varepsilon_{T,\text{test}}$	$\varepsilon_{T,\text{model}}$	$\Delta \varepsilon_T [\%]$
0.4715	35.0	23.9	25.54	25.76	0.22	0.855	0.835	-2.36
0.5668	35.0	23.9	25.75	25.89	0.14	0.830	0.817	-1.59
0.6617	35.0	23.9	26.03	26.15	0.12	0.811	0.800	-1.40
0.7551	35.0	23.9	26.17	26.27	0.10	0.793	0.784	-1.12
0.4725	32.8	23.9	25.41	25.35	-0.05	0.829	0.835	0.70
0.5660	32.7	23.9	25.57	25.52	-0.04	0.812	0.817	0.61
0.6604	32.5	23.9	25.66	25.62	-0.04	0.796	0.800	0.59
0.7558	32.5	23.9	25.89	25.72	-0.16	0.765	0.784	2.45

Table 4.2: model predicted and manufacturers test data for an enthalpy exchanger

The difference $\Delta T_{\text{OA,out}}$ between measured and model predicted temperature is within 0.2 K and on the order of the uncertainty of the measurements. For the first set of data, the model under predicts the effectiveness 1-2%, while effectiveness is higher calculated for the second run. Reasons may be slightly varied testing conditions and measurement uncertainties. When using two of the test data points as reference for the model instead of the official catalog data, $\Delta T_{\text{OA,out}}$ stays below 0.03 K, and the model predicted effectiveness ε_T fits the four experimental results within 0.3 %.

Experimental data for another enthalpy exchanger with an aluminum matrix are compared to the performance predicted by the model in **Figure 4.13**. The reference data was also obtained from the manufacturer, $\varepsilon_T = 84.4\%$ and $\varepsilon_L = 85.8\%$ at 1750 cfm and $\varepsilon_T = 82.7\%$ and $\varepsilon_L = 83.1\%$ at 2500 cfm. It is evident that predicted effectiveness stays within 5% of the experimental data. However, the deviation of predicted from experimental data is larger for highly unbalanced flow than for conditions closer to the reference flow rates, as it will be pointed out by the uncertainty propagation.

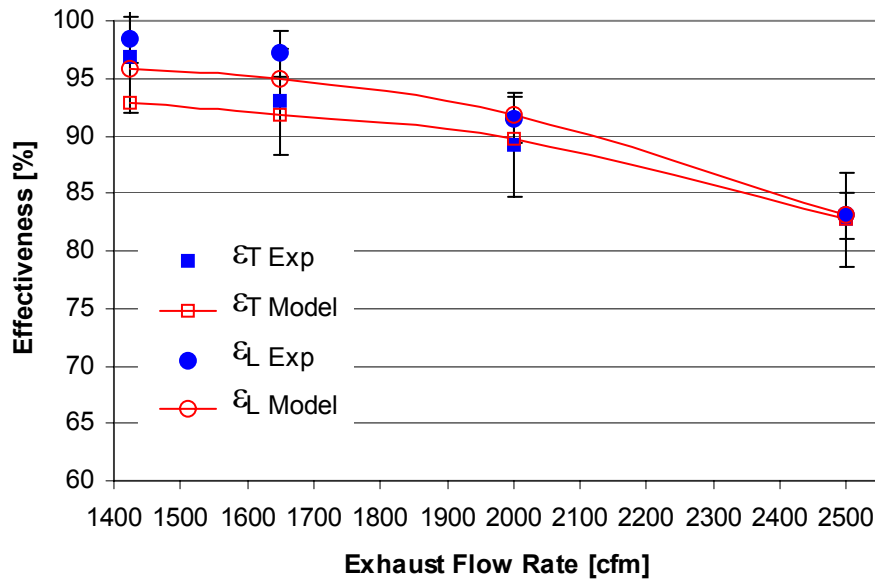


Figure 4.13: Experimental and model predicted effectiveness for unbalanced flow. Intake flow rate is 2500 cfm, 1.18 m³/s. Error bars indicate an assumed 5% experimental uncertainty.

Uncertainty Propagation for the NTU Correction Factor Method

Uncertainty propagations were carried out to investigate the affect of inaccuracies of the reference data on the calculated effectiveness and the outlet temperature and humidity. The results of the uncertainty propagations show that the uncertainty of the calculated effectiveness is less than the uncertainty of the reference effectiveness when the actual flow rate is in between the range of the reference flow rates. **Table 4.3** lists the uncertainties calculated based on manufacturers data [12] for the Airxchange ERV-3615 for balanced flow. Reference flow rates are 0.4719 m³/s and 0.7551 m³/s. An assumed uncertainty for the reference effectiveness is +/- 5%. Exhaust temperature is 21°C and intake temperature -10°C and 30°C for winter and summer conditions, respectively. For summer conditions the uncertainty of temperature is much smaller since the temperature difference between intake and exhaust is less.

Flow [m ³ /s]	Effectiveness	T _{out, winter} [°C]	T _{out, summer} [°C]
0.3776	0.851±0.060	16.46±1.87	22.32±0.54
0.4248	0.844±0.050	16.17±1.56	22.40±0.45
0.4719	0.835±0.042	15.89±1.29	22.48±0.38
0.5191	0.826±0.035	15.61±1.08	22.57±0.31
0.5663	0.817±0.030	15.34±0.94	22.64±0.27
0.6135	0.809±0.029	15.07±0.89	22.72±0.26
0.6607	0.800±0.030	14.81±0.93	22.80±0.27
0.7079	0.792±0.034	14.55±1.05	22.87±0.31
0.7551	0.784±0.039	14.30±1.23	22.94±0.35
0.8023	0.776±0.045	14.06±1.40	23.02±0.41

Table 4.3: Uncertainties for effectiveness and outlet temperature for balanced flow

The uncertainty propagation for imbalanced flow conditions in **Table 4.4** demonstrates the same effect as for balanced flow: the uncertainty of predicted effectiveness is lower than the uncertainty of the reference effectiveness as long as the flow is within the range of the reference flow rates. For this uncertainty propagation, the same conditions as before were applied, with the exception that the exhaust air flow rate is constant 0.6135 m³/s, while the outside air flow rate varies. The flow ratio denotes the relation of outside air flow rate over exhaust flow.

The percentage of uncertainty for humidity and for enthalpy is the same as for temperature due to the interchangeability of the properties in the mathematical equations, provided that the relative uncertainty of the measurements for humidity is the same. The uncertainty propagations were prepared using the equations of the NTU-Correction factor method described above in an EES [11] program.

Flow 1 [m ³ /s]	Flow ratio	Effectiveness	T _{out, winter} [°C]	T _{out, summer} [°C]
0.3776	0.62	0.954±0.067	19.57±2.06	21.42±0.60
0.4248	0.69	0.938±0.047	19.07±1.47	21.56±0.43
0.4719	0.77	0.914±0.031	18.33±0.95	21.77±0.28
0.5191	0.85	0.883±0.026	17.38±0.81	22.05±0.24
0.5663	0.92	0.848±0.028	16.27±0.86	22.37±0.25
0.6135	1.00	0.809±0.0286	15.07±0.89	22.72±0.26
0.6607	1.08	0.778±0.0285	14.08±0.88	23.01±0.26
0.7079	1.15	0.744±0.0291	13.07±0.90	23.30±0.26
0.7551	1.23	0.712±0.0282	12.07±0.87	23.59±0.25
0.8023	1.31	0.681±0.0261	11.11±0.81	23.87±0.24

Table 4.4: Uncertainties for effectiveness and outlet temperature for imbalanced flow

Conclusion

This new method described above allows prediction of enthalpy exchanger performance for any flow conditions based on two reference data points for balanced flow as available for all enthalpy exchangers on the market.

It has proven difficult as shown before in this chapter to calculate effectiveness by evaluating heat and mass transfer coefficients to obtain UA and NTU. If it were possible to accurately calculate UA, NTU and the correction factor c based on enthalpy exchanger's geometry and materials could be found, reference data and the uncertainties of experiments would not be needed. However, no relation has been found yet between the correction factor and certain properties of enthalpy exchangers, like materials, dimensions, flow channels etc. The disadvantage of this model based on experimental performance data is, that it cannot be used to directly study the influence of changing physical properties when developing an enthalpy exchanger.

This method of performance calculation appears to be well suited for being used in a model for transient computer simulations and in general for computation of enthalpy exchanger

effectiveness for different flow conditions. Limitations of this model are sufficient rotational speed, coherent reference data and flow rates on the order of the reference data to keep uncertainties low.

Computer Modeling of Enthalpy Exchangers for TRNSYS

The computer model of an enthalpy exchanger must be able to calculate the outlet states of the intake air stream for any given set of inlet air properties and parameters. Parameters can include geometrical data, mass and capacitance of the matrix to calculate the Nusselt Number and the NTU, rotational speed and desiccant and material properties. The latter are only necessary when actually solving the governing differential equations (4.7) - (4.10). A program able to solve the governing equations numerically is MOSHMX [5]. This program can be used to obtain reference state points, which then can be curve-fitted to obtain a set of simple equations depending only on temperatures and Γ for the effectiveness. The program is not appropriate for transient simulations of HVAC systems due to complex calculations, but using curve fit equations is possible. It has been shown that above a certain speed the effectiveness reaches a maximum and is only dependent on the NTU. This would be the operating point for most conditions, during heating season as well as for cooling. A simplified model based only on NTU would yield the maximum effectiveness for the optimum speed where Γ is set to five for instance. Such a model would not require much computational effort and could be used in transient simulations.

However, there are two reasons for not going through all these calculations and instead using experimental data: first, as it was shown in the analysis of the second matrix (Airxchange), the calculation procedure may not yield accurate results. Uncertainties are much lower when basing performance predictions on secured experimental data. Second, unlike detailed geometrical data and material properties, performance data are available for many enthalpy exchangers on the market. These data have been obtained with experiments according to the standards developed by independent testing institutions like the Air-Conditioning and Refrigeration Institute (ARI) and at the testing sites of the manufacturers.

The purpose of the computer model developed here is to predict the performance of enthalpy exchangers when simulating HVAC systems in the context of building energy analysis using TRNSYS [10]. The program TRNSYS has a modular structure based on components written in FORTRAN. Components are interlinked to each other by input and output variables. A component is a FORTRAN subroutine, which contains the mathematical abstract of the modeled equipment or device. A component is defined with a number of input and output variables and is specified by a list of parameters.

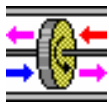


Figure 4.14: TRNSYS icon for the Type 222 Enthalpy Exchanger

The computer model of the enthalpy exchanger is named TRNSYS Type 222 and has the following basic input variables:

- Intake and exhaust temperatures
- Intake and exhaust relative humidity
- Intake and exhaust volumetric air flow rates

The list of parameters contains sensible and latent effectiveness and pressure drop for two different reference flow rates, fan efficiency, a parameter setting the frost control mode from preheat to low speed operation and one parameter for the air-side economizer mode.

Finally, the model outputs incorporate the following variables:

- Outside air temperature [$^{\circ}\text{C}$], relative humidity [%] and humidity ratio
- Exhaust air temperature [$^{\circ}\text{C}$], relative humidity [%] and humidity ratio
- Outside and exhaust air flow rate [m^3/h]
- Intake and exhaust pressure drop [kPa]
- Additional intake and exhaust Fan Power [kW]

- Preheater Energy Demand [kJ/hr]
- Preheater Temperature Rise [K]
- Sensible effectiveness and latent effectiveness
- Exchanged sensible, latent and total heat

Outlet State Calculation

To calculate the outlet states of the leaving airstreams, first the actual heat and mass transfer exchanger effectiveness's ES and EL are evaluated using the NTU Correction Factor Method as described earlier. ES denotes the sensible effectiveness ε_s , while EL stands for the latent heat or mass exchanger effectiveness ε_w . The outside air temperature and humidity ratio are calculated with equation (4.23) and (4.24), and the exhaust air temperature and humidity ratio leaving the enthalpy exchanger with equation (4.25) and (4.26):

$$T_{OAOUT} = T_{OAIN} + C_{MIN}/C_{OA} E_S (T_{EAIN} - T_{OAIN}) \quad (4.23)$$

$$W_{OAOUT} = W_{OAIN} + C_{MIN}/C_{OA} E_L (W_{EAIN} - W_{OAIN}) \quad (4.24)$$

$$T_{EAOUT} = T_{EAIN} + C_{MIN}/C_{EA} E_S (T_{OAIN} - T_{EAIN}) \quad (4.25)$$

$$W_{EAOUT} = W_{EAIN} + C_{MIN}/C_{EA} E_L (W_{OAIN} - W_{EAIN}) \quad (4.26)$$

The humidity ratios are then checked for possible condensation, which would occur if W_{EAOUT} were greater than the saturation humidity ratio w_{sat} , obtained using a subroutine for psychrometric calculations in TRNSYS. In case of condensation, the output humidity ratio is set equal to w_{sat} . Finally, the re-calculation of the relative humidity from the humidity ratio is accomplished again using a psychrometric subroutine.

Frost Control

Before calculating any outlet states, an evaluation is made to determine if frost buildup can occur when the outdoors temperature is below -2°C . Therefore, the outdoor temperature is compared to the lowest inlet temperature, $T_{NOFROST}$, where no condensation would occur when cooling the exhaust air stream. When connecting $T_{NOFROST}$ to the exhaust state point on the psychrometric chart, **Figure 4.4**, the line does not intersect the saturation curve. The saturation curve is given by equation (4.27):

$$w_{sat} = 0.0041375 \exp(0.0964888 T_{EAOUT}) \quad (4.27)$$

This is a curve-fit describing the saturation humidity ratio as a function of temperature at standard pressure based on a saturation vapor pressure p_S correlation as given in [9] for low temperatures $<0^{\circ}\text{C}$.

The temperature $T_{NOFROST}$ is a function of four variables, outdoors temperature T_{OAIN} and relative humidity RH_{OAIN} , and exhaust temperature T_{EAIN} and relative humidity RH_{EAIN} . $T_{NOFROST}$ is given in (4.28) and has been obtained by linear regression of 360 tabulated values:

$$\begin{aligned} T_{NOFROST} = & -21.985 + 1.1269 T_{OAIN} + 0.011921 T_{OAIN}^2 - 0.072838 T_{EAIN} + 0.003083 T_{EAIN}^2 \\ & + 0.24807 RH_{OAIN} + 0.0000013347 RH_{OAIN}^2 + 0.10709 RH_{EAIN} - 0.00037125 RH_{EAIN}^2 \\ & - 0.013653 T_{OAIN} T_{EAIN} + 0.0042011 T_{OAIN} RH_{OAIN} - 0.0072628 T_{OAIN} RH_{EAIN} \\ & 0.0023767 T_{EAIN} RH_{OAIN} + 0.003386 T_{EAIN} RH_{EAIN} - 0.0012644 RH_{OAIN} RH_{EAIN} \end{aligned} \quad (4.28)$$

If $T_{NOFROST}$ is greater than T_{OAIN} , frost buildup is likely. According to the setting of the frost control mode parameter, the rotation speed of the enthalpy exchanger is modeled to be slowed down by setting the effectiveness to zero, or the preheater is activated to raise T_{OAIN} up to $T_{NOFROST}$. The required energy $Q_{PREHEAT}$ is calculated with equation (4.29):

$$Q_{PREHEAT} = Flow \rho_{air} C_{p,air} \Delta T_{PREHEAT} \quad (4.29)$$

The heat capacity $C_{p,air}$ and the density ρ_{air} are set to average values for the expected temperatures of 1.004 kJ/kgK and 1.22 kg/m³, respectively. $\Delta T_{PREHEAT}$ is the temperature difference between T_{OAIN} and $T_{NOFROST}$ in K.

Pressure Drop and Fan Power

The additional fan power required to overcome the pressure drop is calculated in equation (4.30) by multiplying the pressure drop, Δp , in kPa, and the flow rate, in m³/hr, divided by the fan efficiency and by 3600 to convert kJ/hr into kW.

$$Fanpower = 1/\eta_{Fan} \Delta p Flow/3600 \quad (4.30)$$

The pressure drop is a linear function of the flow rate, as experimental data shows, since the flow regime in the matrix of the enthalpy exchanger is laminar. The actual pressure drop Δp is calculated by linear interpolation of the reference pressure drop data over the actual airflow rate.

Enthalpy Exchanger Economizer Control

Buildings with significant internal heat gains require cooling even during spring, fall and even winter when outdoor air temperatures are moderate. Providing the building with ventilation air at the outdoor air temperature can often meet the cooling load. This operation mode is called air-side economizer. When energy recovery equipment is installed, the ventilation air temperature increases and approaches the exhaust air temperature. To offset internal heat gains – from electrical equipment or solar irradiation etc. – the supply air has to be colder than the room temperature set point, when transmission heat losses of the building are smaller than the gains. During the cooling season, i.e. high outdoor air temperatures, high internal gains respectively, the supply air has to be mechanically cooled. With increased

ventilation air temperature due to energy recovery, the cooling load increases. The energy recovery equipment is now wasting rather than saving energy. The straightforward way to solve this problem could be to shut the energy recovery equipment off when the ventilation temperature becomes too high, but this would result in a sharp drop in ventilation air temperature, and additional heating would be necessary. A better strategy is to decrease the effectiveness of the energy recovery, so that the ventilation temperature can be controlled to avoid cooling while recovering enough waste heat to avoid heating. However, these two methods consider sensible heat only; they are applicable to sensible heat exchangers like runaround coil loops. Enthalpy exchangers can also save a significant amount of energy due to their ability to humidify or dehumidify. The amount of energy saved due to lower latent loads when running the enthalpy exchanger can be higher than the energy needed to meet the increased sensible cooling load of the ventilation air. The control methods have to be extended to include humidity; consequently the controls should be based on enthalpy rather than temperature.

There are three points of outside air enthalpy where control settings change:

1. Enthalpy of exhaust air i.e. room air set point
2. Enthalpy of the balance point of the building
3. Enthalpy of the heating point of the building

The balance point (point 2) is the state of outdoor air when neither heating or cooling, nor humidification or dehumidification is required to condition the ventilation air and maintain the building at the desired indoor air set points. The heating point is specified by the temperature and humidity of the outdoor air below which heating and humidifying is required.

When the outdoor air enthalpy is above the room air set point (point 1), the enthalpy exchanger is operational. Energy is transferred from the outside air into the cooler and drier exhaust air.

When the outside air enthalpy has a value between point 1 and point 2, the enthalpy exchanger is cycled off; any energy recovery from exhaust stream would increase the cooling demand. Cooling or dehumidifying with the enthalpy exchanger is not possible since the intake air is cooler and dryer than the exhaust.

For outside air enthalpy between point 2 and point 3 the exchanger's effectiveness is linearly increased by increasing the rotation speed. Instead of controlling the speed, an outside air bypass of the enthalpy exchanger with a controlled damper can be used, leaving the wheel speed constant at optimum and controlling the enthalpy of the mixed outside air behind enthalpy exchanger and bypass. The enthalpy of the ventilation air leaving the exchanger is decreasing for rising outside temperature until reaching the balance point.

When the outdoor air enthalpy is below point 3, the enthalpy exchanger is on to recover the maximum exhaust air energy and minimize heating and humidifying demand.

However, for buildings without humidity control during the cold season i.e. without humidification or with a floating range of humidity, the enthalpy control method for economizer operation does not lead to maximal energy savings. The heating and balance point in those building are only defined by specific temperatures and the room air set point only has a maximum relative humidity. Instead of enthalpy, two of the three control points are here based solely on temperature. For outdoor air temperature between the balance point and the heating point, the effectiveness is linear decreased, hitting zero when reaching the balance point. For outside temperature below the heating point the enthalpy exchanger operates under maximal effectiveness, as well as when either outside temperature or enthalpy are higher than the values of the exhaust air i.e. the room air set point. When the outside air temperature is higher than the balance point but lower than the exhaust air temperature, and the outside air enthalpy is lower than the enthalpy of the exhaust air, the enthalpy exchanger remains shut off.

A control strategy, as described above, leads to the largest possible energy savings in buildings with floating humidity. Both options for economizer operation, full enthalpy

control and the second method of enthalpy control for cooling mode only are incorporated in the TRNSYS Type 222 model of enthalpy exchangers.

Output Plots

Figure 4.15 shows model outputs of outside air conditions leaving the enthalpy exchanger and the preheat temperature rise for an outdoor air temperature increasing from -25°C to -10°C at constant exhaust air conditions of 21°C , 50% RH and constant 60% outdoor air RH.

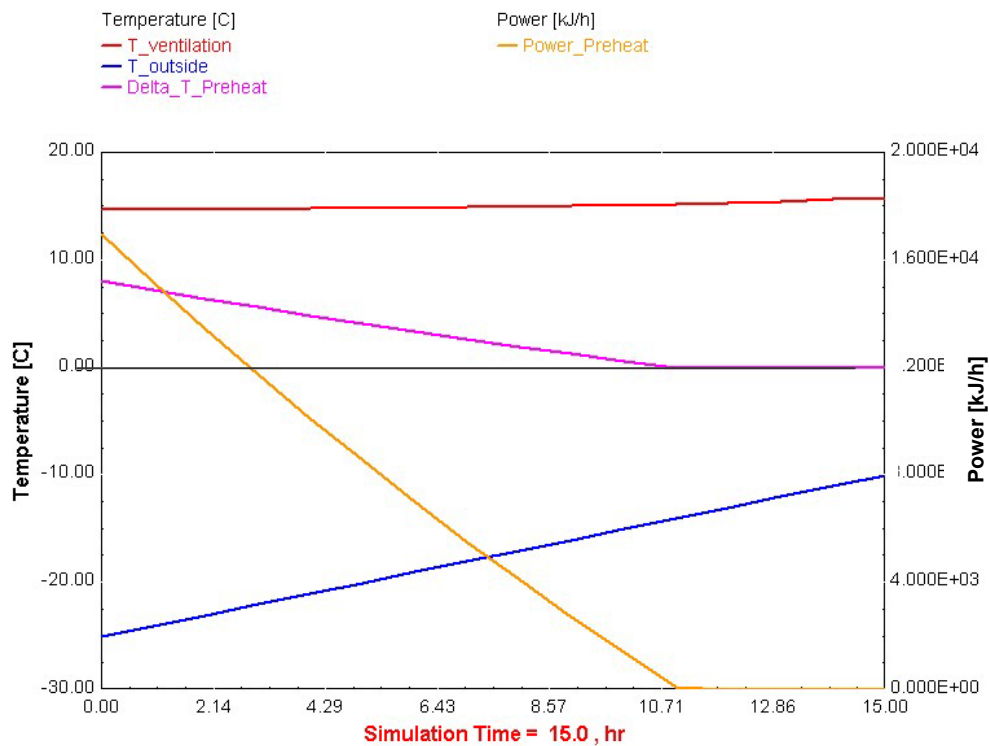


Figure 4.15: TRNSYS Plot of enthalpy exchanger model outputs for rising outdoor temperature and preheat under frost control operation.

Figure 4.16 displays economizer operation under the same exhaust conditions as Figure 4.15, for rising outside air temperature from 0°C to 25°C and constant 60% outdoor air RH. The heating point and balance point for economizer mode are set to 5°C and 13°C .

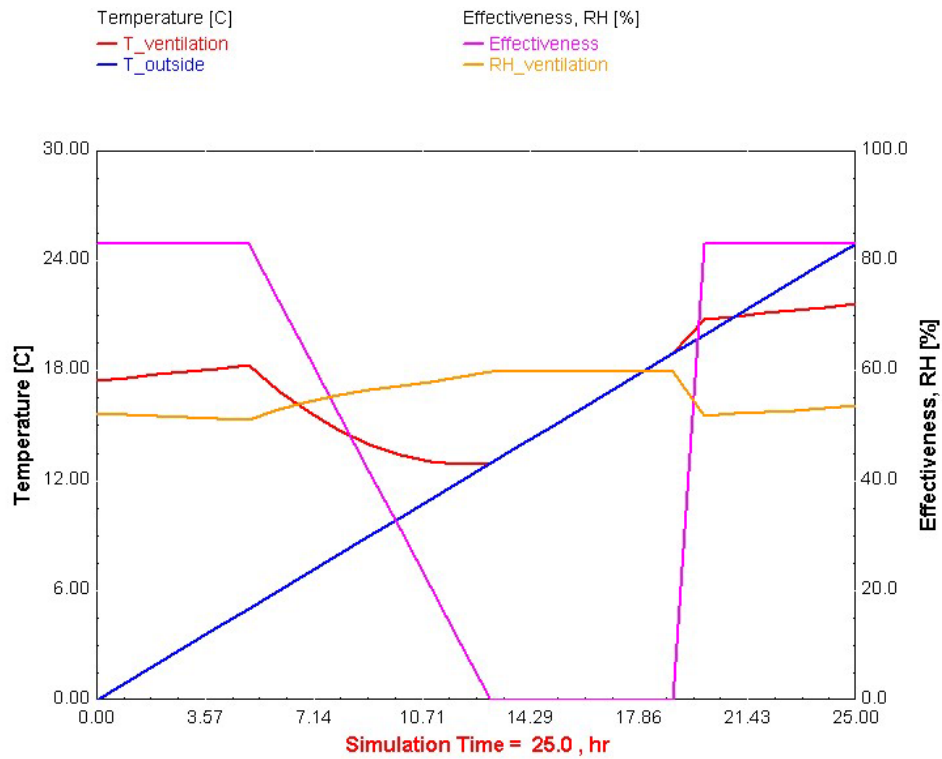


Figure 4.16: TRNSYS Plot of enthalpy exchanger model outputs for rising outdoor temperature and economizer operation.

The entire FORTRAN source code for TRNSYS Type 222 is listed in Appendix A.

Chapter 5 Runaround Loop Heat Exchangers

Introduction

A runaround loop heat exchanger is an air-to-air heat recovery system. It relies on the use of plate-finned coils along with a secondary fluid and a circulating pump. A typical runaround loop has one coil located in the exhaust air stream with the second coil located in the outdoor air intake stream. The heat exchange capability between the two air streams is completed by the use of a heat transfer fluid that is circulated between the two coils; a simple schematic of a runaround loop is shown in **Figure 5.1**. By recovering energy from the exhaust stream, the runaround loop can precondition the intake air to provide:

- outdoor air preheat during wintertime operation
- outdoor air precooling during summertime operation
- dehumidified outdoor air reheat during summertime operation

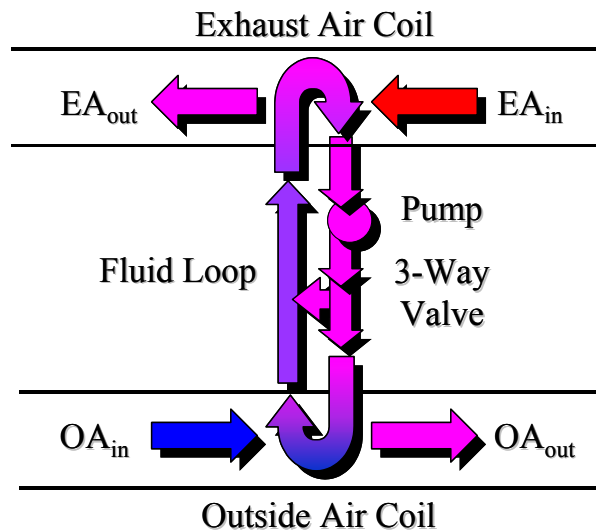


Figure 5.1: Schematic of a runaround loop

The effectiveness of a Runaround Loop is typically 55% - 65% [13]. The effectiveness is defined in equation (5.1):

$$\varepsilon = \frac{\dot{C}_{OA} (T_{OA, in} - T_{OA, out})}{\dot{C}_{min} (T_{OA, in} - T_{EA, in})} \quad (5.1)$$

Here T_{OA} are the entering and leaving outside air temperatures, T_{EA} are the exhaust air temperatures and C_{OA} and C_{min} are the outside air capacitance rate and the minimum air capacitance of outside and exhaust air.

Unlike enthalpy exchangers, runaround loops are only able to accomplish sensible heat transfer in the outside air stream. Latent heat can only contribute to the heat transfer when condensation in the exhaust coil occurs; no moisture can be exchanged between the intake and exhaust air stream and no cross contamination can occur. An advantage of runaround loops over enthalpy exchangers is that intake and exhaust ducts do not have to be located adjacent to each other. This feature makes runaround loops easier to install for retrofit applications as compared to rotary enthalpy exchangers.

Transfer Fluid

The heat transfer fluid used in the runaround loop is typically an inhibited solution of 35% ethylene glycol in water to provide freeze protection. The specific heat of the circulating fluid is 3.51 kJ/kgK and its density is 1058 kg/m³ (at 5°C). During wintertime operation the fluid is circulated from the “hot” side of the exhaust coil to warm the fluid while the exhaust air is cooled to the “hot” side of outside air coil to preheat the outside air. In the summer, this process works the same with reversed temperatures; the outside air temperature has to be lower than the exhaust temperature and the intake air is cooled. The fluid is piped through the multi-row coils so that the system will operate in a counterflow configuration, allowing maximal heat exchanger effectiveness.

The heat transfer fluid flow rate significantly affects the performance of the runaround loop system. At low fluid flow rates, heat transfer will be limited by the reduced capacitance rate of the secondary fluid – even though it will experience a maximum change in temperature. At high flow rates, the fluid experiences almost no temperature change since the capacitance rate of the fluid is much higher than the capacitance rate of the airstreams. Therefore, heat transfer is limited by the small temperature difference such that the cold side outlet temperature will be lower than the hot side outlet. A runaround loop system will reach optimum effectiveness when the heat transfer fluid capacitance rate equals the capacitance rate of the minimum air stream.

Under the assumption that both coils have equal effectiveness, the temperature profile for optimum fluid flow rate will ideally look as shown in **Figure 5.2**, for balanced flow rates, and in **Figure 5.3**, for unbalanced flow. The arrows indicate the direction of temperature change:

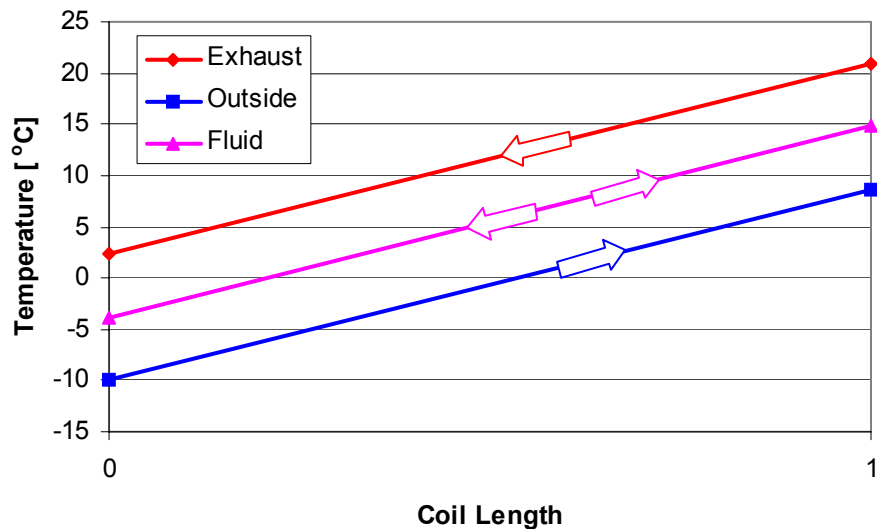


Figure 5.2: Schematic temperature profile over coil length for balanced airflows

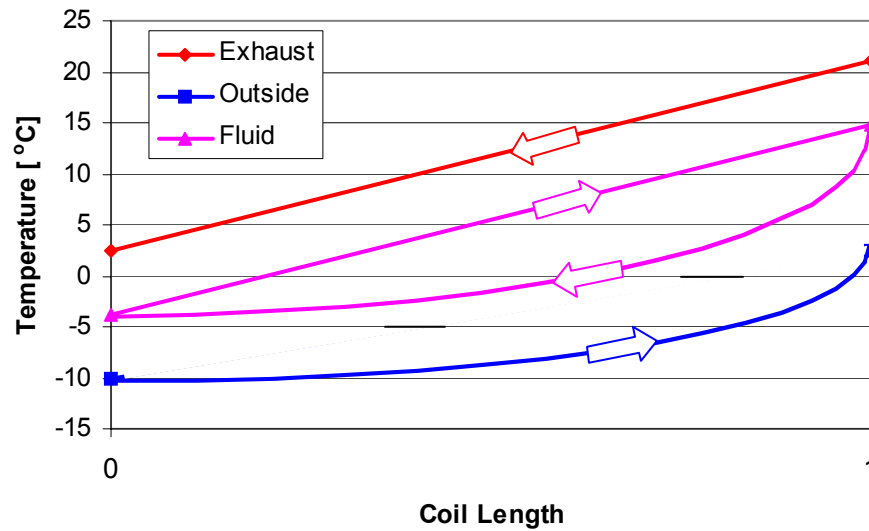


Figure 5.3: Schematic temperature profile over coil length for imbalanced air-side flow, outside airflow 1.5 times exhaust airflow.

Since the optimal liquid flow rate is such that its capacitance rate is equal to the minimum air-side capacity in order to have the maximal temperature change of the transfer fluid, liquid flow rates in runaround loops are small compared to normal water flow rates in standard heating or cooling coil applications. Thus, fluid-side Reynolds numbers tend to be lower resulting in lower fluid-side convection coefficients. A factor that compounds the low heat transfer coefficients is the secondary fluid choice – ethylene glycol. Glycol solutions have higher viscosities and lower thermal conductivities as compared to pure water (the more common working fluid for liquid-to-air coils). To compensate, runaround loops will, in general, be designed with higher fluid-side velocities than common in design for water coils – 2 m/s vs. 1 m/s. Since the standard coil tube diameters of $\frac{1}{2}$ " or $\frac{3}{8}$ " may be too large to establish a sufficiently high velocity at a small flow rate, the actual secondary fluid flow rate will often be higher than required to achieve a capacitance rate to match the minimum air flow.

Frost Control

Frosting or icing can occur in the exhaust coil of runaround loops during wintertime operation. Frosting may increase pressure drop or even block the channels of a finned coil. There are two requisites for frosting to occur: the exhaust coil's finned surface temperature must be below 0°C and it must fall below the dew point temperature of the leaving exhaust air. A method to prevent frosting is to maintain the exhaust coil surface temperature above the freezing point when having a dew point under run of the exhaust air. This can be achieved in three ways:

1. Preheating the intake air
2. Re-circulating the warm fluid leaving the exhaust coil via a temperature controlled 3-way bypass valve
3. Reducing heat transfer fluid flow rate

In the first case, the runaround loop system operates overall at increased temperatures, since outside air inlet temperature is higher and less energy can be recovered from the exhaust than possible without preheat, even though effectiveness stays the same. Preheat energy is added by an electric or hot water preheat coil to hold the intake temperature constant when the outdoor temperature falls below a critical value depending on exhaust inlet states. In the two latter cases, circulation and reduction of fluid flow rate, the effectiveness will be decreased, less energy can be recovered. In the second case, the fluid temperature entering the exhaust coil will be increased due to mixing of warm liquid leaving the exhaust coil and cold liquid from the intake coil, so that either no dew point under run and no condensation occurs, or in case of condensation the coil surface temperature stays above freezing. In case of reduced fluid flow rate, the effectiveness will be decreased to a point where the exhaust will not be cooled to critical conditions at which frosting occurs.

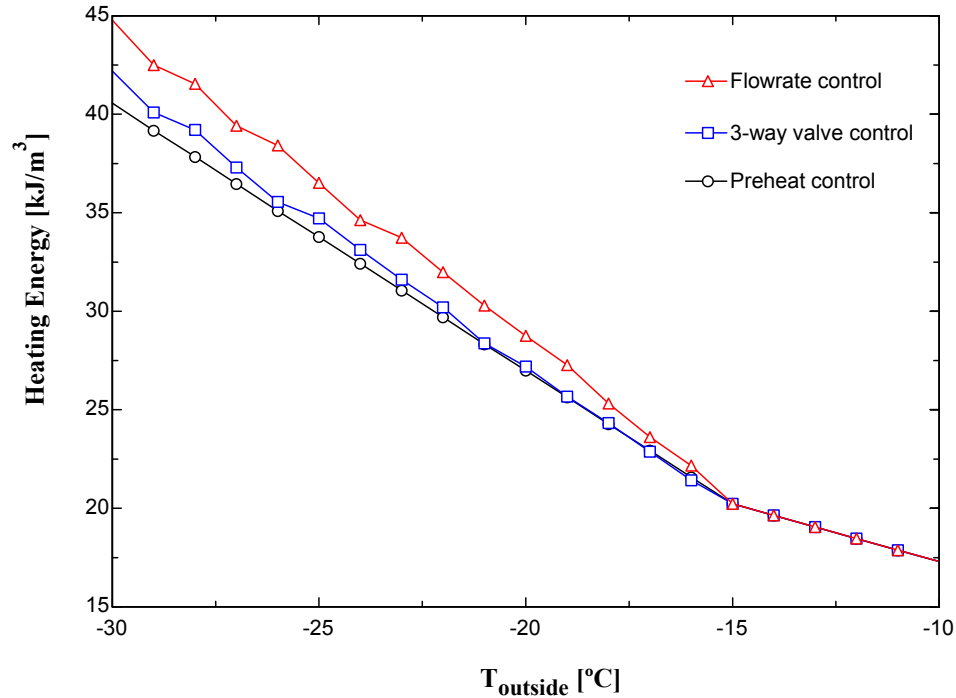


Figure 5.4: Comparison between different frost control strategies, simulated with TRNSYS TYPE 223 for a runaround loop system with 56% design effectiveness. Sensible Heating energy demand to warm leaving outside air to 21°C. Exhaust conditions 21°C, 30% RH. No frosting conditions occur above -15°C .

Figure 5.4 shows a comparison of the three frost control strategies outlined before. It suggests, that 3-way valve and preheat control are about equally efficient for temperatures down to -25°C and have in this case an advantage of about 10% less energy demand over flow rate control. The system simulated here is a 8 row, 8 circuit system, coil dimensions 18" x 33", 5/16" diameter tube with turbulators, air flow rates $0.96\text{ m}^3/\text{s}$ balanced, design liquid flow rate 0.63 l/s.

While preheat appears to be the most efficient frost control strategy, its advantage over the 3-way valve is very small, and since this solution does not require an additional coil, the choice for frost control is likely to fall on the 3-way valve. When a variable speed circulation pump is installed, flow rate control is an interesting option, although it has a penalty of effectiveness at low temperatures.

Economizer Control

During periods of the year when the outdoor air temperatures are moderate, little or no heat recovery is required (or desired) to condition a building (see also chapter Enthalpy Exchangers). In this case it is necessary to reduce the effectiveness of a runaround loop in order to limit heat recovery and prevent overheating a building. Three options of air-side economizer operation are available:

1. Bypass outside air around the coil
2. Bypass heat transfer fluid around the outside air coil using a 3-way valve
3. Reduction of heat transfer fluid flow rate

The advantage of the first option is that the air-side pressure drop will be decreased when opening the bypass damper. The principal disadvantage of an air-side bypass is that it requires more space and controls for implementation. The second possibility of controlling the fluid temperature with the bypass valve is probably the most common solution. The bypass valve is also used for frost control, and it allows maintaining temperature and effectiveness control without changing fluid flow rate, what requires a variable speed pump. In case a variable speed pump including a controller is installed, the third option is preeminent since it reduces pumping power demand; a variable speed pump can also used for frost control and 3-way valve is not needed.

Independent of the method of effectiveness reduction, the economizer will be activated when outdoors temperature is higher than the heating point temperature and will control the system effectiveness with rising temperature down to zero when outdoor temperature reaches the balance point. The system will remain shut off with further increasing temperature until the exhaust temperature is below the outdoor temperature. Then the system operates in cooling mode under maximum effectiveness to cool outside air.

Heat Exchanger Equations

The runaround loop is a liquid-coupled counterflow heat exchanger and the following set of equations has been used to model the heat exchanger performance. Equations (5.2), (5.3) and (5.4) describe effectiveness, capacitance rate ratio and NTU for one of the coils, index 1.

$$\varepsilon_1 = \frac{1 - e^{-NTU_1(1-R_{c,1})}}{1 - R_{c,1}e^{-NTU_1(1-R_{c,1})}} \quad (5.2)$$

$$R_{c,1} = \frac{\min(\dot{C}_1, \dot{C}_{liq})}{\max(\dot{C}_1, \dot{C}_{liq})} \quad (5.3)$$

$$NTU_1 = \frac{U_{o,1}A_1}{\dot{C}_{\min,1}} \quad (5.4)$$

$$\dot{C}_{\min} = \min(\dot{C}_1, \dot{C}_2) \quad (5.5)$$

$$\dot{C}_{\min,1} = \min(\dot{C}_1, \dot{C}_{liq}) \quad (5.6)$$

$$\varepsilon_o = \frac{1}{\frac{\dot{C}_{\min}}{\dot{C}_{\min,1}\varepsilon_1} + \frac{\dot{C}_{\min}}{\dot{C}_{\min,2}\varepsilon_2} + \frac{\dot{C}_{\min}}{\dot{C}_{liq}}} \quad (5.7)$$

Equation (5.7) describes the overall effectiveness of two liquid coupled counterflow heat exchanger as derived from equations developed in [14].

The overall coil heat transfer coefficient U_o for a finned tube heat exchanger as is a heating or cooling coil is given with equation (5.8):

$$U_o = \frac{1}{\frac{1}{\eta h_a} + \frac{B}{h_w}} \quad (5.8)$$

Here h_a denominates the air-side heat transfer coefficient (typically about 100 W/m²K), h_w the water-side (typically on the order of 2800 W/m²K), η is the fin efficiency (0.9) and B is the surface area ratio of total coil surface area to inner tube surface area (typical coil data taken from [11]). The fin efficiency is defined as the ratio of actual heat transfer to the heat

transfer that would occur if the entire fin were at base temperature. The fin efficiency of a rectangular fin can be written as

$$\eta = \frac{\tanh \sqrt{2 \frac{h_a}{k\delta} L}}{\sqrt{2 \frac{h_a}{k\delta} L}} \quad (5.9)$$

where k is the thermal conductivity, δ the thickness and L the length of the fin [14].

The air-side heat transfer coefficient of a coil varies as a function of air flow rate and can be obtained from Equation (5.10) and (5.11). Equation (5.11) gives the Stanton number as a function of the Reynolds number (5.12), and has been derived by curve fitting experimental data of Stanton number vs. Reynolds number given in [22]. D_a is the fin spacing, v_a the air velocity and μ_a the viscosity.

$$St = \frac{h_a}{c_{p,a} \rho_a v_a} \quad (5.10)$$

$$St Pr^{2/3} = 0.166 Re^{-0.4} \quad (5.11)$$

$$Re = \frac{v_a D_a}{\mu_a} \quad (5.12)$$

The liquid-side heat transfer coefficient depends on the Reynolds number for the liquid in the coil tubing and can be estimated based on Nusselt number correlation for smooth tubes. For turbulent flow where $Re > 2300$ the Gnielinski Nusselt number correlation modified for developing flow is used [8]. For laminar flow, $Re < 2300$, the Hausen Nusselt number correlation for developing flow is used [8]. Nusselt numbers are chosen for the constant wall temperature boundary condition, since the temperature along the tube and orthogonal to the airflow is assumed constant. The thermal length of the coil tube used in the correlations for developing flow is set equal to two times the length of the coil. The flow pattern will partially redevelop after passing the 180° bending on the ends of the coil.

As shown in **Figure 5.5**, the Nusselt number and hence the convection coefficient is much higher for turbulent flow, to ensure sufficient heat transfer between water and coil, the flow regime should always be turbulent.

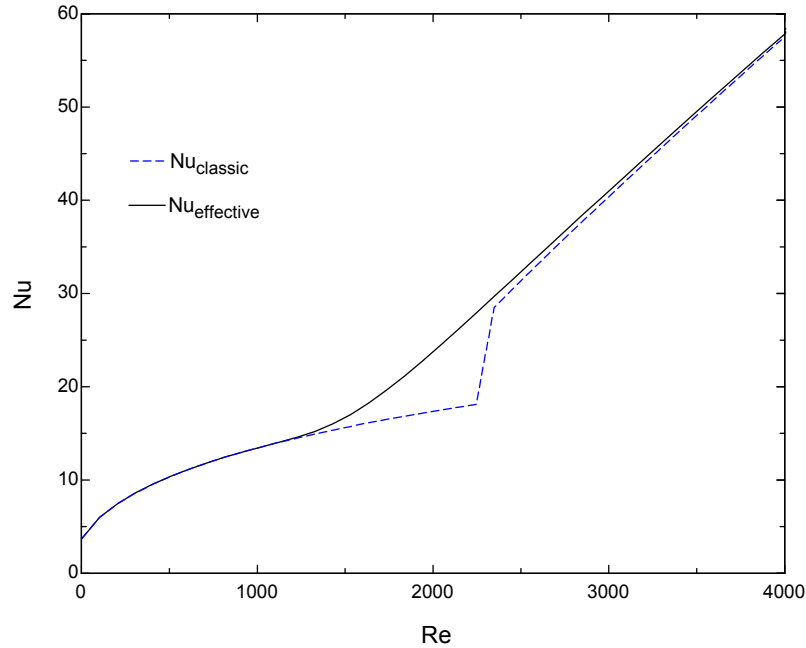


Figure 5.5: Nusselt number as a function of Reynolds number for internal flow in a coil tube

To enhance turbulence in the coil, devices known as “turbulators” can be used. Turbulence-enhancing devices include: twisted tape, spiral inserts, and others that promote turbulence by disturbing the fluid flow pattern and inducing tangential velocity. Pressure drop in coils with turbulators is three times as high at the same flow rate [24] when compared to coils without turbulators. Since the pressure drop is proportional to the square of the velocity, the effective Reynolds Number used in the calculations is increased by a factor of square root of three compared to tubes without turbulators to account for the tangential velocity. The transition of laminar to turbulent flow is assumed to start at Reynolds Numbers as low as 1300, as suggested by comparing the model to experimental data [25, 26]. The effective Nusselt number in the model is calculated with Equation (5.13) to accommodate for enhanced turbulence and shows continuous transition from laminar to fully turbulent:

$$Nu_{effective} = \left(Nu_{laminar}^4 + Nu_{turbulent}^4 \right)^{\frac{1}{4}} \quad (5.13)$$

In **Figure 5.5**, the effective Nusselt number used in the model is compared to the classic Nusselt number for internal flow with a discontinuous jump at the transition at $Re = 2300$.

Verification

A comparison of model-predicted performance and experimental data has been undertaken to verify the mathematical models developed to predict the runaround loop performance. Two sets of experimental data taken from previously published literature are presented here in comparison with data obtained from the model for the same parameters and flow arrangements.

The first set of experimental results comes from “Effectiveness and Pressure Drop Characteristics of Various Types of Air-to-Air Energy Recovery Systems” [25]. The coils of the runaround loop investigated here have 8 rows and 8 circuits and a tubing diameter of 5/16”. The size is 18” by 33” and they have 12 fins per inch made of corrugated aluminum. The simulated and experimental results are shown in **Figure 5.6 – Figure 5.9**.

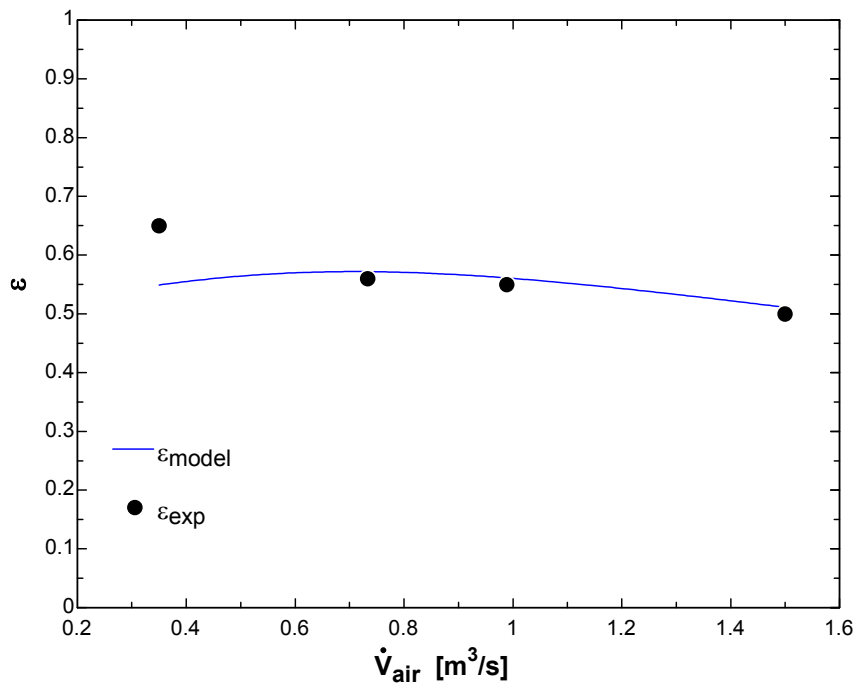


Figure 5.6: Effectiveness versus balanced air flow rate. Transfer fluid flow rate constant 0.63 l/s.

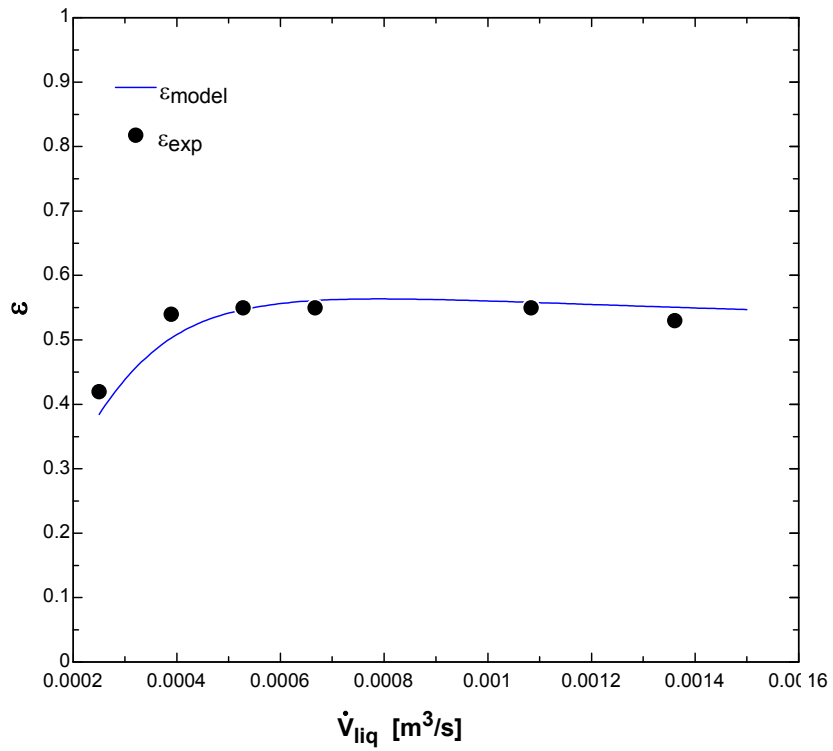


Figure 5.7: Effectiveness versus heat transfer fluid flow rate. Air flow rate balanced 0.966 m³/s.

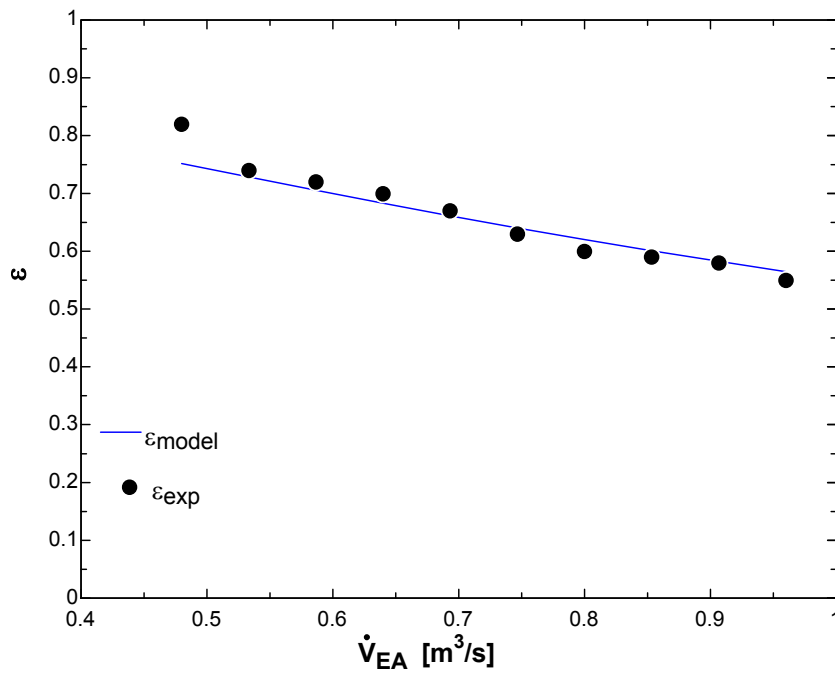


Figure 5.8: Effectiveness for imbalanced flow, outside air flow rate is constant 0.96 m³/s, exhaust air flow rate varies, heat transfer fluid flow rate constant 0.63 l/s.

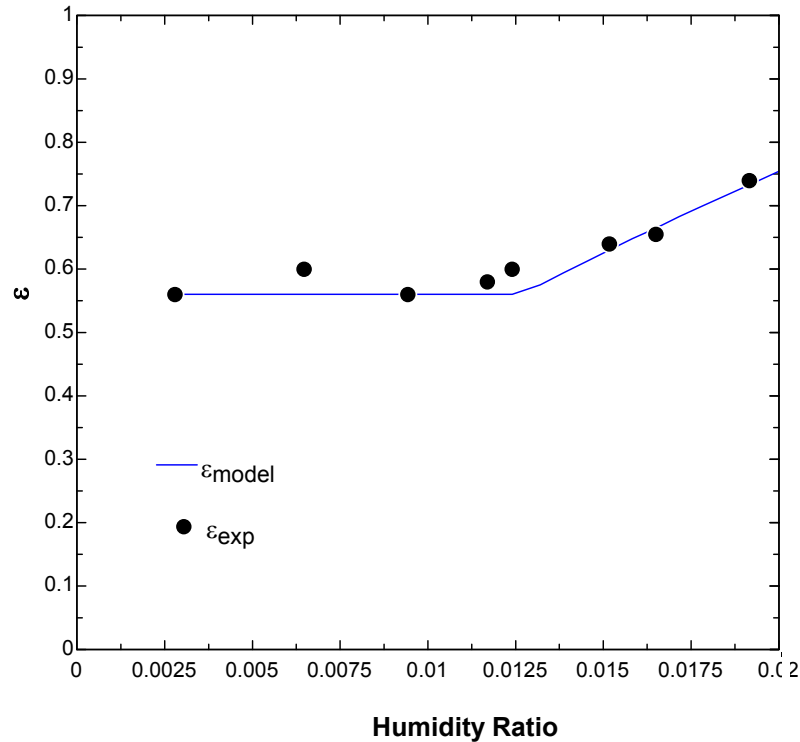


Figure 5.9: The effectiveness changes over humidity ratio (mass of moisture over mass of dry air) when condensation occurs. Condensation in the exhaust coil starts above a humidity ratio of 0.011. Constant air flow rates of $0.95 \text{ m}^3/\text{s}$ and heat transfer fluid flow rate of 0.63 l/s . Exhaust temperature is 26°C , outside air has 5°C .

The second data set originates from “The Performance of a Run-Around Heat Recovery System Using Aqueous Glycol as a Coupling Liquid” [26]. The outside air coil is a 6 row 20 circuit coil with $0.5''$ tubing, 12 corrugated fins per inch and a size of $32.5''$ by $50''$. The exhaust coil has a different size of $29.5''$ by $59''$ and the same parameters. A 50% ethylene glycol solution is used.

For design conditions, the measured effectiveness is given as 0.57 ± 0.02 . The model yields $\epsilon = 0.567$. Intake air flow rate is $2 \text{ m}^3/\text{s}$, while exhaust flow equals $2.7 \text{ m}^3/\text{s}$; the heat transfer fluid flow rate is constant 2.52 l/s . In **Figure 5.10** below the effectiveness for varying transfer fluid flow rate is shown, the air flow rate is balanced $1.9 \text{ m}^3/\text{s}$.

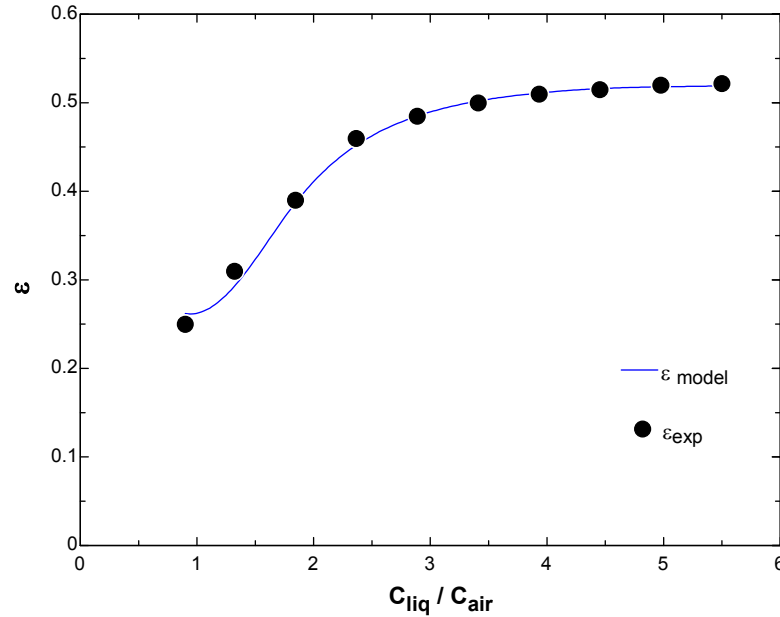


Figure 5.10: Effectiveness versus transfer liquid capacitance rate ratio for balanced air flow rate of $1.9 \text{ m}^3/\text{s}$.

Agreement within 5% or less has been achieved for most data points. However, it can be seen that the inaccuracy of the model increases for operating conditions at low air flow rates or small fluid flow rates. Here the transition of turbulent to laminar flow with significantly decreased heat transfer coefficients dominates the heat transfer resistance of the system. Over the range of normal operation, under optimum effectiveness and rather balanced flow rates, the model agrees $\pm < 1\%$ with the experimental data compared here. Based on the results presented above, the model is considered able to appropriately predict runaround loop performance in computer simulations.

Computer Modeling

To simulate a runaround loop in TRNSYS [10], a computer model has been developed based upon the equations described above.

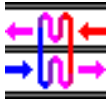


Figure 5.11: TRNSYS icon for the TYPE 223 Runaround Loop Coil Heat Exchanger

The model calculates the outlet states of outside and exhaust air for given inlet conditions and system parameters. Frost control and economizer mode are incorporated. The model is a TRNSYS component called TYPE 223 and has the following basic input variables:

- Intake and exhaust temperatures
- Intake and exhaust relative humidity
- Intake and exhaust volumetric air flow rates
- Liquid flow rate

The parameters of the detailed model encompass all relevant coil data, liquid properties, design pressure drops for airside and liquid system and options for economizer mode and frost control. As an option, a simplified model with a given system effectiveness can be used, which does not need any coil data. Finally, the model outputs incorporate the following variables:

- Outside air temperature [$^{\circ}\text{C}$], relative humidity [%] and humidity ratio
- Exhaust air temperature [$^{\circ}\text{C}$], relative humidity [%] and humidity ratio
- Outside air flow rate [m^3/h]
- Liquid flow rate [m^3/h]
- System effectiveness
- Intake, exhaust and system pressure drop [kPa]
- Additional intake and exhaust Fan Power [kW]
- Pumping power [kW]

- Exchanged heat [kJ/h]
- Preheater energy demand [kJ/h] and Preheater temperature Rise [K]

Outlet State Calculation

The first step in the program towards computation of outlet states is the calculation of the outside and exhaust air coil effectiveness (5.2) based on the given coil parameters and air and liquid flow rates. When simulating a 3-way valve in the runaround loop, the effectiveness equation (5.7) is not valid any longer, since the liquid flow rate in the outside air coil will be lower and the liquid temperature at the exhaust coil will be higher due to the bypass and mixing of warm liquid. A new variable, VC , is introduced (5.14) as a function of the ratio of the intake and exhaust coil liquid capacitance rates for controlling the bypass valve between zero, closed, and unity, fully open.

$$VC = 1 - \frac{\dot{C}_{liq,oa}}{\dot{C}_{liq,ea}} \quad (5.14)$$

To obtain the system effectiveness and outlet states, the effectiveness equations (5.2) for the two coils have to be coupled with the temperatures of the heat transfer liquid:

$$T_{liq,oa,in} = T_{liq,ea,out} \quad (5.15)$$

$$T_{liq,ea,in} = \frac{\dot{C}_{liq,oa} T_{liq,oa,out} + VC \cdot \dot{C}_{liq,ea} T_{liq,ea,out}}{\dot{C}_{liq,ea}} \quad (5.16)$$

The outside air coil outlet temperature $T_{oa,out}$ (5.17) can be calculated rearranging the coil effectiveness when the liquid temperature $T_{liq,oa,in}$ (5.18) is known:

$$T_{oa,out} = T_{oa,in} + \varepsilon_{oa} \dot{C}_{min,oa} / \dot{C}_{oa} (T_{liq,oa,in} - T_{oa,in}) \quad (5.17)$$

$$T_{liq,oa,in} = \frac{T_{oa,in} \frac{\epsilon_{oa} \dot{C}_{min,oa}}{\dot{C}_{liq,ea}} \left[\frac{\epsilon_{ea} \dot{C}_{min,ea}}{\dot{C}_{liq,ea}} - 1 \right] - T_{ea,in} \frac{\epsilon_{ea} \dot{C}_{min,ea}}{\dot{C}_{liq,ea}}}{\left[\frac{\epsilon_{oa} \dot{C}_{min,oa}}{\dot{C}_{liq,ea}} - \frac{\dot{C}_{liq,oa}}{\dot{C}_{liq,ea}} - VC \right] - \left[\frac{\epsilon_{ea} \dot{C}_{min,ea}}{\dot{C}_{liq,ea}} - 1 \right] - 1} \quad (5.18)$$

Once the outside air outlet temperature $T_{oa,out}$ is known, the exchanged heat Q_{xch} can be calculated:

$$Q_{xch} = \dot{C}_{oa} (T_{oa,out} - T_{oa,in}) \quad (5.19)$$

From there on, all other outputs can be calculated based on the inlet temperatures, for the next step especially $T_{ea,out}$ and the humidity ratio $w_{ea,out}$ of mass of moisture over mass of dry exhaust air is of interest.

Wet Coil Analyses

The calculation procedure above can only be applied when transferring sensible heat only. When during winter operation humidity in the exhaust stream condenses, latent heat is added to the fluid from the exhaust coil, causing overall effectiveness to increase and temperatures to rise. To check for condensation, the saturation humidity ratio for the exhaust temperature $T_{ea,out}$ is compared to the exhaust inlet humidity ratio $w_{ea,in}$. If the saturation humidity ratio is lower than $w_{ea,in}$, condensation will occur in the coil. In case of condensation in the exhaust coil, the equations based on the dry surface effectiveness of the exhaust coil and the heat capacity rate \dot{C}_{ea} are not suitable anymore. Rather than temperature, the computations to obtain effectiveness and outlet states rely on enthalpy.

The wet coil effectiveness (5.20) is defined [20, 21] as the actual enthalpy difference of the air entering and leaving the coil, $h_{ea,in} - h_{ea,out}$, divided by the difference of $h_{ea,in}$ and the enthalpy of saturated air $h_{ea,sat}$ at the entering liquid temperature $T_{liq,ea,in}$, which is the minimum possible enthalpy of the leaving air and is given as a curve fit with equation (5.21):

$$\epsilon_{wet} = \frac{h_{ea,in} - h_{ea,out}}{h_{ea,in} - h_{ea,sat}} \quad (5.20)$$

$$h_{ea,sat} = 9.2127 + 1.83256 T_{liq,ea,in} + 0.024948 T_{liq,ea,in}^2 \quad (5.21)$$

Based on an analogy to the dry coil effectiveness, when given the number of transfer units for the wet coil, the effectiveness of the wet coil **(5.22)** can be determined with a counterflow heat exchanger effectiveness equation, as described in [20]:

$$\mathcal{E}_{wet} = \frac{1 - e^{-NTU_{wet}(1-m^*)}}{1 - m^* e^{-NTU_{wet}(1-m^*)}} \quad (5.22)$$

The overall number of transfer units for the wet coil includes sensible and latent heat transfer. The air side and the liquid side heat transfer coefficients with the surface area ratio B and the heat capacity rate of the exhaust air plus the rate of enthalpy change due to condensation are comprised here; the number of transfer units is based upon enthalpy and may be written as derived from [20] as:

$$NTU_{wet} = \frac{h_{ea} A_{coil,ea}}{\dot{C}_{ea} + m^* \dot{C}_{liq,ea} \frac{h_{ea} B}{h_{liq,ea}}} \quad (5.23)$$

The capacitance ratio m^* appearing in these two equations is the ratio of the capacitance rate of the air at saturation while condensation occurs to the capacitance rate of the liquid:

$$m^* = \frac{\dot{m}_{ea} C_s}{\dot{C}_{liq,ea}} \quad (5.24)$$

Here C_s is defined as the change of the enthalpy of the air at the saturation curve over the change of the liquid temperature passing through a cooling coil. It is evaluated at the arithmetic mean liquid temperature $(T_{liq,ea,in} + T_{liq,ea,out}) / 2$ for the complete wet coil:

$$C_s = \left. \frac{dh_{sat,T_{liq,ea}}}{dT} \right|_{T_{liq,ea}} \quad (5.25)$$

By differentiation of the saturation enthalpy for standard pressure moist air over a temperature range from -10°C to 20°C and linear regression, C_s [J/kgK] as a function of temperature T [°C] has been found to be:

$$C_s = 1735.18279 + 42.9767108 T + 1.05363412 T^2 + 0.0494449332 T^3 \quad (5.26)$$

Since the liquid temperatures appear in the properties $h_{ea,sat}$ and C_s before the temperatures are known and both are needed to solve the effectiveness equations (5.20) and (5.22), the coupled heat exchanger equations cannot be solved analytically. An iterative approach to the solution must be taken.

As an estimate to start the iteration, an exhaust temperature is calculated as a mean value of two theoretical exhaust outlet temperatures. One is the temperature previously obtained under the assumption the coil would be dry, before checking for condensation, and the other one is calculated based on the simplified postulation that the effectiveness stays the same when exhaust humidity condenses in the coil [13]. The enthalpy of the exhaust air outlet is calculated by setting Q_{xch} equal to the exhaust air enthalpy change, assuming in a first step that the effectiveness stays constant:

$$Q_{xch} = Flow_{ea} \rho_{ea} (h_{ea,in} - h_{ea,out}) \quad (5.27)$$

Based on the exhaust outlet enthalpy $h_{ea,out}$ and the supposition that in case of condensation the air leaving the exhaust coil will be 99.9% saturated, the temperature can be computed using a curve fit equation:

$$T_{ea,out,2} = -5.9765 + 0.66484664 h_{ea,out} - 0.003841278 h_{ea,out}^2 \quad (5.28)$$

While the first temperature from the dry coil analysis is too low because of the latent heat transfer, $T_{ea,out,2}$ will be too high, the heat transfer Q_{xch} for the wet coil along with the effectiveness will be higher, lowering the outlet temperature. The real outlet temperature is in between those two numbers; as a good approximation $T_{ea,out} = 0.25 T_{ea,out,1} + 0.75 T_{ea,out,2}$ has been found by comparison of this number to the iterative solution of the outlet temperature. This temperature is used to calculate a new value of Q_{xch} , which, along with the air and liquid temperatures calculated based on it, is a first estimate used for the iterative solution for all

temperatures and the effectiveness of the wet coil. This temperature is also been used to calculate outlet states for the simplified model, when only the air inlet states and as a parameter the overall system effectiveness without condensation are known.

In the iteration loop, which starts with the estimates of $T_{liq,ea,in}$ and $T_{liq,ea,out}$ to obtain estimates $H_{ea,sat}$ and C_s , equations (5.23), (5.22), (5.20) are consecutively solved to get a new value of Q_{xch} by solving (5.27), and henceforth (5.28), (5.29), (5.30), (5.31), (5.16) and (5.32) for new temperatures.

$$T_{oa,out} = T_{oa,in} + Q_{xch} / \dot{C}_{oa} \quad (5.29)$$

$$T_{liq,oa,in} = \frac{Q_{xch}}{\varepsilon_{oa} \dot{C}_{min,oa}} + T_{oa,in} \quad (5.30)$$

$$T_{liq,oa,out} = T_{liq,oa,in} - Q_{xch} / \dot{C}_{liq,oa} \quad (5.31)$$

$$T_{liq,ea,out} = T_{liq,ea,in} + Q_{xch} / \dot{C}_{liq,ea} \quad (5.32)$$

The iteration process has not been found to be stable and convergent for any given coil parameters and inlet conditions, unless using the mean values of the old and current liquid temperatures $T_{liq,ea,in}$ and $T_{liq,ea,out}$ as new values to obtain new property values $H_{ea,sat}$ and C_s for the next step. The iteration loop is continued until the difference of the liquid temperatures $T_{liq,ea,out}$ leaving the exhaust coil and $T_{liq,oa,in}$ entering the outside air coil is within a tolerance of +/- 0.01K. Convergence is usually achieved within 5 to 10 iteration steps.

Under conditions when the coil is only partially wet, i.e. condensation takes place only on the colder part of the coil surface and the coil inlet stays above the dew point, the wet coil effectiveness analysis may not yield the exact solution, but instead under-predict the effectiveness. In that case, the heat transfer Q_{xch} obtained with the wet coil analysis may be lower than the Q_{xch} calculated before under the assumption of a dry coil. Depending on which of the values is higher, either the results for the wet or the dry coil analysis are taken as more accurate and used [20]. However, when the wet coil model yields a higher $T_{ea,out}$ but a lower effectiveness, the mean value of the dry coil and wet coil outlet temperatures is used.

The humidity ratio of the leaving exhaust air in case of condensation will be saturated and is set to a value corresponding to 99.9% relative humidity by calling the psychrometric subroutine in TRNSYS. If no condensation occurs, $T_{ea,out}$ is calculated with the exhaust coil effectiveness equation, the humidity ratio $w_{ea,out}$ is set equal to the humidity ratio of the exhaust inlet. The same applies to the outside air humidity ratio, after checking for possible condensation, in which case it would be set to the saturation humidity ratio, it is set equal to the inlet value $w_{oa,in}$, and a corresponding relative humidity $RH_{oa,out}$ is calculated by calling the psychrometric subroutine.

Frost Control

After computing the exhaust air outlet state, the next step in the program is to determine if frosting conditions exist when condensation occurs or when the coil surface temperature falls below the dew point of the leaving exhaust air. The surface temperature of the coldest part of the exhaust coil then has to be above freezing point to prevent frost buildup in the coil. The temperature is a function of the entering liquid temperature $T_{liq,ea,in}$ (5.16), the coil parameters and the exhaust outlet temperature as derived from Fourier's steady state convection equation $Q = hA\Delta T$:

$$T_{coil,ea} = \frac{T_{ea,out} B \frac{h_{ea}}{h_{liq,ea}} + T_{liq,ea,in}}{B \frac{h_{ea}}{h_{liq,ea}} + 1} \quad (5.33)$$

If this temperature is below 0°C and below the dew point, the user-specified frost control strategy is applied:

1. In case of preheating, the intake air temperature will be raised by 1K
2. If frost control by 3-way valve operation, the valve will be opened by a 2.5% increase of VC
3. When the liquid flow rate is to be varied, liquid flow will be reduced by 5%

The program then jumps back to calculate the effectiveness and the outlet states again, and this feedback loop is continued until either no condensation occurs or the coil temperature stays above freezing. Then the final outlet states of outside and exhaust air will be calculated.

Economizer Control

When outside air temperatures are above the heating temperature of the building, the economizer is enabled to lower the effectiveness. The system effectiveness is linearly decreased for outside temperatures between heating temperature and balance point temperature, according to the value of an economizer control variable defined as:

$$CONTROL = (T_{balance} - T_{oa,in}) / (T_{balance} - T_{heat}) \quad (5.34)$$

In case outside temperature is between balance point and exhaust temperature, *CONTROL* is set to zero and system remains shut off. The economizer control works in a loop: after calculating the system effectiveness ε_{des} for normal operation, the program reduces the effectiveness according to the user chosen economizer strategy by either

- opening the 3-way valve by increasing *VC* by 2.5%, or
- reducing liquid flow rate by 5%

Then the new system effectiveness ε is calculated and compared to ε_{des} . This loop continues until the condition of $\varepsilon / \varepsilon_{des} < CONTROL$ is met, then the outlet states are finally calculated.

Fan and Pump Power

The additional fan power needed to overcome the added air-side pressure drop caused by the coils, and the parasitic pumping power are calculated in the last step of the program. Air pressure drop across the coils is approximately proportional to the velocity ratio to the power of 1.7. This exponent is derived from curve fitting catalog data [24. 27] from various coils and agrees within a deviation <15 % for a velocity ratio of < 4 for all analyzed coils and different types of fins. Having design pressure drop and design face velocity, actual pressure drop Δp can be calculated as follows:

$$\Delta p = \Delta p_{design} (V_{air}/V_{air,design})^{1.7} \quad (5.35)$$

To obtain the fan power necessary to overcome the pressure drop, the pressure drop is multiplied with the air flow rate and divided by the fan efficiency:

$$Fanpower = 1/\eta_{Fan} \Delta p Flow_{air} \quad (5.36)$$

Calculation of the pumping power for the heat transfer liquid is similar. The pressure drop in the loop and the coils is proportional to the square of the flow rate ratio, an assumption valid for turbulent flow and backed by data from coil catalogs [24, 27]:

$$\Delta p_{liq} = \Delta p_{liq,design} (Flow_{liq}/Flow_{liq,design})^2 \quad (5.37)$$

$$Pumppower = 1/\eta_{Pump} \Delta p_{liq} Flow_{liq} \quad (5.38)$$

In case the 3-way valve is operated, the pressure drop is lower since only a part of the total liquid flow goes through the outside air coil. The pumping power will be calculated under the assumption that the pressure drop in the connecting tubing and the bypass is negligible and the two coils have the same pressure drop at same flow. Equation (5.38) then transforms into (5.39), taking into account that the pressure drop in the outside air coil decreases with the second power of the liquid flow:

$$Pumppower = 1/\eta_{Pump} (\Delta p_{liq}/2 Flow_{liq,ea} + \Delta p_{liq}/2 (1-VC)^2 Flow_{liq,oa}) \quad (5.39)$$

The entire FORTRAN source code for TRNSYS Type 223 is listed in Appendix B.

Output Plots

TRNSYS Output plots for typical runaround loop applications are below in **Figure 5.12**, **Figure 5.13** and **Figure 5.14**. The parameters for the system are the same as in the system used for the verification shown in **Figure 5.6**, but air flow rate is balanced and constant 0.96 m³/s, liquid flow rate is 0.63 l/s.

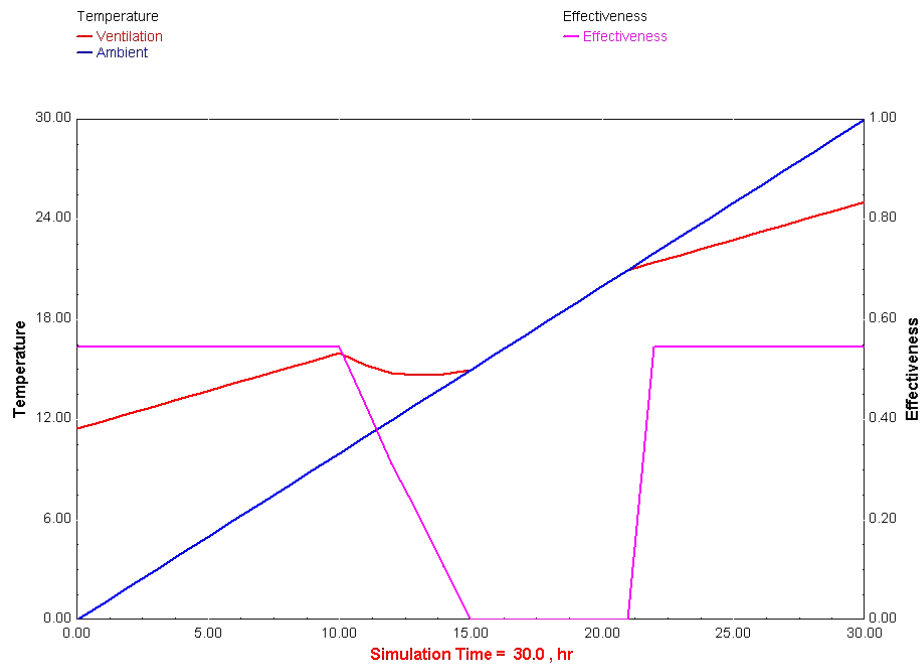


Figure 5.12: Operation of the economizer: for outside air temperatures above the heating point of 10°C, the effectiveness is decreased, above the balance point of 15°C the system remains off, until the ambient temperature is higher than the exhaust temperature of 21°C. The economizer controls the liquid flow rate between zero and 0.63 l/s. Exhaust conditions are constant 21°C, 30% RH, while the outside temperature increases from 0°C to 30°C

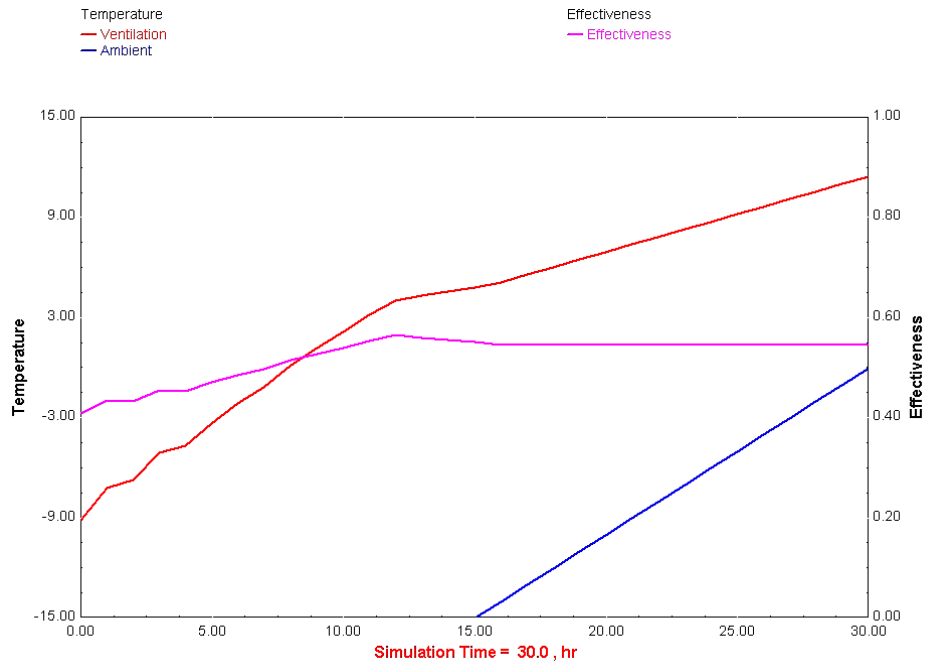


Figure 5.13: operation of the frost controller: below an ambient temperature of -18°C , the 3-way valve opens and maintains the coil temperature above the dew point, while the effectiveness is significantly reduced. Exhaust conditions are 21°C , 30% RH, while the outside temperature increases from -30°C to 0°C .

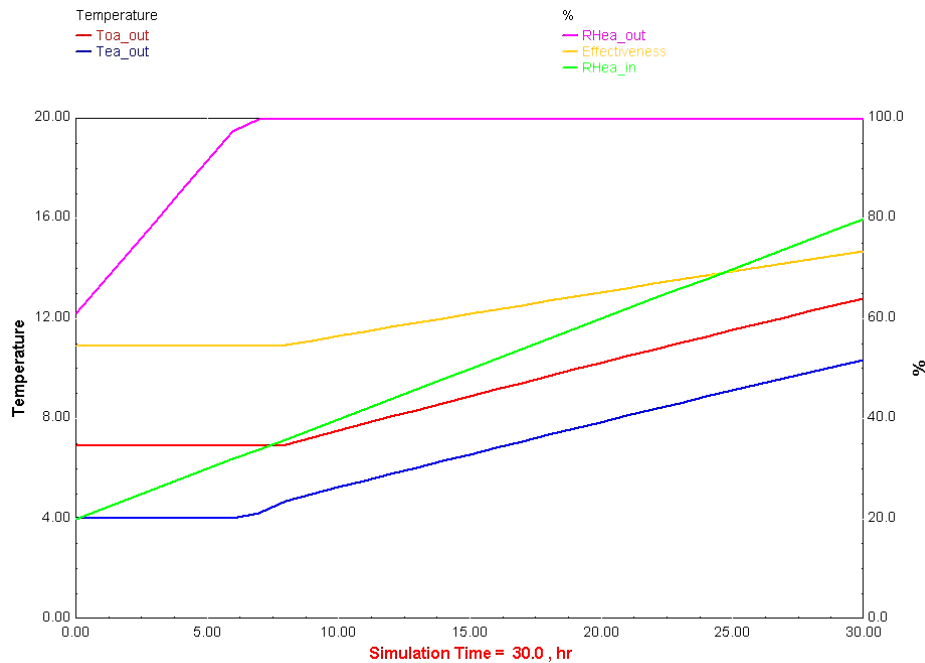


Figure 5.14: Temperatures and effectiveness for exhaust air relative humidity rising from 20% to 80%. Exhaust air inlet temperature constant 21°C , ambient air -10°C .

Chapter 6 Simulations of the Primate House

Validation of the Simulation Model

The first step upon completion of the Primate House TRNSYS Type 56 model is to validate the model. The Primate House model is validated by comparing the simulation results with actual energy consumption measured at the facility. Energy use data over both short-term (3 days, 1 week) and long-term (1 year) intervals provided a basis for comparison with the model. The year 1999 was chosen as a reference period for the simulation since actual gas and electric use data were available and no anomalies in HVAC system operation occurred in 1999. Unlike during later years, the system worked as designed, no unexplained changes in control settings as happened in 2001 have to be taken into account for the simulation. For the 1999 calendar year complete weather data were available, as well as monthly utility bills for the gas and electric consumption. Since the Type 56 model outputs are energy demands in kJ/h and do not include the efficiency of the real HVAC equipment, the utility bill data were processed to obtain estimates of the actual monthly heating and cooling loads for the building.

To calculate the cooling energy from the electric bill, the portion of electric energy consumed by the air-conditioning system and the average COP of the A/C system must be known. The portion of electric energy consumed by the A/C system has been calculated by subtraction of non-A/C related energy from the monthly electric bill. This amount of energy can be estimated by the sum of electric consumption known from the internal gains calculation and from the consumption in winter months, when the condensing units remain off. An average value of 21,244 kWh/month of non-A/C related electric consumption has been found for 1999. The yearly average COP of the condensing units was estimated at 2.8, based on manufacturers data [Carrier, 1995] for the low part load operating conditions of the units. Given the A/C related electric consumption and the COP, the value of A/C energy demand of the building in kJ/month can be calculated.

To calculate the actual heating load of the building, the amount of natural gas used was multiplied by the lower heating value and the efficiency of the boilers. The efficiency depends on the part-load ratio of the boilers. For the January with highest heating demand, average of 614,000 kJ/h, efficiency is estimated at 0.88, and for the winter months of February, March and December with lower demand, average about 350000 kJ/h, 0.85. For the rest of the year heating demand was below 163000 kJ/h, and efficiency is estimated at 0.8 for the boilers while cycling on and off at low part load conditions.

The temperature, maximum relative humidity set points and air change rates for the simulation were set to the following standard values:

- Zone 1: 20°C, 60%, 2.4 ACH
- Zone 2: 23°C, 60%, 1.4 ACH
- Zone 3: 23°C, 60%, 2.68 ACH
- Zone 4: 23°C, 60%, 1.7 ACH

These temperatures are up to 5°C lower than the values measured early in 2001, when the system was out of control but about 1°C higher in Zones 2, 3, and 4 and 3°C higher in Zone 1 than the more conservative settings established later in 2001 to conserve energy. Internal loads and humidity gains are set as described in chapter Building Simulation.

A comparison of the simulation results and the data derived from actual billing data in 1999 is listed in the **Table 6.1** below and plotted in **Figure 6.1**.

Month	Heating, model	Cooling, model	Heating, billing	Cooling, billing
1	424006436	16011	448164167	0
2	236590592	98570	278815431	0
3	237792538	43052	258278688	0
4	116398463	3364321	119517197	0
5	47988047	22714114	31229776	19712000
6	13297396	96784560	2447739	89062400
7	1535453	181530810	2363334	198732800
8	3946085	175788313	2954168	242278400
9	26795173	67165885	3038573	26163200
10	81639422	11589156	101538974	0
11	129638046	2620182	98247187	0
12	246774516	158677	253256602	0
Sum [kJ]	1550200467	575228980	1599851837	575948800
Difference [%]	3.1	0.1	0.0	0.0

Table 6.1: Simulated and billed energy consumption for 1999

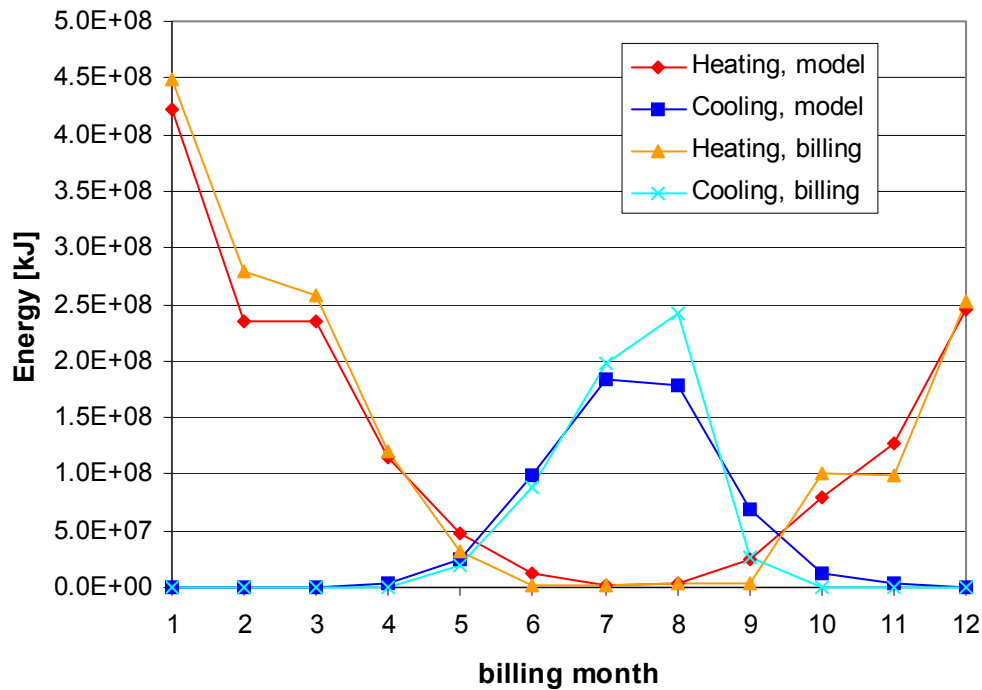


Figure 6.1: Simulated and billed energy consumption for 1999

The Simulation results show good agreement in energy consumption over the entire period of simulation. However, for some months with very low heating demand, e.g. May and

September, the heating energy demand yielded by the model does not reflect the actual consumption. It is likely that during these times the operation schedule of the HVAC system changed and that the indoor temperature may have floated.

To further validate the model, two short-term simulations have been carried out, one for winter, **Figure 6.2**, and one for summer, **Figure 6.3**. The energy demand yielded by the simulation is compared to hourly averaged measurements of gas and electric consumption from the utility, respectively. Again, these data have been processed to obtain the building's heating load and the condensing unit's electric power, thereby the following assumptions have been made:

- Lower heating value of the gas 1000 BTU/ft³ (as obtained by the local utility during the gas consumption measurement period),
- boiler efficiency constant at 0.88.
- The COP of the condensing units is assumed to be constant 3. Non A/C electric consumption of the building averagely 35 kW from 8:30 AM to 16:45 PM when lights are on and 30 kW for the remaining time. The difference of this estimate of non A/C electric consumption and the measured total building load is taken as the condensing unit's load.

The input data used in these simulations are hourly weather data from Madison and average zone temperatures coincidentally measured with data loggers during the time period of the simulation. For February 2002 the averaged zone temperatures were 16.6°C for Zone 1 and 22.2°C for all other zones.

For the July simulation, the cooling set point temperatures and the maximum relative humidity limits are set to the average of the measured values for return air and are based on supply air conditions in the zones:

- Zone 1: 23.2°C, 80%
- Zone 2: 23.6°C, 68%

- Zone 3: 23.1°C, 70%
- Zone 4: 24.2°C, 75%

Ventilation rates and infiltration, as well as internal gains, for these simulations are the same values as used in the previous simulation for 1999.

Figure 6.2 shows the heating load of the building calculated with hourly time steps. The curve based on measured gas consumption and the assumptions described above follows the simulated heating load very close for the first day. For the next two days, which were warmer, the model predicted consumption is lower than the measurements suggest. The model predicted total demand over the period of three days is 15% below the measured consumption of 30,207 MJ.

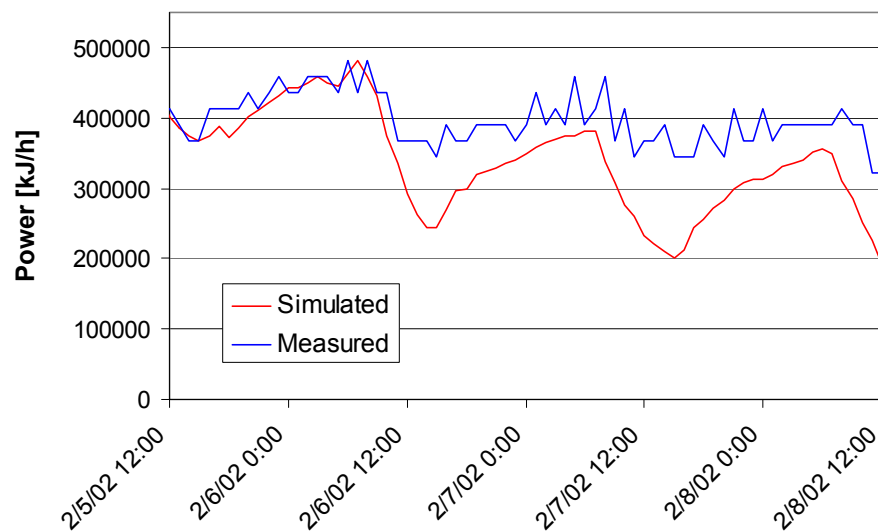


Figure 6.2: Heating power for February 5-8 '02, comparison between simulated and measured data

In **Figure 6.3** the simulated and estimated electric energy demand for the condensing units is compared. The simulation results yield a curve primarily following the measured curve but showing no hourly peaks, instead the model-predicted cooling power demand averages over time to a smooth curve. This leads to the conclusion, that implementation of TRNSYS Type

56 simulations for this investigation are not capable of predicting of instantaneous electric energy demand of cooling equipment since hourly time steps are employed. However, the integrated energy for July 15 – 22 sums up to 4008 kWh estimated based on the measurements, while the model predicts 4236 kWh, or 5% more. Uncertainties for the estimated condensing unit power are on the order of 5 kW, since the actual non-A/C related power demand can only be roughly estimated, and will vary due to equipment that cycles on and off like the walk-in freezer condensing unit. These variations can also appear in the hourly electric peak loads and falsify points of the curve.

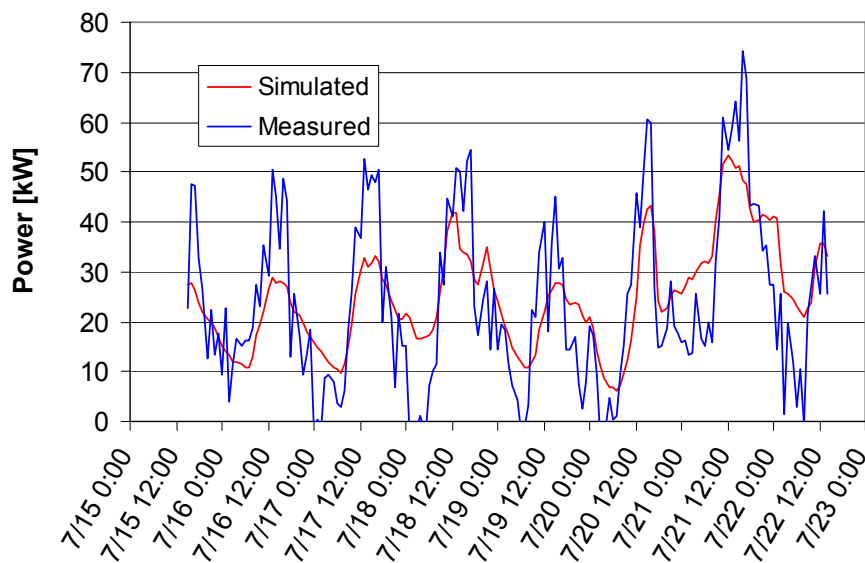


Figure 6.3: Cooling power for July 15-22 '02, comparison between simulated and measured data

The comparison of the energy consumption estimated based on utility bills and field measurements with simulated energy demand from the Type 56 model for heating as well as for cooling shows in general agreement within less than 5% for long term simulations. The model is therefore considered to be appropriately reflecting the energy consumption of the Primate House for long term simulations.

To investigate the effect of different annually weather data on the energy consumption of the building, a simulation using 1999 weather data is compared to a simulation run driven by weather data from a Typical Meteorological Year for Madison. The Typical Meteorological Year (TMY) is a table of hourly weather data, which is representative of the long-term average for a give location. Since it is composed of historic weather data taken from a number of years in the past, it will not be reflective of any climate change effects. However, the TMY is the best representation of the weather for an average year, hence it is best suited for simulations intended to predict future energy consumption for buildings. The reason the TMY data are not used in most simulations here is that the simulated energy demand is compared to the actual energy usage in 1999. As it can be seen in **Table 6.2** and **Figure 6.4**, the heating energy usage under TMY is 6% higher than the usage predicted for 1999. The cooling energy prediction for the TMY simulation is 23% lower. Overall, 1999 was a warmer year than the TMY. It is concluded, that the year 1999 reflects anticipated weather conditions well enough to be used for simulations, even though it differs from TMY for the cooling season.

	Heating TMY	Cooling TMY	Heating 1999	Cooling 1999
Sum [kJ]	1,656,679,269	466,742,472	1,550,200,467	575,228,980
Difference TMY to 1999 [%]	6.4	-23.2	0.0	0.0

Table 6.2: Comparison of results for 1999 and TMY weather data

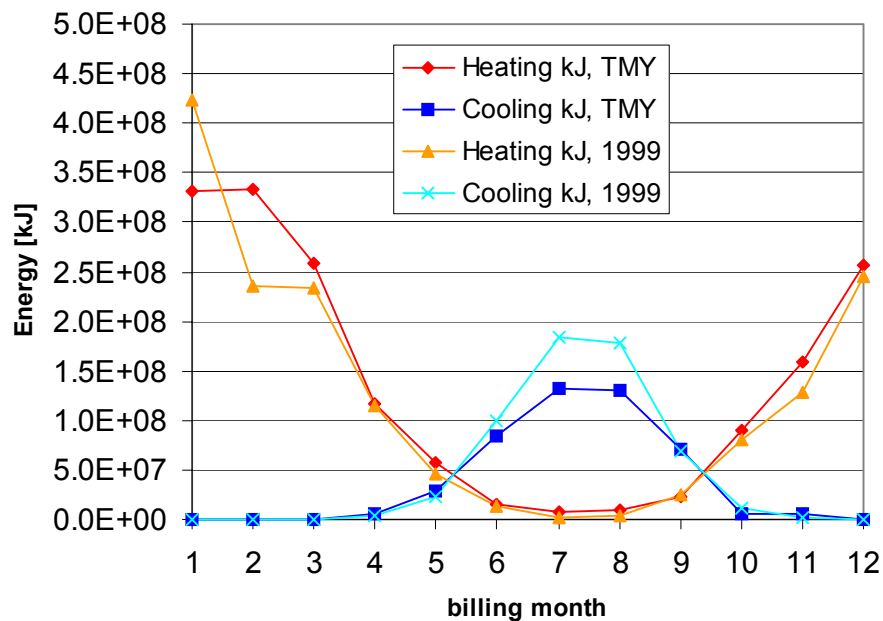


Figure 6.4: Simulation results for 1999 and TMY weather data

Simulation of the HVAC system including Enthalpy Exchangers

Air-to-air energy recovery equipment can save energy in ventilated buildings by reducing heating and cooling loads attributable to outside air. The effect of adding enthalpy exchangers to the HVAC system of the Primate House is studied in this section. The simulation model for the enthalpy exchangers is the TRNSYS Type 222, as described in chapter 4. Each air-handling unit is equipped with a rotary enthalpy exchanger designed to recover both sensible and latent energy from the exhaust air stream. The size of the units is chosen so that the actual air flow rate is within the lower third of the range of the applicable flowrates, resulting in a low pressure loss of about 0.2 kPa and high effectiveness of about 80%.

The enthalpy exchanger data used in this example is taken from a catalog [12] for the following models:

- Zone 1: Airxchange ERC-2511
- Zone 2 and 4: Airxchange ERC-3615
- Zone 3: Airxchange ERC-5856

To prevent the building from overheating during mild temperatures when no heat recovery is required and minimize cooling loads, the enthalpy exchangers operate at economizer mode with decreased or zero effectiveness when outdoors temperature is above the following heating point respectively balance point temperatures:

- Zone 1: 5°C, 15°C
- Zone 2: 7°C, 15°C
- Zone 3: 9°C, day 16°C / night 18°C
- Zone 4: 7°C, day 14°C / night 17°C

The temperature and humidity settings as well as the internal loads are the standard settings and the same as in the first simulation for 1999:

- Zone 2, 3 and 4: 23°C, 60%
- Zone 1: 20°C, 60%

Results of this simulation are listed in the **Table 6.3** and plotted in **Figure 6.5**. They are compared to the previous simulated data for 1999 without energy recovery.

Month	Heating, with EX	Cooling, with EX	Heating, normal	Cooling, normal
1	129200712	541436	422850292	19336
2	59006559	553451	234858972	100271
3	51020452	1178886	234108674	39127
4	18238774	5261261	114460093	3613211
5	6381980	25704514	46921245	23869012
6	1273160	78207820	12661806	99761817
7	116027	127608487	1410551	184545503
8	868208	124631546	3786056	178554251
9	2682280	57813158	25592887	69541499
10	12502522	15768029	80029981	12209155
11	24145084	5365728	127474404	2814345
12	62626250	876026	246045506	161455
Sum [kJ]	368,062,006	443,510,341	1,550,200,467	575,228,980
Savings [%]	76.3	22.9	0.0	0.0
Max. Load [kJ/h]	284,633	444,641	824,922	829,802
Savings [%]	65.5	46.4	0.0	0.0

Table 6.3: HVAC energy consumption with and without enthalpy exchangers (EX)

As the simulation shows, savings of heating energy can be as high as 76% and the savings potential of cooling energy of 23% when enthalpy exchangers are included in the space-conditioning systems serving the Primate House. The economizers reduce the cooling energy demand by 21% compared to continuous operation of the enthalpy exchangers.

The maximal hourly load can be reduced by 66% for heating and 46% for cooling. These results suggest that the heating and cooling capacity of the current HVAC system would be greatly oversized if energy recovery equipment were installed. The efficiency of oversized systems will be somewhat lower due to lower part load ratio over a longer period of operation.

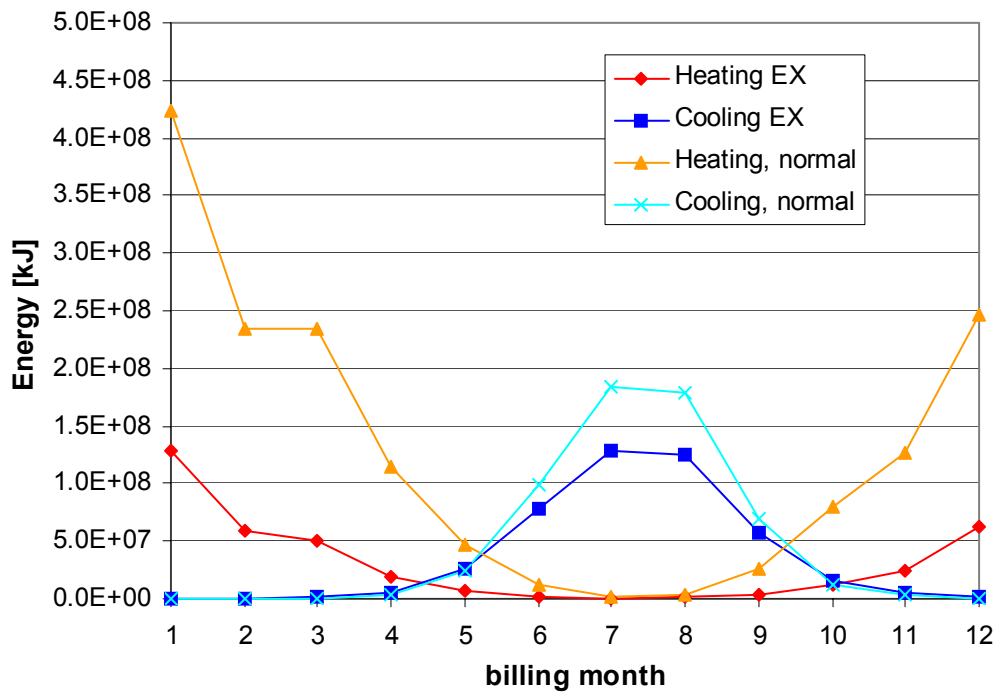


Figure 6.5: HVAC energy consumption with and without enthalpy exchangers (EX)

Additional electric energy used by the fan systems to overcome the added pressure drop of the enthalpy exchangers sums up to 20,950 kWh per year assuming a fan efficiency of 0.5. This additional energy use has to be taken into account in the economic analysis.

An outside air preheater is required to prevent frost buildup on the energy recovery ventilator heat exchanger during cold weather operation. The outside air preheater operates in Zone 1 for 35 h during cold nights in January and 6 h in December, requiring a total of 110,000 kJ; for Zone 2 the preheater runs for 2 h and consumes 850 kJ. The preheater energy demand for the simulated year 1999 sums up to 31 kWh.

Simulation of the HVAC system including Runaround Loops

Although the application of enthalpy exchange results in a significant decrease in the heating and cooling loads, it may be difficult to retrofit the HVAC equipment in the Primate House since enthalpy exchanger require adjacent intake and exhaust ducts. An alternative option of energy recovery are runaround loops, which are considered in this section. In this and a following simulation, the HVAC system is equipped with runaround loop heat exchangers between the exhaust and the intake ducts for energy recovery. The runaround loops are simulated with TRNSYS Type 223. Details of the system for each zone are given in **Table 6.4**, coil data from [24, 27]. The heat transfer liquid flowrate is optimized for maximal effectiveness using an EES [11] program. This results in a liquid velocity of about 1.4 m/s; tube diameter is 5/16", spring-type turbulators are used. Coil dimensions are chosen so that the face air velocity fo the coils is about 2.5 m/s, resulting in a pressure drop of 200 Pa.

Zone	1	2	3	4
Coil width [in]	12	18	30	12
Coil length [in]	16	20	38	24
Rows	8	8	8	8
Circuits	8	12	20	8
Air flow rates [m ³ /s]	0.3	0.56	1.86	0.47
Liquid flow rate [l/s]	0.6	0.84	1.38	0.57
Liquid-side pressure drop [kPa]	84	78	117	84
Effectiveness	0.526	0.536	0.578	0.54

Table 6.4: Parameter of the runaround loop systems

Temperature and dehumidification setpoints and internal loads are according to the normal configuration and the same as in previous simulations. Economizer settings for heating point and balance point respectively are the following temperatures:

- Zone 1: 5°C, 12°C

- Zone 2: 14°C, 16°C
- Zone 3: 11°C, 17°C day / 18°C night
- Zone 4: 10°C, 14°C day / 17°C night

Economizer control as well as frost control is realized with 3-way bypass valves.

The results of this simulation are shown in **Table 6.5** and **Figure 6.6** and energy consumption is compared to the normal configuration:

Month	Heating, RL	Cooling, RL	Heating, normal	Cooling, normal
1	217610954	19336	422850292	19336
2	110522211	99229	234858972	100271
3	103973655	89065	234108674	39127
4	41861067	4156249	114460093	3613211
5	12932881	25778759	46921245	23869012
6	2703896	96385546	12661806	99761817
7	150066	175351800	1410551	184545503
8	1000418	170456674	3786056	178554251
9	6329351	69072901	25592887	69541499
10	27231893	13956783	80029981	12209155
11	50441438	3542951	127474404	2814345
12	115586704	193596	246045506	161455
Sum [kJ]	690,344,533	559,102,890	1,550,200,467	575,228,980
Savings [%]	55.5	2.8	0.0	0.0
Max. Load [kJ/h]	445,362	758,823	817,978	842,547
Savings [%]	45.6	9.9	0.0	0.0

Table 6.5: HVAC energy consumption with and without runaround loops (RL)

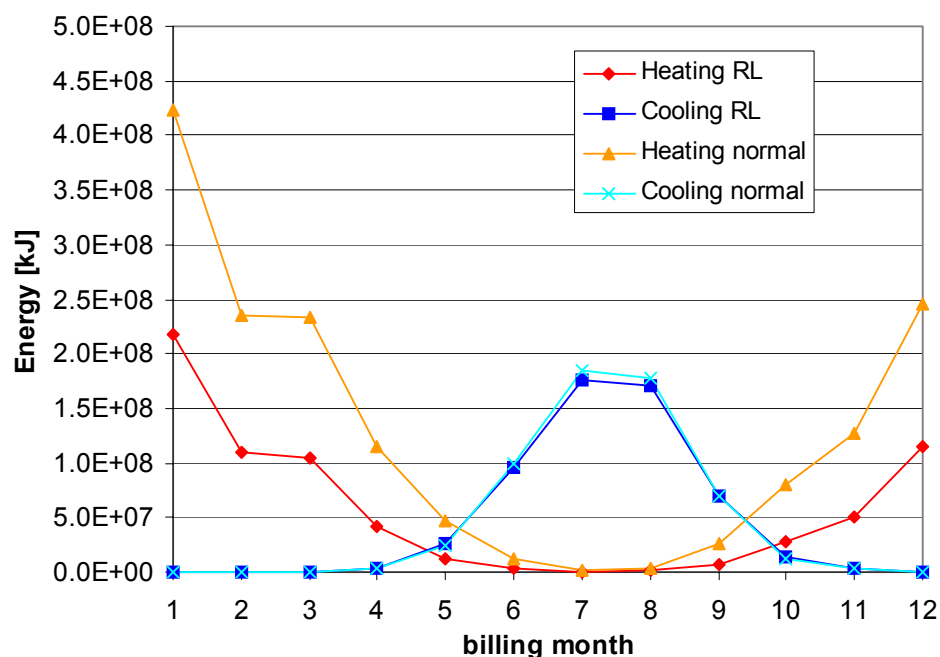


Figure 6.6: HVAC energy consumption with and without runaround loops (RL)

The runaround loop heat exchangers can save 56% of annual heating energy, and lower winter loads by 46%. Since in contrast to enthalpy exchangers only sensible heat can be transferred, no dehumidification of the outdoor air stream in the summer takes place and annual cooling energy use is only reduced by 2.8%. However, maximum hourly summer loads can be lowered by 10% when heat from the intake air is transferred into the cooler exhaust stream.

As with energy recovery ventilation systems, run-around systems are susceptible to frosting of the exhaust air coil under cold weather operation. The tendency to frost the exhaust air coil increases as the outdoor air temperature decreases (thereby, decreasing the fluid temperature supplied to the exhaust air coil) and the zone (exhaust air) relative humidity increases. In the case of the Primate House, frosting only affects Zone 1 due to the higher relative humidity of the exhaust air stream. Humidity in the other zones is very low during the winter, in contrast to energy recovery with enthalpy exchangers, no humidification in the winter takes place, humidity in the building is basically equal to outside levels. The relative humidity in Zones 2,

3 and 4 during January and February averaged 14.5%. In Zone 1 the relative humidity was 21%. These values should be compared to 17.3% and 30% when using enthalpy exchangers.

Including coils in the outdoor air intake and exhaust ducts results in additional air-side pressure drop. The required additional fanpower adds up to 21,750 kWh per year for the eight coils in the four air-handling units serving the Primate House. Annual energy consumption for the circulation pumps to overcome the pressure drop of the systems is 8,630 kWh under the assumption of an efficiency of 0.33. The additional electrical energy use has to be taken into account for economic analysis.

Energy Optimized Control Settings

In order to minimize energy consumption while maintaining the conditioned space at an appropriate IAQ and temperature, there are three parameters which can be adjusted to actual occupancy and specific requirements: temperature set point, humidity set point, and ventilation rate. The key is to find reasonable values. Here we have a tradeoff between maintaining best possible comfort and saving energy. The restriction for energy saving measures in the Primate House is that indoor environmental conditions must not compromise animal health and comfort and a pleasant climatic environment for both keepers and visitors must be provided. One consideration is, that the animals are adaptable to a range of temperatures from winter to summer. The chimpanzees, e.g., spend some time in their outside cages even in the winter. They do not necessarily have to be kept year round at the same temperature since also in their natural habitat they are exposed to variable climatic conditions. According to the “Guide for the Care and Use of Laboratory Animals” [16], a temperature range of 18°C – 29°C is acceptable for non-human primates. While tigers can stand low temperatures, African lions need to be kept warmer. Since they are in the same zone, the minimum temperature is determined by the comfort requirements for the lions. Although they may be exposed to temperatures as low as 6°C in the winter in southern Africa, a minimum of 15°C appears reasonable for Zone 1. Humans adapt themselves to different temperatures by different clothing, varying from a clothing factor of 0.36 in the

summer to 1.3 in the winter. Hence indoor design temperatures for the visitors can be lower in the winter than in the summer. An acceptable range of temperature for human comfort is 20°C in the winter, and 25°C in the summer [Thermal Comfort in ASHRAE Fundamentals, 9]. In principle, temperatures can be lower during the night. Night set back of a few degrees is a good measure to conserve energy, especially in the visitors zone where nobody is present from 5 PM to 10 AM. While in the animal zones ventilation is required all times, in Zone 4 ventilation can be shut down over night.

ASHRAE Standard 55-1992 [19] suggests a indoor relative humidity range of 30% - 60%, while for laboratory primates up to 70% are acceptable [16]. It seems reasonable to limit relative humidity in all zones of the building to 60% to guarantee comfort and prevent mold growth (see chapter 4 “Indoor Humidity”).

In this simulation the heating and cooling set points and the ventilation rates are the following:

- Zone 1: 15°C, 25°C, 60%, 2.4 ACH
- Zone 2: 20°C from 8 AM to 5 PM, 18°C night, 25°C, 60%, 1.4 ACH
- Zone 3: 20°C from 8 AM to 5 PM, 18°C night, 25°C, 60%, 2.68 ACH
- Zone 4: 18°C from 8 AM to 5 PM, 15°C night, 25°C, 60%, 1.7 ACH from 10 AM to 5 PM, 0 ACH night

The results of this simulation are shown in **Figure 6.7**. A comparison with simulated data for the normal conditions is listed in the **Table 6.6** below.

Month	Heating, save	Cooling, save	Heating, normal	Cooling, normal
1	314102723	249557	422850292	19336
2	157603200	772508	234858972	100271
3	151865106	333263	234108674	39127
4	48520822	963673	114460093	3613211
5	6692002	8796443	46921245	23869012
6	302340	66753049	12661806	99761817
7	0	137085363	1410551	184545503
8	0	129265416	3786056	178554251
9	1730181	45544582	25592887	69541499
10	22641534	3670883	80029981	12209155
11	56021272	509221	127474404	2814345
12	162565155	715876	246045506	161455
Sum [kJ]	922,044,335	394,659,833	1,550,200,467	575,228,980
Savings [%]	40.5	31.4	0.0	0.0
Max. Load [kJ/h]	787,373	754,726	817,978	842,547
Savings [%]	3.7	10.4	0.0	0.0

Table 6.6: Comparison of HVAC energy consumption with energy-optimized settings and with normal settings

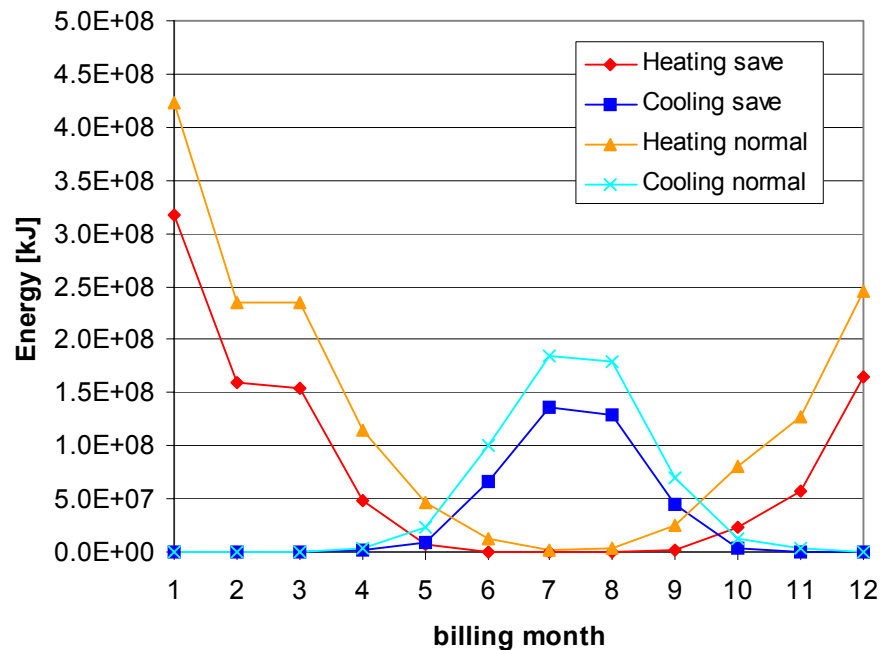


Figure 6.7: Plot of HVAC energy consumption with energy-optimized settings and with normal settings

As the simulation results above show, significant energy savings of 40% for heating energy and 31% for cooling energy can be achieved by optimizing control settings even without sacrificing comfort.

Improved Indoor Air Quality

In these simulation scenarios the ventilation rates are changed according to the suggestions given in chapter 3 “Ventilation” and chapter 4 “Indoor Humidity” to enhance the IAQ in the Primate House. Three simulations are made: one without energy recovery and two runs with the HVAC system including air-to-air heat recovery by enthalpy exchangers respectively runaround loops. To conserve energy, the energy optimized control settings developed in the previous paragraph are applied. The minimum relative humidity to be maintained in the wintertime in Zone 1, 2 and 3 is 30%, moisture is assumed to be provided by electric steam humidifiers. In this simulation the heating and cooling set points and the ventilation rates are the following:

- Zone 1: 15°C, 25°C, 60%, 3 ACH
- Zone 2: 20°C from 8 AM to 5 PM, 18°C night, 25°C, 60%, 3 ACH
- Zone 3: 20°C from 8 AM to 5 PM, 18°C night, 25°C, 60%, 3 ACH
- Zone 4: 18°C from 8 AM to 5 PM, 15°C night, 25°C, 60%, 3 ACH from 10 AM to 5 PM, 0 ACH night

Improved IAQ settings without Energy Recovery

Shown in **Table 6.7** is the energy consumption of the HVAC system without energy recovery. As compared to the standard settings, even for increased IAQ are savings of annual energy costs of 16% for heating and 28% for cooling possible. The humidification of the ventilation air for Zones 1, 2 and 3 consumes 57,500 kWh electricity for the period of the simulation.

	Heating, IAQ	Cooling, IAQ	Heating, normal	Cooling, normal
Sum [kJ]	1,298,583,597	412,492,930	1,550,200,467	575,228,980
Savings [%]	16.2	28.3	0.0	0.0
Max. Load [kJ/h]	1,029,331	940,918	817,978	842,547
Savings [%]	-25.8	-11.7	0.0	0.0

Table 6.7: Comparison between normal configuration and optimized settings for minimal energy consumption and improved IAQ

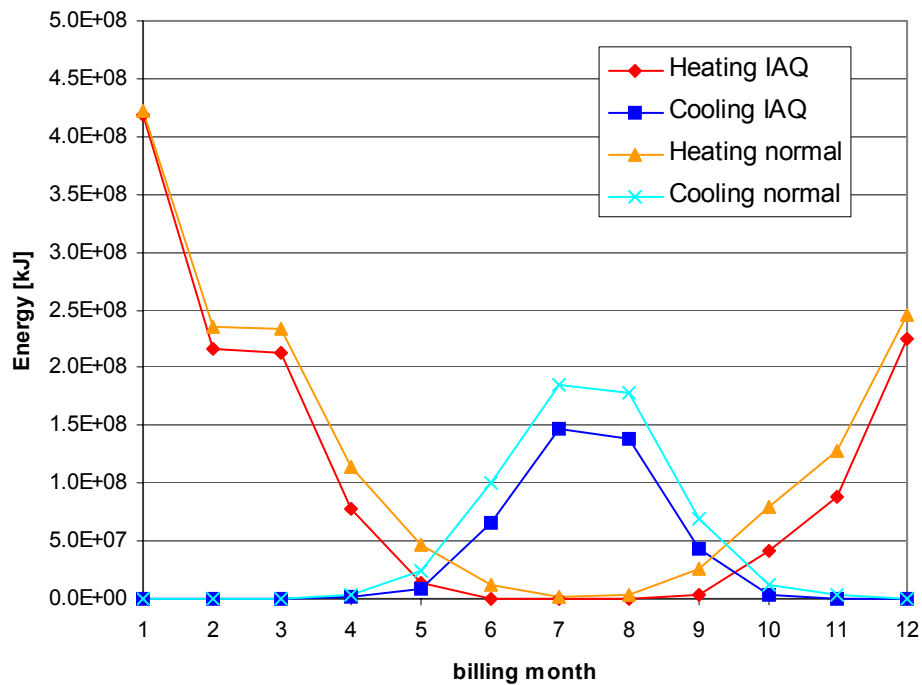


Figure 6.8: Plot of HVAC energy consumption with energy-optimized settings for improved IAQ and with normal settings

The significant savings of cooling energy are caused not only by the high cooling temperature set point, but also by the increased ventilation rate, leading to lower cooling demand during times of moderate outside air temperatures. However, the high ventilation rates causes the maximum hourly heating load to increase by 26% to 1,029,331 kJ/h; this is 37% below the maximal combined heating capacity of the installed equipment of 1,408,500 kJ/h. Also the cooling equipment would be able to handle the 12% increased load.

Improved IAQ settings applying Enthalpy Exchangers

To realize maximum energy savings with improved IAQ, the HVAC system in the following simulation is equipped with four enthalpy exchangers. Temperature and humidity set points are the same as in the previous simulation. Ventilation air flow rates and suitable enthalpy

exchangers picked from [12] with heating respectively balance point temperatures for economizer operation are the following:

- Zone 1: 1350 m³/h, Airxchange ERC-2511, 5°C, 15°C
- Zone 2: 4320 m³/h, Airxchange ERC-4634, 10°C, 15°C
- Zone 3: 7500 m³/h, Airxchange ERC-5856, 8°C, day 16°C, night 17°C
- Zone 4: 3000 m³/h, Airxchange ERC-3622, 8°C, 14°C

The Simulation results of energy consumption for improved IAQ with enthalpy exchangers are in **Table 6.8** and **Figure 6.9** compared with the standard case of 1999:

	Heating, IAQ, EX	Cooling, IAQ, EX	Heating, normal	Cooling, normal
Sum [kJ]	259,455,644	317,568,441	1,550,200,467	575,228,980
Savings [%]	83.3	44.8	0.0	0.0
Max. Load [kJ/h]	360,343	466,416	817,978	842,547
Savings [%]	55.9	44.6	0.0	0.0

Table 6.8: Comparison between normal configuration and optimized settings for minimal energy consumption and improved IAQ with enthalpy exchangers

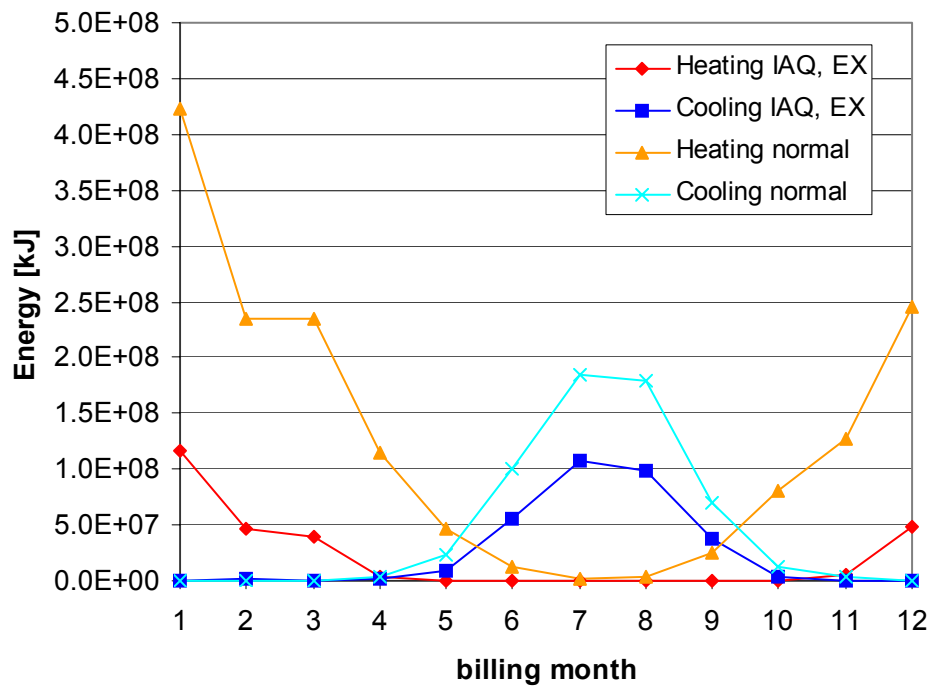


Figure 6.9: Plot of HVAC energy consumption with energy-optimized settings for improved IAQ and enthalpy exchangers and with normal settings

The application of enthalpy exchangers together with conservative control settings can reduce annual heating load by 83% and the cooling energy demand by 45% compared to the normal case of 1999, even though ventilation rates are higher. The maximum hourly heating and cooling loads can be reduced by 60% and 45% according to the simulation results, installed equipment will be oversized. When implementing enthalpy exchangers, the annual humidification load to maintain the zones at 30% RH decreases 69% from 57,000 kWh to 17,800 kWh. The additional fan power for intake and exhaust air streams of the four zones sums up to 27,720 kWh. The preheaters for frost control in Zone 1, 2 and 3 consume 1,093,000 kJ or 303 kWh during their operation time of 56 hours in January of the simulation. Zone 4 does not require frost control due to low wintertime humidity levels and the ventilation shutdown over night.

Heating demand in Zone 1 is zero for all year but 35 hours in January and sums up to 80,000 kJ. The heating demand of Zone 4 follows the ventilation schedule and is zero when ventilation is off, even during cold winter nights.

Improved IAQ settings applying Runaround Loops

Instead of enthalpy exchangers like in the previous simulation run, the HVAC system now is equipped with runaround loop heat exchangers. All ventilation rates, temperature and relative humidity settings are the same as before for improved IAQ and minimized energy consumption. The runaround loops simulated here with TRNSYS Type 223 differ from the runaround loop simulation before since air flow rates are higher. Details of the system for each zone are given in **Table 6.9**, coil data comes from [24, 27]. The heat transfer liquid flow rate is optimized for maximal effectiveness, liquid velocity is about 1.4 m/s, tube diameter is 5/16", spring-type turbulators are used. Coil dimensions are chosen so that air velocity is about 2.5 m/s, resulting in a pressure drop of 200 Pa.

Zone	1	2	3	4
Coil width [in]	12	24	30	18
Coil length [in]	20	32	42	30
Rows	8	8	8	8
Circuits	8	16	20	12
Air flow rates [m³/s]	0.375	1.2	2.08	0.83
Liquid flow rate [l/s]	0.57	1.06	1.42	0.79
Liquid-side pressure drop [kPa]	96	100	128	84
Effectiveness	0.536	0.565	0.587	0.553

Table 6.9: Parameter of the runaround loop systems for the improved IAQ air change rates

The Economizer settings for heating point and balance point respectively are the following temperatures:

- Zone 1: 5°C, 12°C
- Zone 2: 14°C, 16°C

- Zone 3: 11°C, 17°C day / 18°C night
- Zone 4: 10°C, 14°C day / 17°C night

Economizer control as well as frost control is realized with 3-way bypass valves.

The results of the simulation of energy consumption for improved IAQ with runaround loops are listed in **Table 6.10** and plotted **Figure 6.10** and compared with the standard case of 1999:

	Heating, IAQ, RL	Cooling, IAQ, RL	Heating, normal	Cooling, normal
Sum [kJ]	524,639,501	388,832,843	1,550,200,467	575,228,980
Savings [%]	66.2	32.4	0.0	0.0
Max. Load [kJ/h]	644,988	735,512	817,978	842,547
Savings [%]	21.1	12.7	0.0	0.0

Table 6.10: Comparison between normal configuration and optimized settings for minimal energy consumption and improved IAQ with runaround loops (RL)

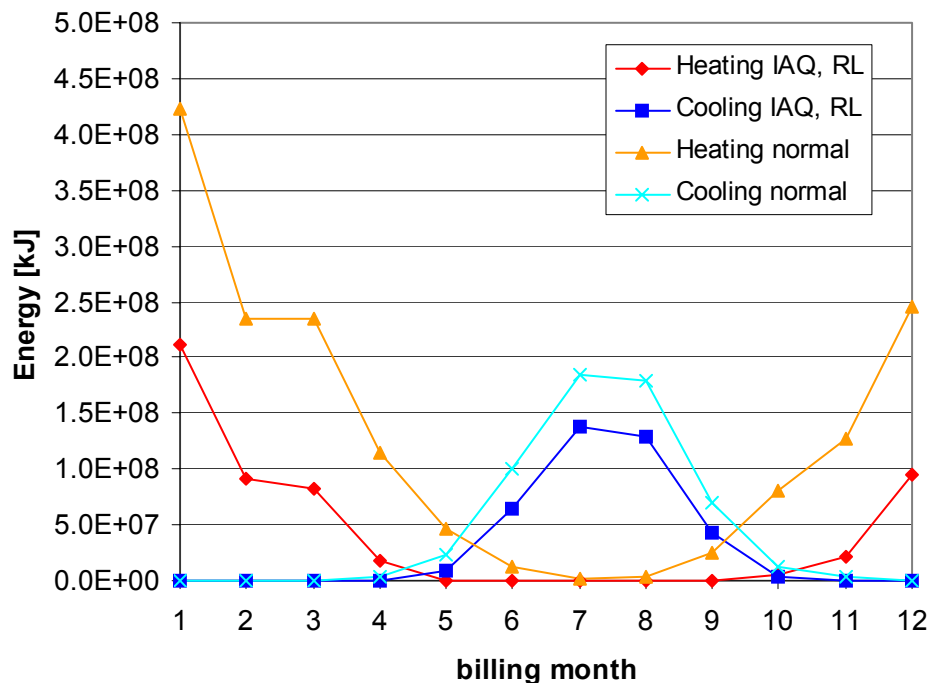


Figure 6.10: Plot of HVAC energy consumption with runaround loops (RL) and energy-optimized settings for improved IAQ and with normal settings

Runaround loops in combination with conservative control settings and improved IAQ can save 66% of the annual heating load and 32% of the cooling load compared to the 1999 normal case, despite higher ventilation rates maximum hourly energy demand is 21% and 13% reduced. However, in comparison to enthalpy exchangers the reduction especially in cooling energy and hourly maxima is less. Since no moisture is transferred into the intake air streams, the humidification energy is higher, 59,000 kWh are necessary to keep the relative humidity in the zones at 30%.

The additional fan power for intake and exhaust air streams of the four zones sums up to 26,980 kWh. The circulation pumps of the runaround loops consume 6565 kWh.

Extreme Weather Conditions and System Sizing

To obtain the maximal expected hourly loads for extreme cold and extreme hot weather conditions, the last two simulations of the Primate House with improved IAQ, energy optimized settings and ERV are repeated with input weather data generated by Extremes [30]. Extremes is a program which generates weather data for the coldest and warmest conditions of a certain location, it can be used to find appropriate heating and cooling system capacities. For Madison the extreme conditions are winter nights with an outdoor temperature of -32.5°C and summer days with up to 38.6°C and 45% RH.

For the Primate House equipped with enthalpy exchangers, the maximum hourly heating load is 401,060 kJ/h. This leads to a part load ratio of 85% for a boiler with a hot water capacity of 469,500 kJ/h, three of those are installed in the Primate House, and only one would be needed. The additional preheater power is listed in **Table 6.11**.

Zone	1	2	3	4
Max. Load [kJ/h]	15475	48306	84533	40265
Max. Load [kW]	4.3	13.4	23.5	11.3

Table 6.11: maximum required preheater power for -32.5°C outdoor temperature and 30% indoor relative humidity

The maximum cooling demand is 552,007 kJ/h. The total capacity of the cooling system is 936,000 kJ/h, the equipment can meet the demand in each zone and operates under part load conditions.

When runaround loops are implemented into the HVAC system of the Primate House, the maximum heating load is 678,415 kJ/h. Two of the boilers with a capacity of 469,500 kJ/h each would be needed, the combined part load ratio would be 0.72. The maximum cooling load is 620,985 kJ/h, 66% of the total installed cooling capacity.

Even under extreme weather conditions, the currently installed heating and cooling equipment is oversized when increasing the ventilation rate, establishing conservative control settings and implementing energy recovery equipment. Reduction of heating and cooling capacity, only one or two boilers and smaller condensing units could lead to higher part load ratio operation, hence higher efficiency.

Conclusions of the Annual Building Energy Simulations

The results for the simulations of the Primate House with improved IAQ and optimized HVAC system with control settings for minimal energy consumption show that it is possible to increase IAQ while saving costs and energy. This is even more the case, when including energy recovery equipment. The highest energy savings are possible with enthalpy exchangers, but also the application of runaround loops leads to considerable reduction in annual energy consumption. An economical analysis of these two cases follows in the next chapter.

The three natural gas boilers in the Primate House have a hot water capacity of 469,500 kJ/h each. Simulations show that the heating demand on very cold days 1999 for the normal configuration is about 825,000 kJ/h, not even the combined capacity of two boilers. On average winter days, only one boiler is needed, and operates under low part load conditions.

When installing energy recovery equipment, the peak heating demand further decreases. If enthalpy exchanger are installed, maximum hourly load is 360,000 kJ/h, the average heating load is 77,500 kJ/h, average part load ratio 0.17. One boiler alone can meet the demand and will operate under part load all the time. For the runaround loop, the peak load is higher when effectiveness is reduced on cold days for frost control, highest demand is 645,000 kJ/h, here two boiler will be needed. The average heating load is 130,000 kJ/h, average part load ratio for one boiler is 0.28.

The additional electric energy needed for the supply and exhaust fans to overcome the pressure losses of energy recovery equipment can be considerable larger than the savings during cooling or economizer operation mode. An air-side bypass economizer and variable speed fans would save electric energy during these operation modes.

Chapter 7 Economic Analysis

An economic analysis for three modifications of the HVAC systems serving the Primate House has been carried out. For all cases, the IAQ in the Primate House is improved with increased ventilation rates and humidification and energy conservative control settings are established. The three different cases analyzed here are:

- Only controls changed, no ERV
- ERV using enthalpy exchangers
- ERV with runaround loops

Estimates of the annual energy savings are developed based on the simulations of the hourly energy consumption for actual 1999 weather data from Chapter 6. The estimate of energy costs are based on utility rates of \$0.0478/kWh for electricity and \$0.6169/therm for natural gas [MG&E, 2002]. The calculation of actual heating fuel (natural gas) consumption for the Primate House requires estimates of the boiler efficiency. The boiler efficiency is assumed to be 0.8 throughout the year due to the low part load ratio operation for the cases when ERV systems are installed. For the case of improved IAQ without ERV as well as for the existing normal case, the heating loads are higher and a boiler efficiency is assumed dependent on the heating demand as follows:

- 0.88 for January
- 0.85 for February and March
- 0.80 for all other months with lower demand

To calculate the electric energy consumption of the condensing units during cooling mode operation, the simulated cooling energy demand is divided by an COP of 2.8. The COP is estimated based on average operation conditions from manufacturer's (Carrier) data.

A summary of the annual heating energy, cooling energy and additional energy are given in **Table 7.1**. Also included in the table are the energy savings and energy cost difference of the alternatives compared with the existing normal operation in 1999 as a base case. The additional energy accounts for humidification and increased fan power due to added ERV pressure drop.

Scenario	Heating [MJ]	Cooling [MJ]	Savings Heating	Savings Cooling	Savings Heating [therm]	Savings Cooling [kWh]	Additional [kWh]	Savings [US \$]
Normal 1999 no ERV	1,566,402	575,229	0.0%	0.0%	0	0	0	0
Improved IAQ no ERV	1,298,584	412,493	16.2%	28.3%	2,986	16,144	57,500	-135
Improved IAQ and enthalpy exchangers	259,456	317,568	83.3%	44.8%	15,484	25,562	45,520	8,598
Improved IAQ runaround loops	524,640	388,833	66.2%	32.4%	12,342	18,492	92,545	4,074

Table 7.1: Summary of simulation results and annual energy savings for heating and cooling. Savings referring to the simulation of normal operation in 1999. Additional energy includes humidification and increased fan power

To investigate the maximum equipment investment costs for the different systems to break even during the time of economic analysis, the P1, P2 Method [28] is applied, **(7.1)**. $P1$ is a present worth factor of the accumulated fuel savings, depending on fuel price inflation rate and market discount rate. $P1$ is essentially on the order of the period of analysis in years. $P2$ is a factor describing the present worth of the total investment costs including annual maintenance costs, depending on the economic parameters interest rates, mortgage terms, down payment, inflation rates and market discount rate.

$$LCS = P1 S_{Fuel} - P2 C_{Invest} \quad (7.1)$$

Where S_{Fuel} are the fuel savings from **Table 7.1**, $C_{Invest,max}$ is the maximum investment cost that would lead to positive life cycle savings during the time of analysis. If the costs of investment are lower, positive LCS will occur within a time horizon shorter than the analysis period.

To obtain the maximum allowable investment cost to break even over the analysis period, the life cycle savings LCS are set to zero:

$$LCS = 0$$

$$C_{Invest,max} = P1/P2 S_{Fuel}$$

Influence of Economic Parameters

Illustrated in **Figure 7.1 - Figure 7.4** is the influence of varying economic parameters on the maximum investment costs over the lifetime of the energy recovery equipment. The assumption made for all cases in this investigation is that the investment is not financed by a mortgage, but the total investment required for retrofitting the HVAC system is available upfront. The sum of investment is either assumed to be discounted at a market discount rate d of 5%, or not discounted for the case the sum came from earmarked funds for public investment in energy saving technology. The general inflation rate is assumed to be 3% per year. Fuel inflation rate i_{Fuel} is a parameter varied from 3% to 5% assuming increasing prices for gas and electricity. The costs C_M for maintenance, replacement parts, parasitic power etc. are also varied from 2% to 5% of the initial investment costs per year.

The following data can be obtained from the curves in **Figure 7.1 - Figure 7.4**:

- the payback time for given investment costs
- the maximum investment costs to break even within an assumed equipment lifetime and have positive LCS

For different values of the parameters C_M , I_{Fuel} and d from the values assumed here, interpolations and extrapolations between the curves can be made.

It is clear that higher future energy prices, lower discount rates d , and lower miscellaneous costs C_M lead to higher LCS with correspondingly higher possible investment costs, or shorter payback times.

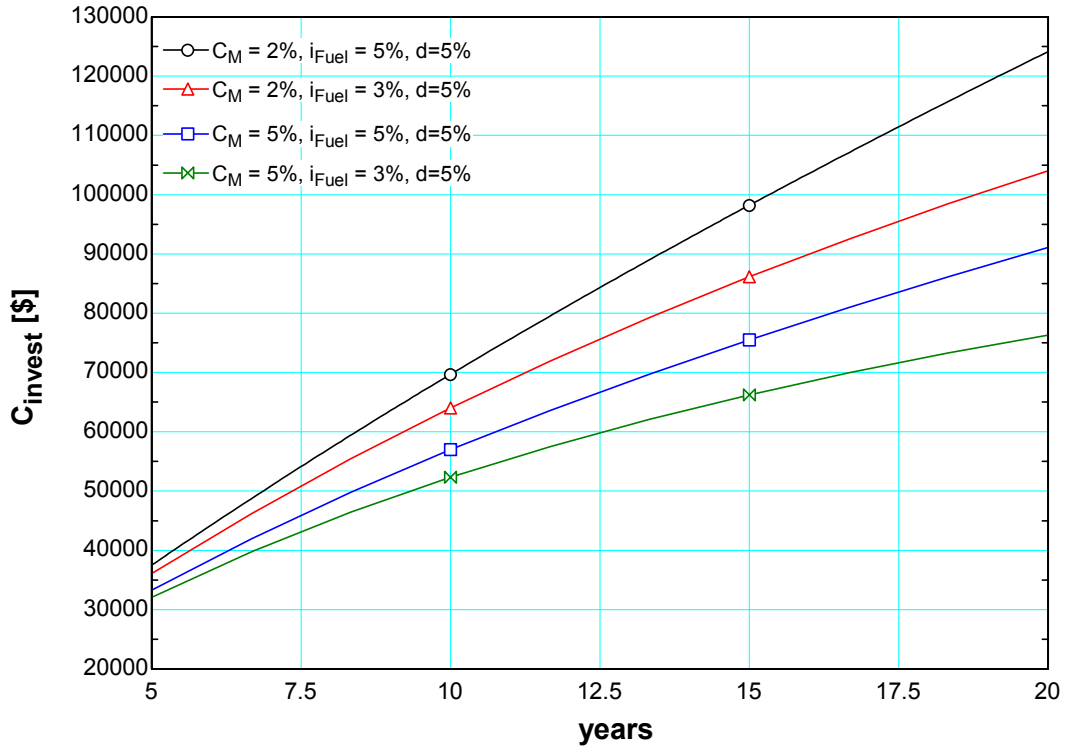


Figure 7.1: Investment costs for the enthalpy exchanger over time to break even for a discount rate d of 5%

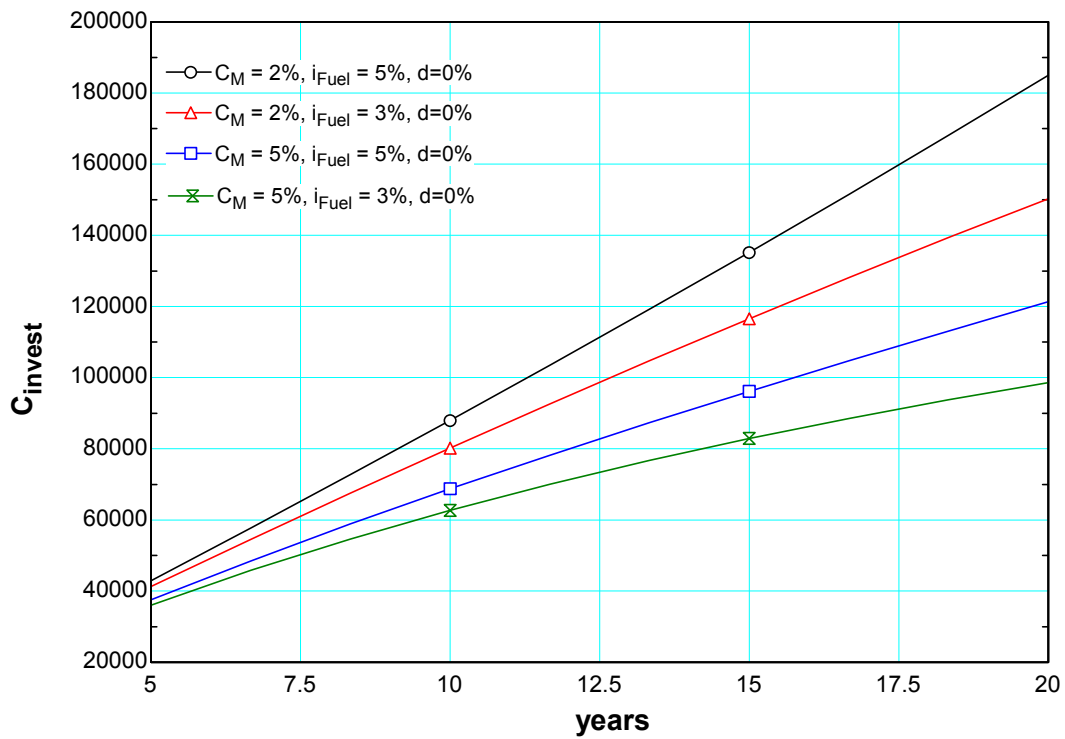


Figure 7.2: Investment costs for the enthalpy exchanger over time to break even for a discount rate d of zero

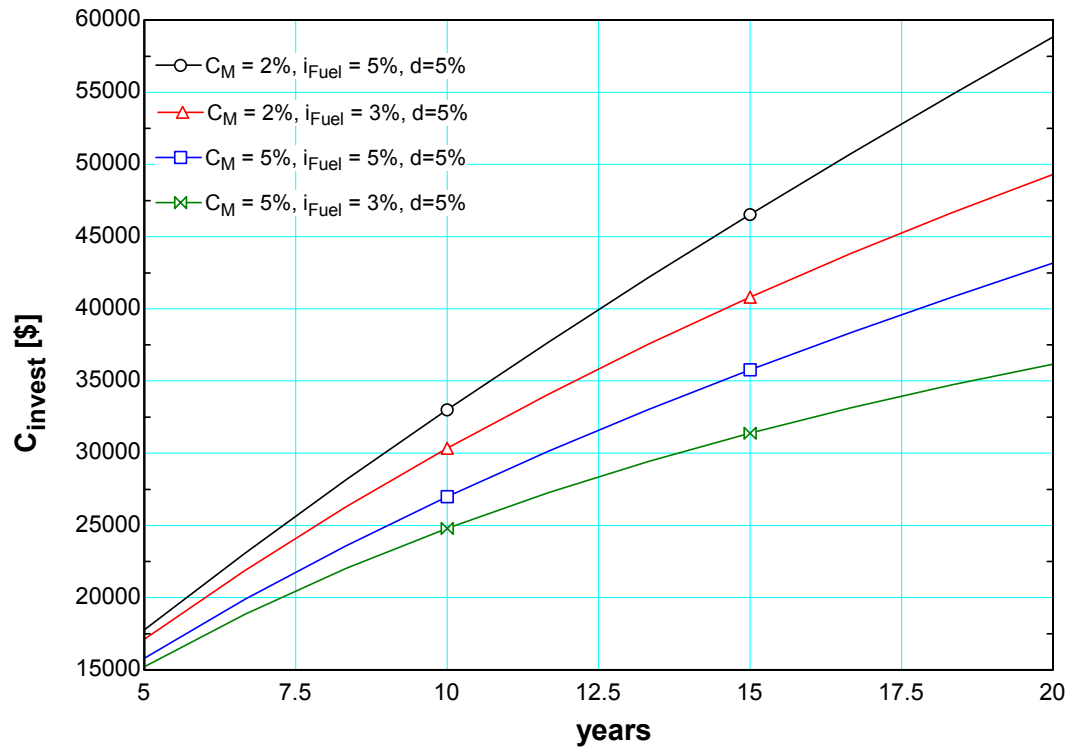


Figure 7.3: Investment costs for the runaround loop over time to break even for a discount rate d of 5%

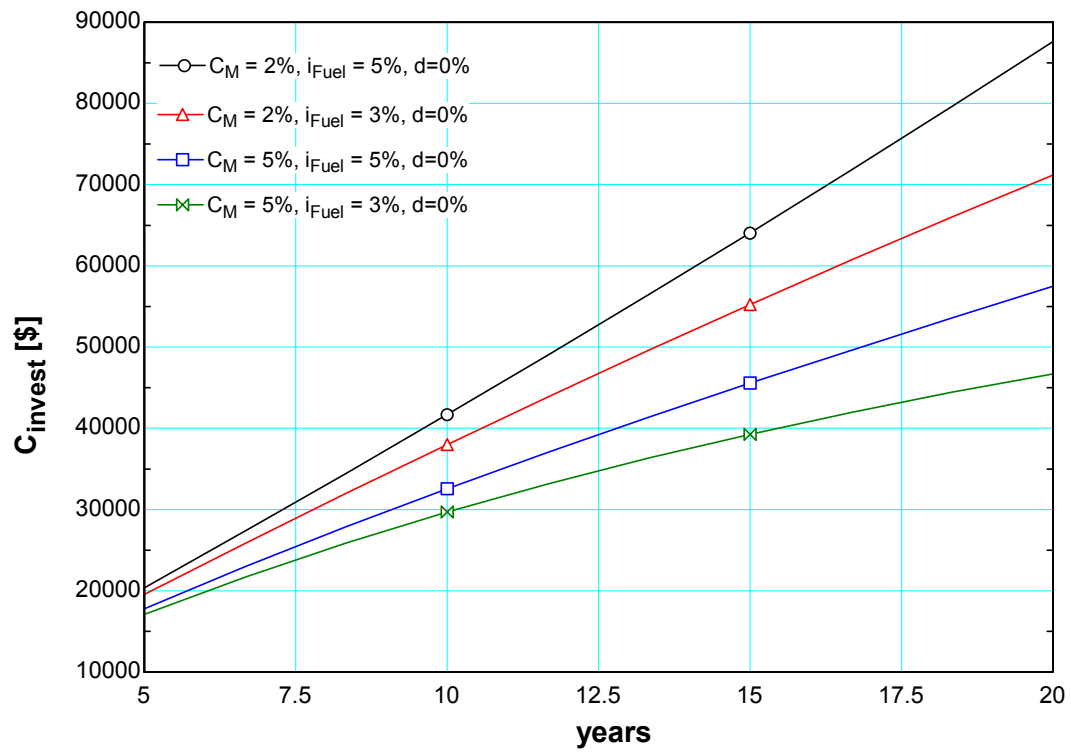


Figure 7.4: Investment costs for the runaround loop over time to break even for a discount rate d of zero

Estimation of Energy Recovery Equipment Cost

An estimation of anticipated costs for retrofitting the HVAC system in the Primate House with enthalpy exchangers and runaround loops ERV systems is carried out based on a computer program for HVAC cost estimation [31]. The costs estimated here are approximated; they shall solely show the order of magnitude of investments for the proposed ERV installations.

An estimate of likely equipment costs for the enthalpy exchangers is listed in **Table 6.11**:

Zone	1	2	3	4
Flow rate max. [cfm]	1000	4000	6000	2000
Price [US \$]	5,050	7,325	8,675	5,950

Table 7.2: estimated prices of enthalpy exchangers including installation costs

The total equipment cost is \$27,000 for all zones. Note that significant additional costs for re-arranging ductwork have to be added, especially in Zone 3, where two exhaust ducts have to be brought from the first floor to the AHU in the basement. An estimate of costs on the order of \$10,000 – \$20,000 is appropriate for this task. Costs for the electric preheaters for Zone 1-3 are not accounted for.

For the runaround loop systems projected costs are given in **Table 6.9**:

Zone	1	2	3	4
Coil	\$ 538	\$ 1,449	\$ 2,200	\$ 1,210
Circulation pump	\$ 700	\$ 900	\$ 1,100	\$ 900
Piping	\$ 1,300	\$ 1,300	\$ 3,150	\$ 1,300
3-Way valve	\$ 200	\$ 200	\$ 200	\$ 200
Controls	\$ 500	\$ 500	\$ 500	\$ 500
Total	\$ 3,776	\$ 5,798	\$ 9,350	\$ 5,320

Table 7.3: estimated prices of the runaround loop systems including installation

The total cost of the runaround loops for all zones is about \$24,244.

The cost estimations for enthalpy exchangers and runaround loops suggest that the investment costs of runaround loops are lower. However, enthalpy exchangers lead to significantly higher annual energy savings. Payback time for the runaround loop solution according to **Figure 7.4** and **Figure 7.3** may be 7 to 10 years based on the estimate of \$24,244. Payback time for the enthalpy exchangers assuming the approximate estimate of \$40,000 would be 5 to 7 years, from **Figure 7.2** and **Figure 7.1**. In addition to a shorter payback time, LCS of the enthalpy exchangers are much higher. Thus, enthalpy exchangers appear to be the most economical solution for conserving energy at the Primate House while improving the indoor air quality.

Chapter 8 Environmental Impacts

The benefits of installing energy recovery systems should not only be considered on account of economics. Reduction of energy consumption not only saves costs, but may also lead to significant reduction of pollution caused by burning coal to generate electricity and natural gas. An analysis of the reduction in greenhouse gas emissions is carried out to evaluate the environmental benefits of the proposed energy conservation strategies. The assumptions made in the analysis are as follows:

- The lower heating value of the natural gas used for heating is 1000 BTU/ft³ [MG&E, 2002]; the density is 0.718 kg/m³.
- The electricity generated to serve the facility originates from a hard coal-fired power plant operating with a first-law efficiency of 0.38.
- The lower heating value of the coal is 30 MJ/kg and the carbon content is 80% on a mass basis.
- The CO₂ generation caused during manufacturing, transport and installation of the ERV equipment is considered negligible in comparison with the savings during operation.

The environmental impacts of the proposed changes to the Primate House's HVAC system are expressed in terms of annual CO₂ emission reductions as given in **Table 8.1**:

Scenario	Savings Heating [tons]	Savings Cooling [tons]	Additional [tons]	Savings total [tons]
Improved IAQ no ERV	16.7	11.2	40.0	-12.0
Improved IAQ and enthalpy exchangers	86.6	17.8	31.6	72.7
Improved IAQ runaround loops	69.0	12.8	64.3	17.6

Table 8.1: Summary of annual CO₂ emission reductions. Savings referring to the simulation of normal operation in 1999.

Energy recovery equipment and optimized control settings can lead to an annual reduction of 17.6 to 72.7 tons of CO₂. The amount of electricity used to humidify the building in the winter when no enthalpy exchangers are installed totals 40 tons of CO₂. However, this pollution will be partially compensated or even over compensated by the heating and cooling savings optimized control settings and ERV can provide.

Not only from an economical point of view, but also in terms of emission reductions the option of enthalpy exchangers appears to be the most favorable. Over a period of 20 years about 1454 tons of CO₂ emissions could be saved. In case a “carbon tax” would be established in future, the economics for the enthalpy exchangers would look even better due to tax savings based on the reduced CO₂ emissions.

Chapter 9 Conclusions and Recommendations

The analysis of the retrofit options for the HVAC system of Primate House has shown that significant savings of energy and costs with improved IAQ are possible.

Based on the conclusions of the simulations in Chapter 6, the economic analysis in Chapter 7 and the environmental impact in Chapter 8, the following list summarizes the measures for maximum costs savings and improved IAQ:

1. Optimization of HVAC control settings
2. Increase of outside air flow rates
3. Installation of enthalpy exchangers

The optimized control settings are given in **Table 9.1**:

Zone	1	2	3	4
Heating set point day	15°C / 59°F	20°C / 68°F	20°C / 68°F	18°C / 64°F
Heating set point night	15°C / 59°F	18°C / 64°F	18°C / 64°F	15°C / 59°F
Cooling set point	25°C / 77°F			
Humidifying set point	30%	30%	30%	-
Dehumidifying set point	60%			
Night set back time	-	5PM - 8AM	5PM - 8AM	5PM - 10AM

Table 9.1: HVAC set points and schedule

The proposed outside air flow rates are given in **Table 9.2**. Note that during night set back the ventilation in Zone 4 shall be shut down.

Zone	1	2	3	4
Flow rate	0.375 m ³ /s 795 cfm	1.2 m ³ /s 2543 cfm	2.083 m ³ /s 4414 cfm	0.83 m ³ /s 1766 cfm

Table 9.2: air flow rates for proper IAQ

The following enthalpy exchangers were modeled for the simulations, it is recommended to install equipment with comparable or better characteristics to achieve the same results:

Zone	1	2	3	4
Model *	ERC-2511	ERC-4643	ERC-5856	ERC-3622
Effectiveness	77.8%	78.3%	77.9%	78.1%
sensible / latent	69.9%	73.1%	72.5%	72.7%
Pressure drop	0.24 kPa	0.2 kPa	0.2 kPa	0.2 kPa

Table 9.3: recommended enthalpy exchangers (*manufactured by Airxchange, Rockland, Ma)

The expected payback time for these measures is 5 to 7 years for an approximate investment cost of \$ 40,000. Annual energy costs savings are \$ 8,598; 72.7 tons of CO₂ can be saved per year.

The recommendations given here are based on simulations applying weather data from 1999. Since future weather may be different, also the energy consumption of the building may differ. In general, more extreme conditions will lead to higher consumption and higher savings, while milder conditions lead to less expenditure and lower conservation compared to the base case of 1999.

Appendix A: FORTRAN Source Code for TRNSYS Type 222

Enthalpy Exchanger

```

SUBROUTINE TYPE222 (TIME,XIN,OUT,T,DTDT,PAR,INFO,ICNTRL,*)
C*****
C Object: Enthalpy Exchanger
C IISiBat Model: TYPE222
C
C Author: Sebastian Freund
C Editor:
C Date: 4/22/2002 last modified: 8/02/2002
C
C
C ***
C *** Model Parameters
C ***
C          Flow 1   m^3/hr [0;+Inf]
C          Sensible Effectiveness 1   - [0;1]
C          Latent Effectiveness 1     - [0;1]
C          Pressure Drop 1   kPa [0;+Inf]
C          Flow 2   m^3/hr [0;+Inf]
C          Sensible Effectiveness 2   - [0;1]
C          Latent Effectiveness 2     - [0;1]
C          Pressure Drop 2   kPa [0;+Inf]
C          Fan Efficiency   - [0;1]
C          Frost Control Mode   - [0;2]
C          Economizer Mode     - [0;2]
C
C ***
C *** Model Inputs
C ***
C          Intake Air Temperature   C [-Inf;+Inf]
C          Exhaust Air Temperature  C [-Inf;+Inf]
C          Intake Air Relative Humidity   - [0;100]
C          Exhaust Air Relative Humidity  - [0;100]
C          Intake Air Flow   m^3/hr [0;+Inf]
C          Exhaust Air Flow m^3/hr [0;+Inf]
C          Control Signal   - [0;1]
C          Balance Point Temperature   C [-Inf;+Inf]
C          Balance Point Relative Humidity - [0;100]
C          Heating Point Temperature   C [-Inf;+Inf]
C          Heating Point Relative Humidity - [0;100]
C
C ***
C *** Model Outputs
C ***
C          Ventilation Temperature   C [-Inf;+Inf]
C          Ventilation Relative Humidity - [0;100]
C          Ventilation Humidity Ratio - [0;1]
C          Exhaust Temperature   C [-Inf;+Inf]
C          Exhaust Relative Humidity - [0;100]

```

```

C          Exhaust Humidity Ratio - [0;1]
C          Ventilation Air Flow   m^3/hr [0;+Inf]
C          Intake Pressure Drop   kPa [0;+Inf]
C          Exhaust Pressure Drop  kPa [0;+Inf]
C          Additional Intake Fan Power    kW [0;+Inf]
C          Additional Exhaust Fan Power   kW [0;+Inf]
C          Preheater Energy Demand kJ/hr [0;+Inf]
C          Preheater Temperature Rise     - [0;+Inf]
C          Sensible Effectiveness - [0;1]
C          Latent Effectiveness  - [0;1]
C          Exchanged Sensible Heat kJ/hr [-Inf;+Inf]
C          Exchanged Latent Heat  kJ/hr [-Inf;+Inf]
C          Exchanged Total Heat   kJ/hr [-Inf;+Inf]
C          Exchanged Total Heat Heating    kJ/hr [0;+Inf]
C          Exchanged Total Heat Cooling    kJ/hr [0;+Inf]

```

C*****

IMPLICIT NONE

```

C          STANDARD TRNSYS DECLARATIONS
          DOUBLE PRECISION XIN,OUT
          INTEGER NI,NP,ND,NO, STATUS
          PARAMETER (NI=11,NP=11,NO=20,ND=0)
          INTEGER*4 INFO,ICNTRL
          REAL T,DTDT,PAR,TIME
          DIMENSION XIN(NI),OUT(NO),PAR(NP),INFO(15)
          CHARACTER*3 YCHECK(NI),OCHECK(NO)

          INTEGER PsyMode, PsyWBMode, Units, FROSTMODE, ECONOMODE
          REAL PSYDAT, ES1, ES2, ES, ESEA, ESOA, EL1, EL2, EL
          REAL ELEA,ELOA,PD1, PD2, PDEA, PDOA
          REAL TOAIN,TOAOUT, TEAIN, TEAOUT, RHOAIN
          REAL RHOAOUT, RHEAIN, RHEAOUT, WOAIN, WOAOUT, WEAIN, WEAOUT
          REAL FLOW1, FLOW2, FLOWEA, FLOWOA, FLOWMIN, CR
          REAL ETAFAN, FANPOWEREA, FANPOWEROA
          REAL NTUS, NTUL, CFCFS, CFCFL, AHCS, AHCL
          REAL TNOFRO, TPREHEAT, QPREH, WSAT, CONTROL
          REAL TBALANCE, HBALANCE, RHBALANCE, THEAT, HHEAT, RHHEAT
          REAL HEAIN, HOAIN, ECONOCONTROL
          DIMENSION PSYDAT(7)

```

```

C
C-----

```

```

C          IF ITS THE FIRST CALL TO THIS UNIT, DO SOME BOOKKEEPING
          IF (INFO(7).GE.0) GO TO 100

```

```

C          FIRST CALL OF SIMULATION, CALL THE TYPECK SUBROUTINE TO CHECK THAT
THE
C          USER HAS PROVIDED THE CORRECT NUMBER OF INPUTS,PARAMETERS, AND
DERIVS

```

```

          INFO(6)=NO
          INFO(9)=1
          CALL TYPECK(1,INFO,NI,NP,ND)
          RETURN 1

```

C END OF THE FIRST ITERATION BOOKKEEPING

C-----

C GET INPUTS AND PARAMETERS

100 CONTINUE

C

 TOAIN = XIN(1)

 TEAIN = XIN(2)

 RHOAIN = XIN(3)

 RHEAIN = XIN(4)

 FLOWOA = XIN(5)

 FLOWEA = XIN(6)

 CONTROL = XIN(7)

 TBALANCE = XIN(8)

 RHBALANCE = XIN(9)

 THEAT = XIN(10)

 RHHEAT = XIN(11)

C

 FLOW1 = PAR(1)

 ES1 = PAR(2)

 EL1 = PAR(3)

 PD1 = PAR(4)

 FLOW2 = PAR(5)

 ES2 = PAR(6)

 EL2 = PAR(7)

 PD2 = PAR(8)

 ETAFAN = PAR(9)

 FROSTMODE = PAR(10)

 ECONOMODE = PAR(11)

 Units = 1 ! SI units

 PSYDAT(1) = 1 ! ATMOSPHERIC PRESSURE

 ECONOCONTROL = 1.0

 TPREHEAT = 0.0

 QPREH = 0.0

 DTDT = 0.0

 FLOWMIN = MIN(FLOWOA, FLOWEA)

 CR = FLOWMIN/MAX(FLOWOA, FLOWEA)

 IF (PD1.EQ.PD2) THEN

 PD2=PD1+0.00001

 ENDIF

C-----

C GET HUMIDITY RATIO WOAIN AND ENTHALPY HOAIN

 PsyMode = 2 ! Inputs are Tdb and RH

 PsyWBMode = 0 ! DON'T Compute Twb

 PSYDAT(2) = TOAIN

 PSYDAT(4) = RHOAIN/100

 CALL PSYCH(TIME,INFO,Units,PsyMode,PsyWBMode,PSYDAT,0,STATUS)

C GET INFO FROM PSYCH

 WOAIN = PSYDAT(6)

 HOAIN = PSYDAT(7)

C-----

C GET HUMIDITY RATIO WEAIN

 PSYDAT(2) = TEAIN

```

PSYDAT(4) = RHEAIN/100
CALL PSYCH(TIME,INFO,Units,PsyMode,PsyWBMode,PSYDAT,0,STATUS)
WEAIN = PSYDAT(6)

C      -----
C      ECONOMIZER MODE ENTHALPY CONTROL
C
      IF (ECONOMODE. EQ. 1) THEN !TEMPERATURE ECONOMIZER AND ENTHALPY COOLING
POINT CONTROL

C      GET ENTHALPIES
PSYDAT(2) = TEAIN
PSYDAT(4) = RHEAIN/100
CALL PSYCH(TIME,INFO,Units,PsyMode,PsyWBMode,PSYDAT,0,STATUS)
HEAIN = PSYDAT(7)

C      SET CONTROL VARIABLE

      IF (TOAIN. GT. THEAT .AND. TOAIN. LT. TBALANCE) THEN
ECONOCONTROL = (TBALANCE-TOAIN)/(TBALANCE-THEAT)
ENDIF
      IF (TOAIN. GE. TBALANCE. AND. HOAIN. LE. HEAIN) THEN
ECONOCONTROL = 0
ENDIF
      IF (HOAIN. GT. HEAIN .OR. TOAIN. GT. TEAIN) THEN
ECONOCONTROL = 1
ENDIF

C
      ENDIF

      IF (ECONOMODE. EQ. 2) THEN !FULL ENTHALPY ECONOMIZER CONTROL

C      GET ENTHALPIES
PSYDAT(2) = TBALANCE
PSYDAT(4) = RHBALANCE/100
CALL PSYCH(TIME,INFO,Units,PsyMode,PsyWBMode,PSYDAT,0,STATUS)
HBALANCE = PSYDAT(7)

PSYDAT(2) = THEAT
PSYDAT(4) = RHHEAT/100
CALL PSYCH(TIME,INFO,Units,PsyMode,PsyWBMode,PSYDAT,0,STATUS)
HHEAT= PSYDAT(7)

C
PSYDAT(2) = TEAIN
PSYDAT(4) = RHEAIN/100
CALL PSYCH(TIME,INFO,Units,PsyMode,PsyWBMode,PSYDAT,0,STATUS)
HEAIN = PSYDAT(7)

C      SET CONTROL VARIABLE

      IF (HOAIN. GT. HHEAT .AND. HOAIN. LT. HBALANCE) THEN
ECONOCONTROL = (HBALANCE-HOAIN)/(HBALANCE-HHEAT)
ENDIF
      IF (HOAIN. GE. HBALANCE .AND. HOAIN. LE. HEAIN) THEN
ECONOCONTROL = 0

```

136

```
ENDIF
IF (HOAIN. GT. HEAIN .OR. TOAIN. GT. TEAIN) THEN
ECONOCONTROL = 1
ENDIF
```

```
C
    ENDIF
```

```
C-----
C    FROST CONTROL
```

```
    IF (FROSTMODE. EQ. 0) THEN
        GOTO 200    !NO FROST CONTROL
    ENDIF
```

```
C
C    CHECK IF FROST BUILDUP CAN OCCUR AND PREHEAT OR SHUTOFF EQUIPMENT
    IF (TOAIN.LT.-2) THEN !CONDENSED WATER MIGHT OCCUR AND FREEZE ON THE
SURFACE
```

```
        TNOFRO = -21.985+1.1269*TOAIN+0.011921*TOAIN**2-0.072838*TEAIN
        &+0.003083*TEAIN**2+0.24807*RHOAIN+0.0000013347*RHOAIN**2
        &+0.10709*RHEAIN-0.00037125*RHEAIN**2-0.013653*TOAIN*TEAIN
        &+0.0042011*TOAIN*RHOAIN-0.0072628*TOAIN*RHEAIN
        &-0.0023767*TEAIN*RHOAIN+0.003386*TEAIN*RHEAIN
        &-0.0012644*RHOAIN*RHEAIN
```

```
        IF (TNOFRO.GT.TOAIN) THEN
            IF (FROSTMODE. EQ. 2) THEN
                CONTROL = 0.0
                GOTO 200
```

```
            ENDIF
```

```
            IF (FROSTMODE. EQ. 1) THEN
```

```
                TPREHEAT = TNOFRO - TOAIN
```

```
                QPREH = 1.004*FLOWOA*1.22*TPREHEAT    !HEAT ADDED BY
```

```
PREHEATER IN kJ/hr
```

```
                TOAIN = TNOFRO
```

```
            ENDIF
```

```
        ENDIF
```

```
    ENDIF
```

```
C-----
```

```
C    CALCULATE EFFECTIVENESS BASED ON COUNTERFLOW HEAT EXCHANGER NTU
METHOD
200    CONTINUE
```

```
    AHCS =(FLOW1*ES1-FLOW2*ES2)/(ES2-ES1) !AHCS = NTU*FLOW
```

```
    CFCFS = ES1*(FLOW1/AHCS+1) !COUNTERFLOW HEAT EXCHANGER CORRECTION
FACTOR FOR BALANCED FLOW
```

```
    AHCL =(FLOW1*EL1-FLOW2*EL2)/(EL2-EL1)
```

```
    CFCFL = EL1*(FLOW1/AHCL+1)
```

```
    IF (CFCFS.LT.1) THEN
```

```
        CFCFS = CFCFS*(CR+1/CFCFS-CR/CFCFS)!MODIFICATION FOR UNBALANCED
```

```
FLOW
```

```

ENDIF
IF (CFCFL.LT.1) THEN
    CFCFL = CFCFL*(CR+1/CFCFL-CR/CFCFL)
ENDIF

IF (CR.EQ.1) THEN
    CR=1.000001 !AVOID DIVISION BY ZERO FOR BALANCED FLOW
ENDIF

NTUS = AHCS/FLOWMIN
ES = (1-exp(-NTUS*(1-CR)))/(1-CR*exp(-NTUS*(1-CR)))*CFCFS*CONTROL*
&ECONOCONTROL

NTUL = AHCL/FLOWMIN
EL = (1-exp(-NTUL*(1-CR)))/(1-CR*exp(-NTUL*(1-CR)))*CFCFL*CONTROL*
&ECONOCONTROL

C
C    CALCULATION OF ESOA, ESEA, ELOA, ELEA, FOR ACTUAL FLOWRATES

ESOA = ES*FLOWMIN/FLOWOA
ESEA = ES*FLOWMIN/FLOWEA
ELOA = EL*FLOWMIN/FLOWOA
ELEA = EL*FLOWMIN/FLOWEA

C    CALCULATE OUTLET TEMPERATURES BASED ON SENSIBLE HEAT EFFECTIVENESS
TOAOUT = TOAIN + ESOA*(TEAIN - TOAIN)
TEAOUT = TEAIN + ESEA*(TOAIN - TEAIN)

C
C    CALCULATE OUTLET HUMIDITY RATIOS BASED ON LATENT HEAT EFFECTIVENESS

WOAOUT = WOAIN + ELOA*(WEAIN - WOAIN)

PSYDAT(2) = TOAOUT
PSYDAT(4) = 1
CALL PSYCH(TIME,INFO,Units,PsyMode,PsyWBMode,PSYDAT,0,STATUS)
WSAT = PSYDAT(6)
IF (WSAT.LT.WOAOUT) THEN !CHECK FOR CONDENSATION
    WOAOUT = WSAT
ENDIF

WEAOUT = WEAIN + ELEA*(WOAIN - WEAIN)

PSYDAT(2) = TEAOUT
PSYDAT(4) = 1
CALL PSYCH(TIME,INFO,Units,PsyMode,PsyWBMode,PSYDAT,0,STATUS)
WSAT = PSYDAT(6)
IF (WSAT.LT.WEAOUT) THEN !CHECK FOR CONDENSATION
    WEAOUT = WSAT
ENDIF

C    LINEAR INTERPOLATION TO FIND PDOA, PDEA
PDOA = (FLOWOA - FLOW1)*(PD2 - PD1)/(FLOW2 - FLOW1)+ PD1
PDEA = (FLOWEA - FLOW1)*(PD2 - PD1)/(FLOW2 - FLOW1)+ PD1
C

```

138

C CALCULATE REQUIRED FAN POWER TO OVERCOME EXHAUST AND INTAKE PRESSURE
DROP

FANPOWEREA = 1/ETAFAN*PDEA*FLOWEA/3600
FANPOWEROA = 1/ETAFAN*PDOA*FLOWOA/3600

C

C-----

C GET RELATIVE HUMIDITY RHOAOUT
PsyMode = 4 ! Inputs are Tdb and HR

PSYDAT(2) = TOAOUT
PSYDAT(6) = WOAOUT
CALL PSYCH(TIME,INFO,Units,PsyMode,PsyWBMode,PSYDAT,0,STATUS)
RHOAOUT = PSYDAT(4)*100

C GET RELATIVE HUMIDITY RHEAOUT

PSYDAT(2) = TEAOUT
PSYDAT(6) = WEAOUT

CALL PSYCH(TIME,INFO,Units,PsyMode,PsyWBMode,PSYDAT,0,STATUS)
RHEAOUT = PSYDAT(4)*100

C

C-----

C

C SET THE OUTPUTS

C VENTILATION AIR TEMPERATURE

OUT(1)= TOAOUT

C VENTILATION AIR RELATIVE HUMIDITY

OUT(2)= RHOAOUT

C VENTILATION AIR HUMIDITY RATIO

OUT(3)= WOAOUT

C EXHAUST AIR TEMPERATURE

OUT(4)= TEAOUT

C EXHAUST AIR RELATIVE HUMIDITY

OUT(5)= RHEAOUT

C EXHAUST AIR HUMIDITY RATIO

OUT(6)= WEAOUT

C VENTILATION AIR FLOW

OUT(7)= FLOWOA

C PRESSURE DROP

OUT(8)= PDOA

OUT(9)= PDEA

C FAN POWER

OUT(10) = FANPOWEROA

OUT(11) = FANPOWEREA

C PREHEATER ENERGY DEMAND

OUT(12)= QPREH

C PREHEAT TEMPERATURE RISE

OUT(13)= TPREHEAT

C SENSIBLE EFFECTIVENESS

OUT(14)= ES

C LATENT EFFECTIVENESS

OUT(15)= EL

C Exchanged Sensible Heat

OUT(16) = 1.004*1.22*FLOWOA*(TOAOUT-TOAIN)

C Exchanged Latent Heat

```
OUT(17)= 1.004*1.22*FLOWOA*2543.5*(WOAOUT-WOAIN)
C      Exchanged Total Heat
OUT(18) = OUT(17) + OUT(16)
C      Exchanged Total Heat Heating
OUT(19) = MAX(0.0,OUT(16)) + MAX(0.0,OUT(17))
C      Exchanged Total Heat Cooling
OUT(20) = - MIN(0.0,OUT(16)) - MIN(0.0,OUT(17))
RETURN 1
END
```

Appendix B: FORTRAN Source Code for TRNSYS Type 223

Runaround Loop

```

SUBROUTINE TYPE223 (TIME,XIN,OUT,T,DTDT,PAR,INFO,ICNTRL,*)
C*****
C Object: Runaround Loop Heat Recovery
C IISiBat Model: TYPE223
C
C Author: Sebastian Freund
C Editor: Sebastian Freund
C Date: 8/17/2002 last modified: 11/21/2002
C
C
***
C *** Model Parameters
C ***
C           Simplified      - [0;1]
C           Effectiveness   - [0;1]
C           Frost Control Mode - [0;2]
C           Economizer Mode - [0;1]
C           System Hydraulic Pressure Drop kPa [0;+Inf]
C           System Design Flow Rate l/s [0;+Inf]
C           Fan Efficiency   - [0;1]
C           Pump Efficiency  - [0;1]
C           Fluid Specific Heat kJ/kg.K [0;+Inf]
C           Fluid Density kg/m^3 [0;+Inf]
C           Fluid Thermal Conductivity W/m.K [0;+inf]
C           Fluid Viscosity kg/m.s [0;+Inf]
C           Number of Circuits OA - [1;+Inf]
C           Number of Rows OA - [1;+Inf]
C           Coil Tube Diameter OA - [0;+Inf]
C           Coil Width OA - [0;+Inf]
C           Coil Lenth OA - [0;+Inf]
C           Number Fins per Inch OA - [0;+Inf]
C           Fin Area Increase Factor OA - [0;+Inf]
C           Turbulators OA - [0;2]
C           Design Pressure Drop OA kPa [0;+Inf]
C           Design Air Velocity OA - [0;+Inf]
C           Number of Circuits EA - [01;+Inf]
C           Number of Rows EA - [01;+Inf]
C           Coil Tube Diameter EA - [0;+inf]
C           Coil Width EA - [0;+Inf]
C           Coil Lenth EA - [0;+Inf]
C           Number Fins per Inch EA - [0;+Inf]
C           Fin Area Increase Factor EA - [0;+Inf]
C           Turbulators EA - [0;2]
C           Design Pressure Drop EA kPa [0;+Inf]
C           Design Air Velocity EA - [0;+Inf]
C
C ***
C *** Model Inputs
C ***

```

C Intake Air Temperature C [-Inf;+Inf]
 C Exhaust Air Temperature C [-Inf;+Inf]
 C Intake Air Relative Humidity - [0;100]
 C Exhaust Air Relative Humidity - [0;100]
 C Intake Air Flow m³/hr [0;+Inf]
 C Exhaust Air Flow m³/hr [0;+Inf]
 C Control Signal - [0;1]
 C Balance Point Temperature C [-Inf;+Inf]
 C Heating Point Temperature C [-Inf;+Inf]
 C Liquid Flow Rate l/s [0;+Inf]

C ***

C *** Model Outputs

C ***

C Ventilation Temperature C [-Inf;+Inf]
 C Ventilation Relative Humidity - [0;100]
 C Ventilation Humidity Ratio - [0;1]
 C Exhaust Temperature C [-Inf;+Inf]
 C Exhaust Relative Humidity - [0;100]
 C Exhaust Humidity Ratio - [0;1]
 C Ventilation Air Flow Rate m³/hr [0;+Inf]
 C Fluid Flow Rate m³/hr [0;+Inf]
 C Effectiveness - [0;1]
 C Recovered Heat kJ/hr [-Inf;+Inf]
 C Removed Heat kJ/hr [-Inf;+Inf]
 C Outside Air Pressure Drop kPa [0;+Inf]
 C Exhaust Air Pressure Drop kPa [0;+Inf]
 C System Hydraulic Pressure Drop kPa [0;+Inf]
 C Additional Intake Fan Power kW [0;+Inf]
 C Additional Exhaust Fan Power kW [0;+Inf]
 C Pumping Power kW [0;+Inf]
 C Preheater Energy Demand kJ/hr [0;+Inf]
 C Preheater Temperature Rise K [0;+Inf]

C*****

IMPLICIT NONE

DOUBLE PRECISION XIN,OUT

INTEGER NI,NP,ND,NO, STATUS

PARAMETER (NI=10,NP=32,NO=19,ND=0)

INTEGER*4 INFO,ICNTRL

REAL T,DTDT,PAR,TIME

DIMENSION XIN(NI),OUT(NO),PAR(NP),INFO(15)

CHARACTER*3 YCHECK(NI),OCHECK(NO)

DIMENSION PSYDAT(7)

INTEGER PsyMode, PsyWBMode, Units, FROSTMODE, ECONOMODE, SIMPLI

REAL PSYDAT, E, Eoa, Eea, Eeawet, Edes, Ewet

REAL TOAIN, TOAOUT, TEAIN, TEAOUT, TEAOUT2, Toaout2

REAL hsatliqain, QXCH, QXCH2, HEAIN, HEAOUT, hoain, WSAT

REAL RHOAOUT, RHOAIN, RHEAIN, RHEAOUT, WOAIN, WOAOUT, WEAIN, WEAOUT

REAL FLOWea, FLOWoa, FLOWliqdes, FLOWliqea, FLOWliqoa

REAL Cliqea, Cliqoa, Cminoa, Cminea, Cairmin, mstar, Cs

REAL Voa, Vea, REoa, REea, Hoa, Hea, Coa, Cea, RCoa, RCea

REAL Vliqoa, Vliqea, RELiqa, RELiqa
 REAL NUturboa, NUturbea, NULamoa, NULamea
 REAL NUeffectiveoa, NUeffectiveea, Hliqoa, Hliqea

REAL MUliq, PRliq, RHoliq, CPliq, Kliq, MUair, PRair, RHOair,CPair

REAL ETAFAN, PDEA, PDOA, PDEADES, PDOADES, FANPOWEROA,FANPOWEREA
 REAL ETAPUMP, PUMPPOWER, PDliq, PDliqdes

REAL Tliqmea, Tliqmeaold, Tliqainold
 REAL Tliqoain, Tliqain, Tliqoaout, Tliqeaout, Tcoilea, TDP

REAL TPREHEAT, QPREH, VC
 REAL ECONOCONTROL, CONTROL, TBALANCE, THEAT, I, Iter

REAL Ncircuitsoa, Nrowsoa,Dtubeoa,Wcoiloa,Lcoiloa,Nfinsoa
 REAL SAFcoiloa, TURBoa, Voades
 REAL Ncircuitsea, Nrowsea,Dtubea,Wcoilea,Lcoilea,Nfinsea
 REAL SAFcoilea, TURBea, Veades
 REAL Ltubeoa, Ltubea, Aductoa, Aductea, DEcoiloa, DEcoilea
 REAL Doa, Dea, SARcoiloa, SARcoilea, FARcoiloa, FARcoilea
 REAL Acoiloa,Acoilea, UAoa, UAea, NTUoa, NTUea, NTUeawet

C

C-----

C IF ITS THE FIRST CALL TO THIS UNIT, DO SOME BOOKKEEPING
 IF (INFO(7).GE.0) GO TO 100

C FIRST CALL OF SIMULATION, CALL THE TYPECK SUBROUTINE TO CHECK THAT
 THE
 C USER HAS PROVIDED THE CORRECT NUMBER OF INPUTS,PARAMETERS, AND
 DERIVS

 INFO(6)=NO
 INFO(9)=1
 CALL TYPECK(1,INFO,NI,NP,ND)
 RETURN 1

C END OF THE FIRST ITERATION BOOKKEEPING

C*****

C-----

C GET INPUTS AND PARAMETERS

100 CONTINUE

C

TOAIN = XIN(1)
 TEAIN = XIN(2)
 RHOAIN = XIN(3)
 RHEAIN = XIN(4)
 FLOWoa = XIN(5)/3600
 FLOWea = XIN(6)/3600
 CONTROL = XIN(7)
 TBALANCE = XIN(8)
 THEAT = XIN(9)
 FLOWliqea = XIN(10)/1000

C VC = XIN(11)

SIMPLI = PAR(1)
 Edes = PAR(2)
 FROSTMODE = PAR(3)
 ECONOMODE = PAR(4)
 PDliqdes = PAR(5)
 FLOWliqdes = PAR(6)/1000
 ETAfan = PAR(7)
 ETApump = PAR(8)
 CPliq = PAR(9)*1000
 RHOliq = PAR(10)
 Kliq = PAR(11)
 MUIq = PAR(12)

Ncircuitsoa = PAR(13)
 Nrowsoa = PAR(14)
 Dtubeoa = PAR(15)
 Wcoiloa = PAR(16)
 Lcoiloa = PAR(17)
 Nfinsoa = PAR(18)
 SAFcoiloa = PAR(19)
 TURBoa = PAR(20)
 PDoades = PAR(21)
 Voades = PAR(22)

Ncircuitsea = PAR(23)
 Nrowsea = PAR(24)
 Dtubeea = PAR(25)
 Wcoilea = PAR(26)
 Lcoilea = PAR(27)
 Nfinsea = PAR(28)
 SAFcoilea = PAR(29)
 TURBea = PAR(30)
 PDeades = PAR(31)
 Veades = PAR(32)

C-----
 C PRESET VARIABLES AND CONSTANTS

PSYDAT(1) = 1 !ATMOSPHERIC PRESSURE

ECONOCONTROL = 1.0
 TPREHEAT = 0.0
 QPREH = 0.0
 DTDI = 0.0
 VC = 0.0
 I = 0

MUair = 0.00001754
 PRair = 0.735
 CPair = 1006
 RHOair = 1.269

```
PRLIQ = MULIQ*CPLIQ/KLIQ
```

```
Coa = FLOWoa*RHOair*CPair
```

```
Cea = FLOWea*RHOair*CPair
```

```
Cairmin = MIN(COA, CEA)
```

```
IF (SIMPLI. EQ. 1. AND. FROSTMODE. GT. 1) THEN      !Frostmode for SIMPLIFIED MODEL
```

```
FROSTMODE = 4
```

```
ENDIF
```

```
C-----
C      GET HUMIDITY RATIOS WOAIN AND WEAIN
```

```
    PsyMode = 2 ! Inputs are Tdb and RH
```

```
    PsyWBMode = 0 ! DON'T Compute Twb
```

```
    PSYDAT(2) = TOAIN
```

```
    PSYDAT(4) = RHOAIN/100
```

```
    CALL PSYCH(TIME,INFO,1,PsyMode,PsyWBMode,PSYDAT,0,STATUS)
```

```
    WOAIN = PSYDAT(6)
```

```
    HOAIN = PSYDAT(7)
```

```
    PSYDAT(2) = TEAIN
```

```
    PSYDAT(4) = RHEAIN/100
```

```
    CALL PSYCH(TIME,INFO,1,PsyMode,PsyWBMode,PSYDAT,0,STATUS)
```

```
    WEAIN = PSYDAT(6)
```

```
    HEAIN = PSYDAT(7)
```

```
C-----
C      CALCULATE COIL DATA
```

```
    IF (SIMPLI. LT. 1) THEN      !SKIP FOR SIMPLIFIED MODEL
```

```
    Ltubeoa = Lcoiloa * Nrowsoa
```

```
    Aductoa = Lcoiloa * Wcoiloa
```

```
    DEcoiloa = (Nrowsoa*1.5+3.5)*0.0254
```

```
    Doa = 0.0254/Nfinsoa
```

```
    Acoiloa = 2*Lcoiloa/Doa*(DEcoiloa*Wcoiloa*SAFcoiloa-Nrowsoa*
&Ncircuitsoa*Dtubeoa**2*3.1416/4)+Ltubeoa*Ncircuitsoa*Dtubeoa
&*3.1416*0.8
```

```
    SARcoiloa = Acoiloa/(Ltubeoa*Ncircuitsoa*Dtubeoa*3.1416)
```

```
    FARcoiloa = (1-0.006*Nfinsoa)*(1-Ncircuitsoa*Dtubeoa/Wcoiloa)
```

```
    Ltubeea = Lcoilea * Nrowsea
```

```
    Aductea = Lcoilea * Wcoilea
```

```
    DEcoilea = (Nrowsea*1.5+3.5)*0.0254
```

```
    Dea = 0.0254/Nfinsea
```

```
    Acoilea = 2*Lcoilea/Dea*(DEcoilea*Wcoilea*SAFcoilea-Nrowsea*
&Ncircuitsea*Dtubea**2*3.1416/4)+Ltubeea*Ncircuitsea*Dtubea*
&*3.1416*0.8
```

```
    SARcoilea = Acoilea/(Ltubeea*Ncircuitsea*Dtubea*3.1416)
```

```
    FARcoilea = (1-0.006*Nfinsea)*(1-Ncircuitsea*Dtubea/Wcoilea)
```

```
    ENDIF
```

```

C-----
C    ECONOMIZER MODE TEMPERATURE CONTROL

    IF (ECONOMODE. GE. 1) THEN !TEMPERATURE CONTROLLED ECONOMIZER

C    SET CONTROL VARIABLE

        IF (TOAIN. GT. THEAT .AND. TOAIN. LT. TBALANCE) THEN
            ECONOCONTROL = (TBALANCE-TOAIN)/(TBALANCE-THEAT)
        ENDIF
        IF (TOAIN. GE. TBALANCE. AND. TOAIN. LE. TEAIN) THEN
            ECONOCONTROL = 0
        ENDIF
    ENDIF

    GOTO 400    !SKIP ECONOMIZER CONTROL BEFORE CHECKED

200  CONTINUE

    I = I + 1

    IF (ECONOMODE. EQ. 1) THEN
        VC = VC + 0.025 !Open 3-Way Valve by 2.5%
        IF (VC. GE. 1) THEN
            ECONOCONTROL = 0
            GOTO 401
        ENDIF
    ENDIF
    IF (ECONOMODE. EQ. 2) THEN
        FLOWliqea = FLOWliqea*0.95    !Reduce Flow rate by 5%
    ENDIF

C-----
C    FROST CONTROL, PREHEAT OR LOWER EFFECTIVENESS

    GOTO 400    !SKIP FROST CONTROL BEFORE CHECKED

300  CONTINUE

    I = I + 1

    IF (FROSTMODE. EQ. 1) THEN
        TOAIN = TOAIN + 1
        TPREHEAT = TPREHEAT + 1
        QPREH = Coa*TPREHEAT*3.6    !HEAT ADDED BY PREHEATER IN kJ/hr
        GOTO 300
    ENDIF
    IF (FROSTMODE. EQ. 2) THEN
        VC = VC + 0.025    !Open 3-Way Valve by 2.5%
    ENDIF
    IF (FROSTMODE. EQ. 3) THEN
        FLOWliqea = FLOWliqea*0.95    !Reduce Flow rate by 5%
        FLOWliqoa = FLOWliqoa*0.95
    ENDIF

```

```

IF (FROSTMODE. EQ. 4) THEN
  Edes = Edes*0.975      !Reduce Effectiveness by 2.5% for simplified model
ENDIF

```

```

C-----
400  CONTINUE

```

```

IF (SIMPLI. EQ. 1) THEN          !SKIP FOR SIMPLIFIED MODEL
  GOTO 500
ENDIF

```

```

C
IF (CONTROL. EQ. 0) THEN
  E = 0
  Toaout = Toain
  Teaout = Teain
  FLOWliqea = 0
  GOTO 600
ENDIF

```

C CALCULATION OF EFFECTIVENESS

```

FLOWliqoa = FLOWliqea*(1-VC)

```

```

Vliqoa = 4*FLOWliqoa/Ncircuitsoa/Dtubeoa**2/3.1416      !OUTSIDE AIR COIL
REliqoa = (TURBoa*0.7321+1)*Vliqoa*Dtubeoa*RHOliq/MUliq

```

```

NUturboa=(((1/(0.79*log(RELIQoa)-1.64)**2)/8*(RELIQoa-1000)
&*PRLIQ))/(1+12.7*sqrt((1/(0.79*log(RELIQoa)-1.64)**2)/8)
&*(PRLIQ**0.6667-1))*(1+(Dtubeoa/Lcoiloa/2)**0.7)

```

```

NULamoa = 3.66+0.0668/((LCOILOa*2/RELIQoa/PRLIQ/Dtubeoa)**0.333
&*(0.04+(LCOILOa*2/RELIQoa/PRLIQ/Dtubeoa)**0.6667))

```

```

NUeffectiveoa = (MAX(NUturboa,0.0)**4+NULamoa**4)**0.25
Hliqoa = NUeffectiveoa*Kliq/Dtubeoa

```

```

Voa = FLOWoa/Aductoa
REoa = Voa/FARcoiloa*RHOair*Doa/MUair
Hoa = 0.166*REOA**(-0.4)/PRair**0.6667*VOA/FARcoiloa*RHOair*CPair

```

```

Vliqea = 4*FLOWliqea/Ncircuitsea/Dtubeea**2/3.1416      !EXHAUST AIR COIL
REliqea = (TURBea*0.7321+1)*Vliqea*Dtubeea*RHOliq/MUliq

```

```

NUturbea=(((1/(0.79*log(REliqea)-1.64)**2)/8*(REliqea-1000)
&*PRLIQ))/(1+12.7*sqrt((1/(0.79*log(REliqea)-1.64)**2)/8)
&*(PRLIQ**0.6667-1))*(1+(Dtubeea/Lcoilea/2)**0.7)

```

```

NULamea = 3.66+0.0668/((LCOILEa*2/RELIQea/PRLIQ/Dtubeea)**0.333
&*(0.04+(LCOILEa*2/RELIQea/PRLIQ/Dtubeea)**0.6667))

```

```

NUeffectiveea = (MAX(NUturbea,0.0)**4+NULamea**4)**0.25
Hliqea = NUeffectiveea*Kliq/Dtubeea

```

```

Vea = FLOWEa/Aductea
REea = Vea/FARcoilea*RHOair*Dea/MUair
Hea = 0.166*REea**(-0.4)/PRair**0.6667*Vea/FARcoilea*RHOair*CPair

Cliqoa = FLOWliqoa * RHOLIq * CPliq           !CAPACITY RATES
Cliqea = FLOWliqea * RHOLIq * CPliq
Cminoa = MIN(COA,Cliqoa)
Cminea = MIN(CEA,Cliqea)

UAoa=Acoiloa/(1/Hoa/0.9+SARcoiloa/Hliqoa)       !HEAT EXCHANGER EQUATIONS
UAea=Acoilea/(1/Hea/0.9+SARcoilea/Hliqea)
NTUoa = UAoa/Cminoa
NTUea = UAea/Cminea
RCoa = Cminoa/MAX(COA, Cliqoa)
RCea = Cminea/MAX(CEA, Cliqea)

Eoa = (1-exp(-NTUoa*(1-RCoa)))/(1-RCoa*exp(-NTUoa*(1-RCoa)))
Eea = (1-exp(-NTUea*(1-RCea)))/(1-RCea*exp(-NTUea*(1-RCea)))

IF (I. EQ. 0) THEN
Edes =1/((Cairmin/Cminoa)/Eoa+(Cairmin/Cminea)/Eea-Cairmin/Cliqea)
ENDIF
C-----
C      CALCULATE OUTLET TEMPERATURES

Tliqoain = (Cminoa*Eoa*Toain/Cliqea*(Eea*Cminea/Cliqea -1)
&- Eea*Cminea*Teain/Cliqea)/((Cminoa*Eoa/Cliqea - Cliqoa/Cliqea
&- VC)*(Eea*Cminea/Cliqea-1) -1)

Tliqeaout =      Tliqoain

Tliqoaout = (Toain - Tliqoain + Cliqoa/Cminoa*Tliqoain/Eoa)/
&Cliqoa*Cminoa*Eoa

Tliqeaain = 1/Cliqea*(Cliqoa*Tliqoaout+Cliqea*VC*Tliqeaout)

Teaout = Teain - Eea*Cminea/Cea*(Teain - Tliqeaain)

Toaout = Toain + Eoa*Cminoa/Coa*(Tliqoain - Toain)

IF (I. EQ. 0) THEN
E = Edes
ELSE
E = Coa/Cairmin*(Toaout - Toain)/(Teain - Toain)
ENDIF

401  CONTINUE

IF (ECONOMODE. GE. 1) THEN !CHECK FOR ECONOMIZER CONTROL

      IF (ECONOCONTROL. EQ. 0) THEN      !SHUT OFF THE SYSTEM
          E = 0
          FLOWliqea = 0
          FLOWliqoa = 0
          TOAout = TOAin

```

148

```
TEAout = TEAin
GOTO 600
ENDIF
IF (ECONOCONTROL. LT. (E/Edes)) THEN      !OPERATE ECONOMIZER AND
REDUCE EFFECTIVENESS
GOTO 200
ENDIF
ENDIF
```

500 CONTINUE

```
IF (SIMPLI. EQ. 1) THEN      !Calculate Outlet temperatures based on Effectiveness
TOAOUT = TOAIN+Edes*ECONOCONTROL*CONTROL*Cairmin/Coa*(TEAIN-TOAIN)
TEAOUT = TEAIN+Edes*ECONOCONTROL*CONTROL*Cairmin/Cea*(TOAIN-TEAIN)
ENDIF
```

```
QXCH = COA*(TOAOUT-TOAIN)/1000
```

```
PsyMode = 2 ! Inputs are Tdb and RH
PSYDAT(2) = TEAOUT
PSYDAT(4) = 1
CALL PSYCH(TIME,INFO,1,PsyMode,PsyWBMode,PSYDAT,0,STATUS)
WSAT = PSYDAT(6)
```

```
Tcoilea = (SARcoilea*Hea/Hliqea*Teaout+Tliqea)/
& (1+ SARcoilea*Hea/Hliqea)      !TEMPERATURE OF THE COLDEST PART OF THE
EXHAUST COIL
```

C-----

```
IF (WSAT.LE.WEAIN) THEN !CHECK FOR CONDENSATION
```

```
HEAOUT = HEAIN - QXCH/RHOair/FLOWea      !CORRELATION FOR DRY BULB
TEMPERATURE AT 99.9% RH IF Eea WOULD BE THE SAME
TEAOUT2=-5.9765+0.66484664*heaout-0.0038412777*heaout**2
```

```
!TEMPERATURES AND EFFECTIVENESS IN CASE OF CONDENSATION
```

```
TEAOUT2 = TEAOUT*0.25 + 0.75*TEAOUT2      !ESTIMATES FOR SIMPLIFIED MODEL
```

```
PsyMode = 2 ! Inputs are Tdb and RH
PSYDAT(2) = TEAOUT2
PSYDAT(4) = 1
CALL PSYCH(TIME,INFO,1,PsyMode,PsyWBMode,PSYDAT,0,STATUS)
HEAout = PSYDAT(7)
```

```
QXCH2 = (HEAIN - HEAOUT)*RHOair*FLOWea
TOAOUT2 = TOAIN + QXCH2*1000/COA
```

```
IF (SIMPLI. EQ. 1) THEN
TOAout = TOAout2
Teaout = Teaout2
```

```
ELSE !SKIP FOR SIMPLIFIED MODEL
```

!CALCUALTION OF WET COIL EFFECTIVENESS AND OUTLET STATES

```

Iter = 0
Tliqoain = QXCH2*1000/Eoa/Cminoa + Toain
Tliqeaout = Tliqoain
Tliqeaain = Tliqeaout - QXCH2*1000/Clieqa
Tliqoaout = Tliqoain - QXCH2*1000/Clieqa

Tliqmea = max((Tliqeaout + Tliqeaain)/2,Tliqmeaold) !ESTIMATE OF MEAN LIQUID
TEMPERATURE

510 CONTINUE !START OF ITERATION

Iter = Iter + 1

Tliqmeaold = Tliqmea
Tliqeaainold = Tliqeaain

Cs=1735.18279+42.9767108*Tliqmea+1.05363412*Tliqmea**2 !SATURATION
SPECIFIC HEAT
& +0.0494449332*Tliqmea**3
mstar=RHOair*FLOWea*Cs/Clieqa
NTUeawet = (Hea*Acoilea)/(Cea+mstar*(Clieqa*Hea*SARcoilea/Hliqea)) !NTU FOR
COMBINED HEAT AND MASS TRANSFER
& Eeawet = (1-exp(-NTUeawet*(1-mstar)))/
(1-mstar*exp(-NTUeawet*(1-mstar))) !ENTHALPY EFFECTIVENESS

hsatliqeaain=9.2127+1.83256*Tliqeaain+0.024948*Tliqeaain**2 !SATURATION ENTHALPY
heaout = heain - Eeawet*(heain - hsatliqeaain)
QXCH2 = (heain - heaout)*RHOair*FLOWea
Teaout2=-5.9765+0.66484664*heaout-0.0038412777*heaout**2
Tliqoain = QXCH2*1000/Eoa/Cminoa + Toain
Tliqoaout = Tliqoain - QXCH2*1000/Clieqa
Tliqeaout = Tliqeaain + QXCH2*1000/Clieqa
Tliqeaain = 1/Clieqa*(Clieqa*Tliqoaout+Clieqa*VC*Tliqeaout)
Toaout2 = TOAIN + QXCH2*1000/COA
Ewet = Coa/Cairmin*(Toaout2 - Toain)/(Teain - Toain)

IF ((Tliqeaout-Tliqoain). LT. (-0.01).
& OR. (Tliqeaout-Tliqoain). GT. (0.01).
& AND. Iter. LE. 1000) THEN
Tliqmea = ((Tliqeaout + Tliqeaain)/2 + Tliqmeaold)/2 !NEW MEAN
LIQUID TEMPERATURE
Tliqeaain = (Tliqeaain + Tliqeaainold)/2
goto 510
ENDIF !END OF ITERATION LOOP

IF (Teaout2. GT. Teaout) THEN !CHECK IF WET TEAOUT GT DRY TEAOUT
Teaout = (Teaout2+Teaout)/2 !USE MEAN TEMPERATURE
ELSE
Teaout = Teain - QXCH/CEA*1000
ENDIF

IF (Ewet. GE. E) THEN !CHECK FOR WET COIL EFFECTIVENESS GT DRY COIL
E=Ewet

```

150

```

      QXCH = QXCH2                !SET VALUES FOR WET COIL
      Toaout = Toaout2
      Teaout = Teaout2
    ELSE
      Toaout = Toain + QXCH/COA*1000    !SET VALUES FOR DRY COIL IF
ONLY PARTIALLY WET
      Tliqoain = QXCH*1000/Eoa/Cminoa + Toain
      Tliqeaout = Tliqoain
      Tliqeaain = Tliqeaout - QXCH*1000/Clieqa
      Tliqoaout = Tliqoain - QXCH*1000/Clieqa
    ENDIF

    ENDIF !END OF DETAILED WET COIL ANALYSIS

    ENDIF !END OF CONDENSATION
```

C-----

```

      IF (SIMPLI. EQ. 1) THEN          !CALCULATE COLDEST EXHAUST COIL SURFACE
TEMPERATURE
      Tcoilea = Teaout - 1.5    !FOR SIMPLIFIED MODEL
    ELSE
      Tcoilea = (SARcoilea*Hea/Hliqea*Teaout+Tliqeaain)/
& (1+ SARcoilea*Hea/Hliqea)    !FOR DETAILED MODEL
    ENDIF

    IF (Tcoilea. LT. 0. AND. FROSTMODE. GT. 0) THEN    !FROST CONTROL ENABLED,
CHECK IF FROST BUILDUP CAN OCCUR
      PsyMode = 4 ! Inputs are Tdb and HR
      PSYDAT(2) = Teaout
      PSYDAT(6) = weain
      CALL PSYCH(TIME,INFO,1,PsyMode,PsyWBMode,PSYDAT,0,STATUS)
      TDP = PSYDAT(5)

      IF (Tcoilea. LT. TDP) THEN !FROSTING LIKELY OR CONDENSED WATER WILL
OCCUR AND FREEZE ON THE COIL SURFACE
        IF (VC. LT. 1. AND. FLOWliqea. GT. 0.0000001) THEN
          GOTO 300    !FROST CONTROL
        ENDIF
      ENDIF
    ENDIF !END OF FROSTCONTROL
```

C-----

600 CONTINUE

C SET FINAL OUTPUTS

```

      E = Coa/Cairmin*(TOAout - TOAin)/(Teain - TOAin + 0.000000001)

      PsyMode = 2 ! Inputs are Tdb and RH
      PSYDAT(2) = TOAOUT
      PSYDAT(4) = 1
```

```

CALL PSYCH(TIME,INFO,1,PsyMode,PsyWBMode,PSYDAT,0,STATUS)
  WSAT = PSYDAT(6)
  IF (WSAT.LT.WOAIN) THEN !CHECK FOR CONDENSATION IN OA COIL
    WOAOUT = 0.999*WSAT
  ELSE
    Woaout = Woain
  ENDIF

  PSYDAT(2) = TEAOUT
  PSYDAT(4) = 1
  CALL PSYCH(TIME,INFO,1,PsyMode,PsyWBMode,PSYDAT,0,STATUS)
    WSAT = PSYDAT(6)
    IF (WSAT.LT.WEAIN) THEN !CHECK FOR CONDENSATION IN EA COIL AGAIN
      Weaout = 0.999*WSAT
    ELSE
      WEAout = Weain
    ENDIF

C    GET RELATIVE HUMIDITY RHOAOUT

    PsyMode = 4 ! Inputs are Tdb and HR
    PSYDAT(2) = TOAOUT
    PSYDAT(6) = WOAOUT
    CALL PSYCH(TIME,INFO,1,PsyMode,PsyWBMode,PSYDAT,0,STATUS)
    RHOAOUT = PSYDAT(4)*100

C    GET RELATIVE HUMIDITY RHEAOUT
    PSYDAT(2) = TEAOUT
    PSYDAT(6) = WEAOUT
    CALL PSYCH(TIME,INFO,1,PsyMode,PsyWBMode,PSYDAT,0,STATUS)
    RHEAOUT = PSYDAT(4)*100

C-----

C    CALCULATE REQUIRED FAN AND PUMPING POWER

    PDoa = PDoades*(Voa/Voades)**1.7
    PDea = PDeades*(Vea/Veades)**1.7
    PDliq = PDliqdes*(FLOWliqea/FLOWliqdes)**2

    FANPOWERoa = 1/ETAfan*PDoa*FLOWoa
    FANPOWERea = 1/ETAfan*PDea*FLOWea
    PUMPPOWER = (PDliq/2*FLOWliqea+PDliq/2*(1-VC)**2*FLOWliqea)/ETAmpump

C-----

C
C    SET THE OUTPUTS

C    VENTILATION AIR TEMPERATURE
    OUT(1)= TOAOUT
C    VENTILATION AIR RELATIVE HUMIDITY
    OUT(2)= RHOAOUT
C    VENTILATION AIR HUMIDITY RATIO
    OUT(3)= WOAOUT
C    EXHAUST AIR TEMPERATURE

```

152

OUT(4)= TEAOUT
C EXHAUST AIR RELATIVE HUMIDITY
OUT(5)= RHEAOUT
C EXHAUST AIR HUMIDITY RATIO
OUT(6)= WEAOUT
C VENTILATION AIR FLOW
OUT(7)= FLOW_{oa}*3600
C LIQUID FLOW RATE
OUT(8)= FLOW_{liqea}*3600
C EFFECTIVENESS
OUT(9)= E
C Exchanged Heat Heating
OUT(10) = MAX(0.0,QXCH)/3.6
C Exchanged Heat Cooling
OUT(11) = - MIN(0.0,QXCH)/3.6
C PRESSURE DROP
OUT(12)= P_{Doa}
OUT(13)= P_{Dea}
OUT(14)= P_{Dliq}/2+P_{Dliq}/2*(1-VC)**2
C FAN POWER
OUT(15) = FANPOWER_{oa}
OUT(16) = FANPOWER_{ea}
C PUMPING POWER
OUT(17)= PUMPPOWER
C PREHEATER ENERGY DEMAND
OUT(18)= QPREH
C PREHEAT TEMPERATURE RISE
OUT(19)= TPREHEAT

RETURN 1
END

References

1. C. J. Simonson, R. W. Besant, "Heat and Moisture Transfer in Desiccant Coated Rotary Energy Exchangers", HVAC&R Research, Volume 3, Number 4, 1997
2. G. Stiesch, "Performance of Rotary Enthalpy Exchangers", MS Thesis, SEL UW-Madison, 1994
3. E. Van den Bulck, "Analysis of Solid Desiccant Rotary Dehumidifiers", MS Thesis, SEL UW-Madison, 1983
4. H. Klein, S. A. Klein, J. W. Mitchell, "Analysis of Regenerative Enthalpy Exchangers", Int. Journal of Heat and Mass Transfer, Vol. 33, 1990
5. Maclaine-cross, "A Theory of Combined Heat and Mass Transfer in Regenerators", PhD Thesis, Monash University, Australia, 1974
6. ASHRAE, Standard 62-2001 "Ventilation Requirements for Acceptable Indoor Air Quality", American Society of Heating, Refrigerating and Air-Conditioning Engineers, Atlanta, GA, 2001
7. W.M. Kays and M.E. Crawford, "Convective Heat and Mass Transfer", McGraw Hill Book Company, NY, 1993
8. S. Kakac and R. K. Shah, "Handbook of Single Phase Convective Heat Transfer", John Wiley & Sons, NY, 1987
9. ASHRAE Handbook Fundamentals 1997, American Society of Heating, Refrigerating and Air-Conditioning Engineers, Atlanta, GA, 1997
10. TRNSYS, a transient systems simulation software package developed at the University of Wisconsin-Madison's Solar Energy Laboratory. Version 15, 2001
11. EES, Engineering Equation Solver, F-Chart Software, www.fChart.com, 2002
12. Airxchange Catalog, Airxchange, Rockland, MA, 2002
13. ASHRAE Handbook Systems and Equipment 2000, American Society of Heating, Refrigerating and Air-Conditioning Engineers, Atlanta, GA, 2000
14. W.M. Kays and A. L. London, "Compact Heat Exchangers", McGraw-Hill, 1964

15. T. Kusuda, O. Piet, J. W. Bean, “Annual Variation of Temperature Field and Heat Transfer under Heated Ground Surfaces”, National Bureau of Standards, 1983
16. “Guide for the Care and Use of Laboratory Animals”, U.S. Department of Health and Human Services, National Institutes of Health, Revised 1985
17. FEHT, Finite Element Heat Transfer, F-Chart Software, www.fChart.com, 2001
18. Jim Kelsey, “The Energy Use Implications of Design Choices in Commercial Buildings”, M.S. Thesis, SEL UW-Madison 1996
19. ASHRAE, Standard 55-1992 “Thermal Environmental Conditions for Human Occupancy”, American Society of Heating, Refrigerating and Air-Conditioning Engineers, Atlanta, GA, 1992
20. James E. Braun, “Methodologies for the Design and Control of Central Cooling Plants”, PhD Thesis, SEL UW-Madison, 1988
21. James L. Threlkeld, “Thermal and Environmental Engineering”, Prentice-Hall, NJ, 1962
22. Sadic Kakac, Hongtan Liu, “Heat Exchangers”, Figure 9.4, CRC Press LLC, 1988
23. Todd B. Jekel, “Experimental Determination of Heat and Mass Transfer in Desiccant Matrices”, PhD Thesis, SEL UW-Madison, 1997
24. Trane Heating and Cooling Coils, Coil Catalog DS1, The Trane Company, 1985
25. H. J. Sauer et al. “Effectiveness and Pressure Drop Characteristics of Various Types of Air-to-Air Energy Recovery Systems”, ASHRAE RP-173, ASHRAE Transactions 1981
26. B. I. Forsyth and R.W. Besant, “The Performance of a Run-Around Heat Recovery System Using Aqueous Glycol as a Coupling Liquid”, ASHRAE Transactions 1988
27. Bohn O.E.M. Coil Manual, Bohn Heat Transfer, 1988
28. Jeff J. Jurinak, “Open Cycle Desiccant Cooling – Component Models and System Simulations”, PhD Thesis, SEL UW-Madison, 1982
29. John A. Duffie, William A. Beckman, “Solar Engineering of Thermal Processes”, 2nd Edition, John Wiley & Sons Inc, 1991
30. Extremes Version 1.02, Extreme Weather Sequence Generator, ASHRAE Project 962, 1997
31. Mechanical Cost Data, RS Means, Kingston, MA, 1998

32. John S. Nelson, "An Investigation of Solar Powered Open Cycle Air Conditioners", MS Thesis, SEL UW-Madison, 1976
33. C. J. Simonson et al. "Part Load Performance of Energy Wheels" ASHRAE Transactions 2000
34. ADL Inc. and DOE, "Energy Consumption Characteristics of Commercial Building HVAC Systems", 2001